USNTPS-T-No.1
8 March 1968

USNTPS-T-No.1

LEVEL II

NAVAL TEST PILOT SCHOOL TEXTBOOK

PRINCIPLES OF HELICOPTER PERFORMANCE

BY

R. B. RICHARDS

NAVAL AIR TEST CENTER
PATUXENT RIVER, MARYLAND

SECURITY CLASSIFICATION OF THIS PAGE *(When Data Entered)*

REPORT DOCUMENTATION PAGE

READ INSTRUCTIONS BEFORE COMPLETING FORM

1. REPORT NUMBER: USNTPS-T-No. 1	2. GOVT ACCESSION NO.
3. RECIPIENT'S CATALOG NUMBER	
4. TITLE *(and Subtitle)*: Principles of Helicopter Performance	5. TYPE OF REPORT & PERIOD COVERED
	6. PERFORMING ORG. REPORT NUMBER
7. AUTHOR(s): R. B. Richards	8. CONTRACT OR GRANT NUMBER(s)
9. PERFORMING ORGANIZATION NAME AND ADDRESS: U. S. Naval Test Pilot School, Naval Air Test Center, Patuxent River, Maryland 20670	10. PROGRAM ELEMENT, PROJECT, TASK AREA & WORK UNIT NUMBERS
11. CONTROLLING OFFICE NAME AND ADDRESS: Head of Academics, U. S. Naval Test Pilot School	12. REPORT DATE: 8 March 1968
	13. NUMBER OF PAGES: 139
14. MONITORING AGENCY NAME & ADDRESS*(if different from Controlling Office)*	15. SECURITY CLASS. *(of this report)*: UNCLASSIFIED
	15a. DECLASSIFICATION/DOWNGRADING SCHEDULE

16. DISTRIBUTION STATEMENT *(of this Report)*

Approved for public release; distribution unlimited

17. DISTRIBUTION STATEMENT *(of the abstract entered in Block 20, if different from Report)*

18. SUPPLEMENTARY NOTES

19. KEY WORDS *(Continue on reverse side if necessary and identify by block number)*

Aircraft performance
Helicopter
Helicopter performance
Performance
Rotary Wing Aircraft

20. ABSTRACT *(Continue on reverse side if necessary and identify by block number)*

This textbook is used as the primary reference for the Helicopter Performance Course at the U. S. Naval Test Pilot School. The Helicopter Performance Course is an integral part of the School curriculum, the particular requirements of which influence the manner and degree of development of these notes. The course is intended to provide a background for the helicopter performance flight projects conducted by the students. The helicopter, with emphasis on the main rotor, is analyzed in various flight

DD FORM 1 JAN 73 1473 EDITION OF 1 NOV 65 IS OBSOLETE

conditions to determine the major factors which influence the performance. Simplified analysis is first applied to hover and then extended to include translational conditions after which consideration is given to the effect of some of the more significant simplifications.

LEVEL II

USNTPS-T-[redacted] 1

(14)

(6)

PRINCIPLES OF HELICOPTER PERFORMANCE

by

(10) ROBERT B. RICHARDS

(11) 8 Mar[redacted]68

(12) 135 p.

U. S. NAVAL TEST PILOT SCHOOL TEXTBOOK
NAVAL AIR TEST CENTER

401 776

INTRODUCTION

This textbook is used as the primary reference for the Helicopter Performance Course at the U. S. Naval Test Pilot School and is presented for review by interested persons as a source of information and with the intention of stimulating suggestions constructive to the course of instruction.

The Helicopter Performance Course is an integral part of the School curriculum, the particular requirements of which influence the manner and degree of development of these notes. The course is intended to provide a background for the helicopter performance flight projects conducted by the students.

References were heavily relied upon and few aspects of the material presented are original. The helicopter, with emphasis on the main rotor, is analyzed in various flight conditions to determine the major factors which influence the performance. Simplified analysis is first applied to hover and then extended to included translational conditions after which consideration is given to the effect of some of the more significant simplifications.

CONTENTS

POWER REQUIRED

For an aircraft to operate at any given airspeed, the engine must supply power to overcome the following losses:

(a) Mechanical losses associated with the operation of the power plant, such as frictional losses, transmission losses, accessory drive and cooling fan power.

(b) Aerodynamic losses associated with transmitting the engine power to the air.

(c) Induced drag, which is a consequence of a three-dimensional lifting surface.

(d) Real-fluid (viscous) effects, which are basically skin friction drag and base pressure drag.

For the fixed-wing aircraft all surfaces are subjected to essentially the same dynamic pressure and the forces produced by the real-fluid effects on all surfaces can be conveniently predicted as:

$$D_p = C_{D_p} q_f S_w$$

where:

D_p = Parasite Drag (lb)

C_{D_p} = Parasite Drag Coefficient = $f(C_L, M)$

q_f = Freestream Dynamic Pressure (lb/ft^2)

S_w = Wing Planform Area (ft^2)

The helicopter, however, has the fuselage subjected to essentially free-stream dynamic pressure but the lifting surface (the rotor), due to its rotation, is subjected to an entirely different dynamic pressure. Thus the real-fluid effects of the fuselage (termed parasite effects) and of the lifting surface (termed profile effects) must be considered separately, unlike the fixed-wing case. The power required for helicopters is more appropriately expressed as:

(a) Power to overcome mechanical losses associated with the operation of the power plant and transmission.

(b) Power supplied to the main rotor, which includes profile and induced effects.

(c) Power supplied to the tail rotor.

(d) Power to overcome the parasite drag of the fuselage.

When considering power requirements of a rotor it is necessary to have a general understanding of the actual rotor operation. The aerodynamics of a rotor is very complex and first order approximations are generally used for analysis and to establish methods of extrapolating rotor power requirements. The analyses need not be completely rigorous because the intent is to show trends, important parameters and major effects, and also to determine results of a qualitative nature which can be useful in evaluating and predicting the quantitative results obtained in flight testing. If secondary effects could not be neglected or if first order approximations could not be made it would be very difficult to establish the generalizations which allow many performance flight tests

to be practical. Profile drag, tip loss, blade interference, etc. are sometimes targets of the first approximation approach. In many cases the simplifying assumptions are restrictive and although applicable to one flight regime may not be reasonable in another. This is not a serious problem if the restriction of the assumption is understood and a correction is predictable.

The least complicated flight condition from an aerodynamic standpoint is hover (when the rotor is not translating with respect to the air mass) because the aerodynamic situation of any portion of the rotor blade does not change with azimuth position. This condition will be considered first and translational flight conditions will be discussed in later sections.

II. HOVER ANALYSIS

A. FLOW VISUALIZATION

In a three-dimensional situation, such as a rotor of finite span, the lifting surface creates a downward acceleration of the air passing the surface. If the air is considered to have a velocity equal and opposite to the blade rotational speed, considering the blade to be stationary, the flow is deflected as it passes the blade, as shown in Figure 1.

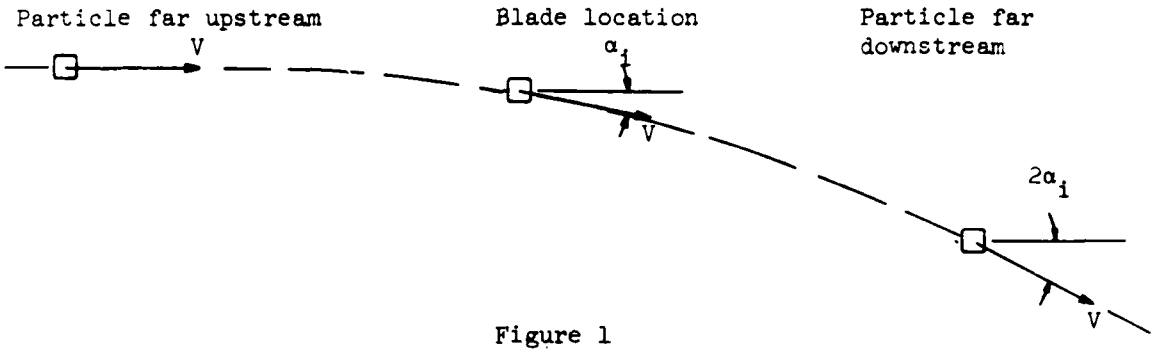

Figure 1
Motion of Air Particle Relative to Blade

The downward velocity imparted to the air as it passes the lifting blade is called induced velocity, v_i, and the angle through which the stream is deflected at the blade is the induced angle, α_i. Notice that the air is deflected upstream of the blade and continues to turn downstream of the blade, ultimately to an angle equal to twice that at the blade. It is also useful to visualize the same phenomenon considering the blade moving relative to the stationary air, as shown in Figure 2.

NAVY
3042

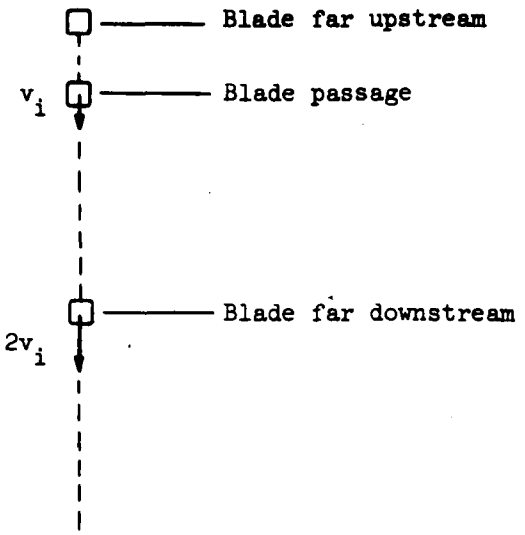

Figure 2
Motion of Air Particle Relative to Air Mass

B. BLADE ELEMENT THEORY

To examine the effect of the induced velocity on the aerodynamic reactions at the blade, let us cut an element out of a hovering rotor at an arbitrary radius, r, from the center of rotation (Figure 3). The resultant aerodynamic force, dR, acting on the blade element is composed of two components: (1) dL, the element lift, which is normal to the local resultant velocity (V_r); and (2) dD_o, the element profile drag, which is parallel to the local velocity, or:

$$\vec{dR} = \vec{dL} + \vec{dD}_o$$

These components of the resultant force are of interest because they are predictable aerodynamically, however, the components of dR normal and

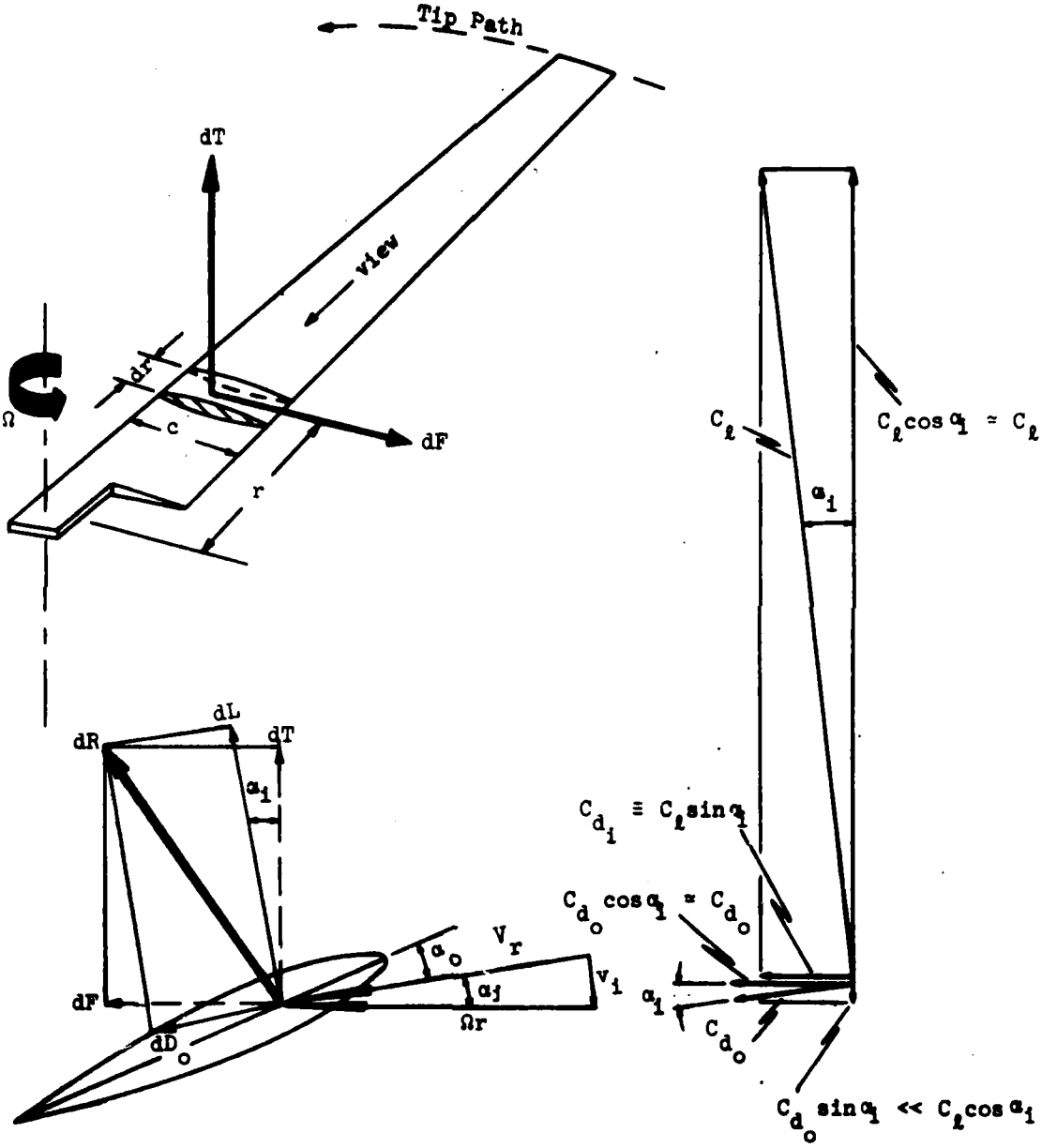

Figure 3
Rotor Blade Element in Hover

parallel to the plane of rotation are more pertinent to performance analysis:

$$\vec{dR} = \vec{dT} + \vec{dF}$$

The component of the resultant aerodynamic force perpendicular to the plane of rotation, dT (thrust), is composed of a component of dL minus a component of dD_o, and is the "useful" force being produced by the rotor. The other component of dR, parallel to the plane of rotation, is dF (torquing force) and is composed of a component of dL (usually called induced drag) plus a component of dD_o. Thus:

$$dT = dL \cos\alpha_i - dD_o \sin\alpha_i$$

$$dF = dL \sin\alpha_i + dD_o \cos\alpha_i$$

The elemental lift and drag can be expressed as:

$$dL = C_\ell q_e dS \qquad dD_o = C_{d_o} q_e dS$$

where $dS = cdr$, $q_e \equiv \frac{1}{2} \rho V_r^2$ and $V_r = \Omega r \cos\alpha_i$

First considering the thrust:

$$dT = \frac{1}{2} \rho (\Omega r)^2 \cos^2\alpha_i \, cdr(C_\ell \cos\alpha_i - C_{d_o} \sin\alpha_i)$$

Analysis of the induced velocity will show that $\Omega r >> v_i$ and thus α_i is a small angle, so that $\cos\alpha_i \approx 1.0$ and $\sin\alpha_i \approx \alpha_i$. Also, in general, $C_\ell >> C_{d_o}$. Then, for these conditions, the second term in the differential

thrust can be neglected compared to the first term (see Figure 3) and

$$dT = \frac{1}{2} \rho(\Omega r)^2 c\,dr\, C_\ell$$

The total thrust per blade can be determined by integration along the blade:

$$T_{\text{per blade}} = \int dT = \int_0^R \frac{1}{2} \rho(\Omega r)^2 c\,dr C_\ell$$

For a first approximation, the integration is simplified by specifying:

(a) Density constant (incompressible).

(b) Element chord constant (no taper).

(c) The element lift coefficient be replaced by the <u>average value</u> along the blade ($\bar{C}_\ell$).

For "b" number of blades, the total thrust produced is:

$$T_{b\ \text{blades}} = \frac{1}{6} \sigma_R \bar{C}_\ell \rho A_D (\Omega R)^2$$

where: $\sigma_R \equiv \frac{bc}{\pi R}$ and $A_D \equiv \pi R^2$

Defining the thrust coefficient,

$$C_T \equiv \frac{T}{\rho A_D (\Omega R)^2} = f\left(\frac{T}{\sigma}, \Omega\right)$$

and from the equation for thrust:

$$C_T = \frac{1}{6} \sigma_R \bar{C}_\ell$$

which shows the manner by which C_T can be determined from aerodynamic

considerations of the blade. The value of C_T, and thus the value of $\bar{C}_\ell$, can be controlled as indicated by the functional relationship. In a hover, T ≈ W and:

$$C_T = f(\frac{W}{\sigma}, \text{RPM}) \qquad \text{where } \sigma \equiv \rho/\rho_{SL} = \rho/0.002377$$

Note that W, ρ and RPM refer to the particular test conditions.

Analysis of the torquing force is done in a similar manner.

$$dF = \tfrac{1}{2}\rho(\Omega r)^2 \cos^2 \alpha_i \, cdr(C_\ell \sin \alpha_i + C_{d_o} \cos \alpha_i)$$

The small angle approximation is again applied but, in this case, it can not be justified that either term be neglected (see Figure 3). The equation can then be written as:

$$dF = \tfrac{1}{2}\rho(\Omega r)^2 cdr(C_{d_i} + C_{d_o})$$

where: $C_{d_i} \equiv C_\ell \alpha_i$, the element induced drag coefficient. The power required, in ft-lb/sec, to rotate the blade element about the shaft axis is:

$$dP = dF(r)\Omega$$

and the integration produces:

$$P_{b\ \text{blades}} = \tfrac{1}{8}\sigma_R(\bar{C}_{d_o} + \bar{C}_{d_i})\rho A_D(\Omega R)^3$$

where $\bar{C}_{d_o}$ and $\bar{C}_{d_i}$ are the average values along the blade.

To simplify the integration C_{d_o} and C_{d_i} were taken to be constant along the blade. The element profile drag coefficient C_{d_o}, varies little over the normal

angle of attack and Mach number range of the operating rotor and, for these conditions, can be assumed constant (Figure 4). A realistic value of the average profile drag coefficient is difficult to predict from wind tunnel section data. The surface finish of actual rotor blades is often relatively poor compared to "aero-dynamically smooth" surfaces because of protuberances and wavyness. Also, blade twist is commonly utilized for improved performance so that at zero thrust most sections are not at zero angle of attack and experience drag associated with the production of lift.

Either high angle of attack or high Mach number may cause large increases in C_{d_o} and, therefore, increases in power required (see Power Corrections Section). The element induced drag coefficient, C_{d_i}, varies considerably with changes of α, or C_L, as perdicted by aerodynamic theory. Thus, in general, the changes in rotor power required are due to changes in rotor induced power.

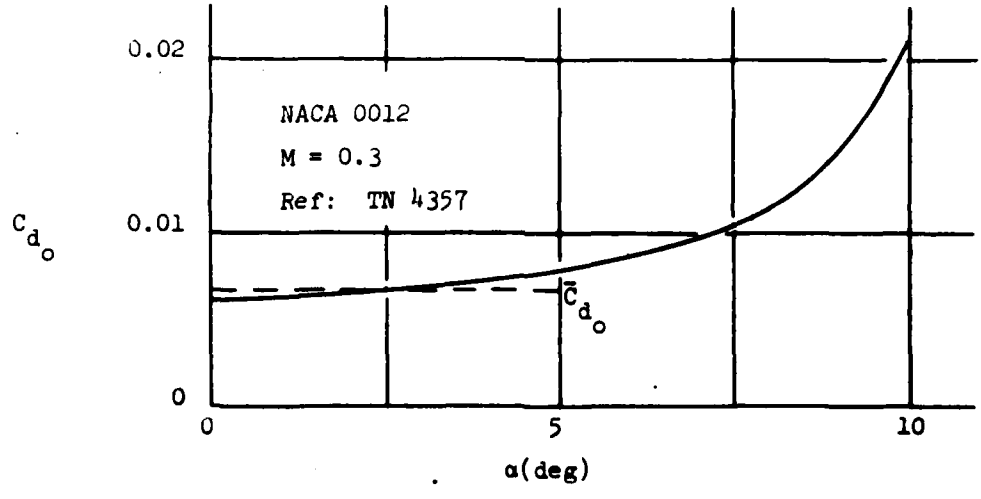

Figure 4
Variation of Section Profile Drag Coefficient
with Angle of Attack

Defining the power coefficient:

$$C_P \equiv \frac{P}{\rho A_D (\Omega R)^3} = f(\frac{P}{\sigma}, \Omega)$$

and, from the power expression:

$$C_P = \frac{1}{8}\sigma_R (\bar{C}_{d_o} + \bar{C}_{d_i})$$

which shows how C_P is related to predictable aerodynamic force coefficients. In the test situation, C_P is controlled by P/σ and RPM.

Analysis of power required is more easily handled if the induced power term is predicted by the momentum theory and blade element theory is used only to analyze the profile term. The above development shows the profile power to be:

$$P_o = \frac{1}{8}\sigma_R \bar{C}_{d_o} \rho A_D (\Omega R)^3$$

to which must be added the induced power to determine total main rotor power required.

C. MOMENTUM ANALYSIS

The momentum theory of rotor (propeller) action visualizes the thrust created as a reaction to the force required to accelerate the air mass through an idealized actuator disc. The analysis affords a simple solution to the induced power required (i.e. the power to overcome the induced drag of the rotor blades) by making many simplifying but restrictive assumptions. The results, then, are only approximations because of the many differences between the idealized rotor and the

real rotor, but many useful relationships are produced and corrections can later be applied to the results to account for the major discrepancies (see Power Corrections Section).

Listed below are the basic assumptions of the momentum theory and, parenthetically, the major corresponding consequence:

(1) Inviscid, frictionless fluid (no profile drag).

(2) Rotor acts as a disc with an infinite number of blades imparting a constant energy to the fluid (no periodicity of the wake).

(3) Flow through the disc is uniform (optimum induced velocity and no tip losses).

(4) Wake is irrotational (no power required to rotate slipstream).

(5) Constant energy flow ahead of and behind the disc ($P_t = \phi$).

Although the static pressure in the flow being affected by the rotor changes in accordance with the Bernoulli equation and the disc sustains a pressure difference, the air far upstream of the rotor in hover must be initially at zero velocity and at ambient pressure (P_a) and far downstream the ultimate wake must be at ambient pressure once again but moving with a velocity, v_w. Considering the flow to be <u>incompressible</u>, and examining the conditions far upstream and far downstream:

$$P_{t_u} = P_a = \text{constant})_1$$

$$P_{t_d} = P_a + q_w = \text{constant})_2$$

so that:

$$\Delta P = P_{t_d} - P_{t_u} = q_w$$

This pressure difference sustained by the actuator disc is the force produced per unit disc area, or:

$$\frac{T}{A_D} = \Delta P = \frac{1}{2}\rho v_w^2$$

The above equation shows the dependence of the wake dynamic pressure on the disc loading (T/A_D) and, as an approximation, describes the velocity imposed on the surroundings under the lifting disc. Typical wake velocities of various lifting systems are compared to that of the rotor in Figure 5.

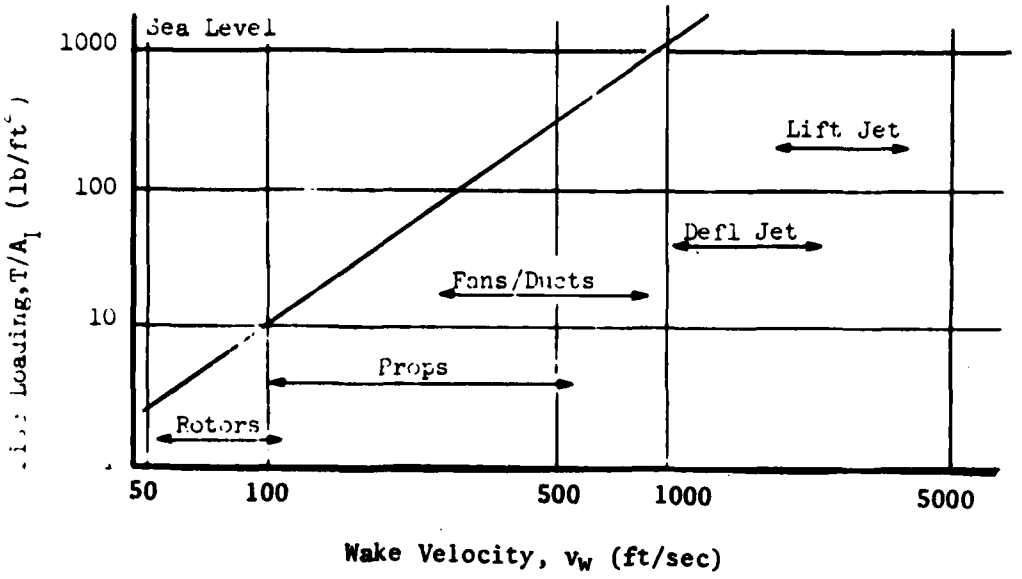

Figure 5
Variation of Wake Velocity With Disc Loading

For steady flow, Newton's law states:

$$F = \dot{m}\Delta V$$

or, the thrust produced by the rotor is the product of the flow rate of

mass being acted upon and the change in velocity of that mass. It is convenient to describe the flow rate at the disc, in which case Newton's law can be written:

$$(\Delta P)A_D = \rho A_D (v_w)$$

and $\Delta P = q_w = \rho v_i v_w$ therefore $\boxed{v_w = 2v_i}$

where: v_i = induced velocity through disc

v_w = ultimate wake velocity

The distance downstream for the wake velocity to become fully developed is usually between one and two rotor radii.

From the above, it is seen that the pressure and velocity along the stream vary as shown in Figure 6. The variations of stream tube size is given by the continuity equation, AV = C.

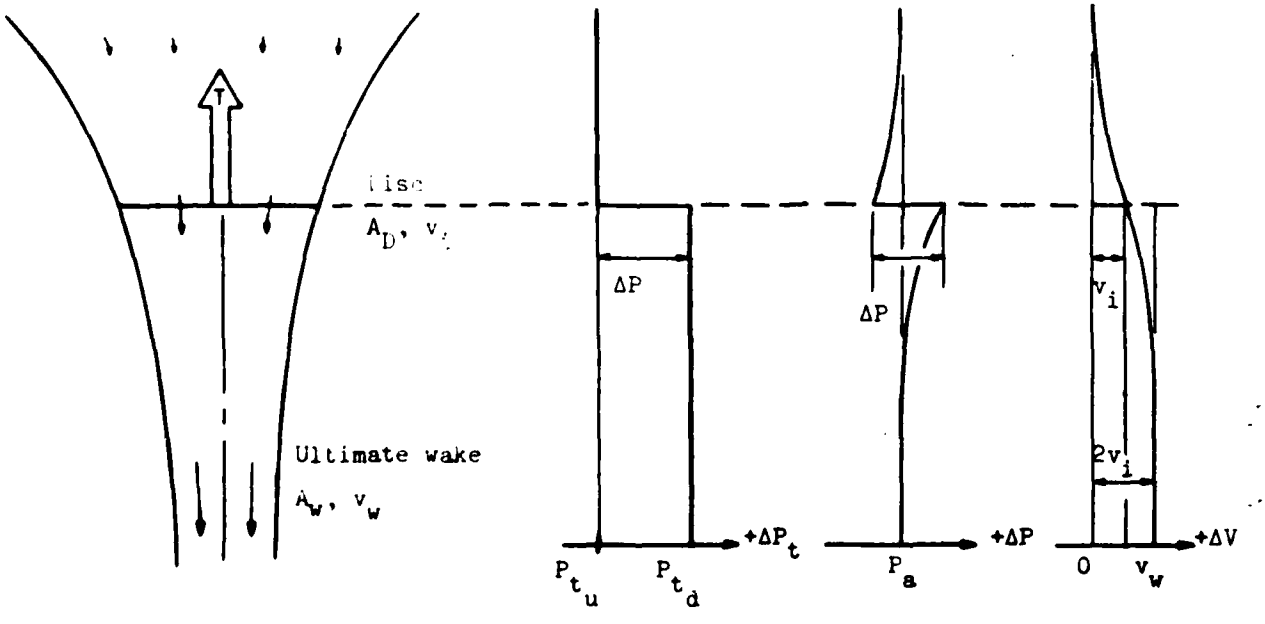

Figure 6
Actuator Disc in Hover

Using the relationship between wake velocity and induced velocity:

$$T = \dot{m}\Delta V = 2\rho A_D v_i^2$$

or, because our interest lies in the magnitude of the induced effects,

$$v_i = \sqrt{\frac{T}{2\rho A_D}} \approx \sqrt{\frac{W}{2\rho A_D}}$$

assuming $T \approx W$ in hover. The power required to accelerate the air mass thorugh the disc, induced power is:

$$P_i = Tv_i$$

$$P_i = \sqrt{\frac{T^3}{2\rho A_D}} \approx \sqrt{\frac{W^3}{2\rho A_D}}$$

assuming $T \approx W$. It should be noted that the induced velocity, v_i, was assumed to be constant across the disc which is an optimum situation and, thus, the induced power indicated by this analysis is the minimum.

D. TOTAL POWER REQUIRED

The major portion of the total power being produced by the engine (ESHP) is abosrbed by the main rotor shaft. The main rotor power (RSHP) is composed of the induced power and the profile power. The induced power is the power required to accelerate the air mass through the rotor and can be conveninetly estimated by momentum analysis. The profile power is the power required to rotate the rotor blades against the viscous action of the air and is analyzed by blade element theory.

The ratio of RSHP to ESHP is defined as mechanical efficiency, η_m:

$$\eta_m \equiv \frac{RSHP}{ESHP}$$

and is, typically, about 0.85 in hover. The mechanical efficiency is a measure of the engine power required to overcome various mechanical losses and includes the power required to drive the tail rotor, which has its own components of induced and profile power. An analysis of the tail rotor power required is presented later. It is sufficient to mention here that the purpose of the tail rotor is to balance the torque reaction to the rotation of the main rotor and thus the tail rotor power requirement, in hover, is simply a percentage of the power input to the main rotor.

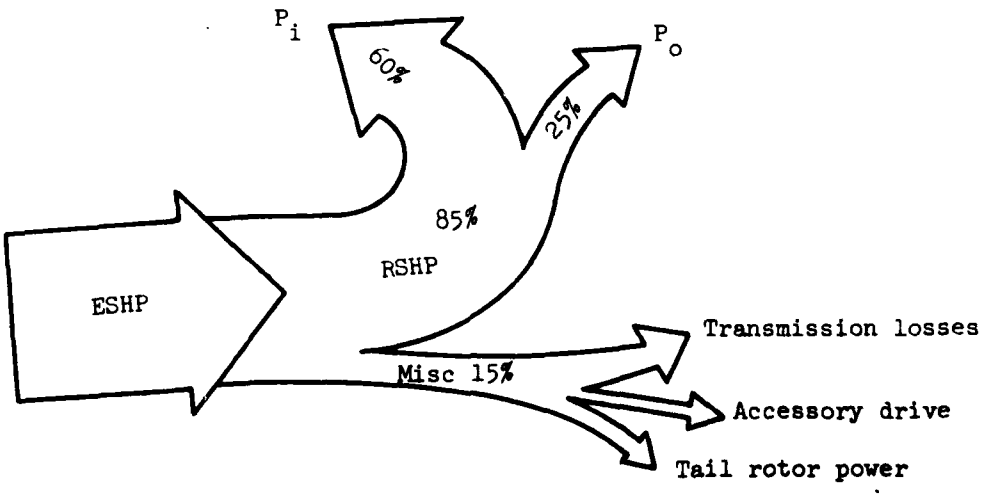

Figure 7
Typical Power Usage in Hover

Accessory drive is the engine power supplied to pumps and generator, etc., necessary to run the many auxiliary systems in the aircraft and may vary widely depending on the loads imposed on the systems. The transmission losses are a result of friction in the drive train and are primarily a function of RPM thus remaining about constant for the helicopter.

The total main rotor power required to hover, P_{MR}, can be written:

$$P_{MR} = P_i + P_o$$

$$P_{MR} = \sqrt{\frac{T^3}{2\rho A_D}} + \frac{1}{8}\sigma_R \bar{C}_{d_o} \rho A_D (\Omega R)^3$$

using the ideal (minimum) induced power, and in coefficient form:

$$C_P = \sqrt{\frac{C_T^3}{2}} + \frac{1}{8}\sigma_R \bar{C}_{d_o}$$

Realizing that the second term in the equation for C_P is constant, a convenient manner by which hover data can be faired is to linearize the power data as a function of $C_T^{3/2}$:

$$C_P = \frac{1}{\sqrt{2}} C_T^{3/2} + K_1$$

Figure 8 shows the generalized hover performance of a typical rotor. The linear relationship expressed above will be typical of actual data only if $\bar{C}_{d_o}$ is representative of the actual rotor profile drag throughout the range of C_T. As mentioned previously, C_{d_o} may vary considerably under certain operating conditions.

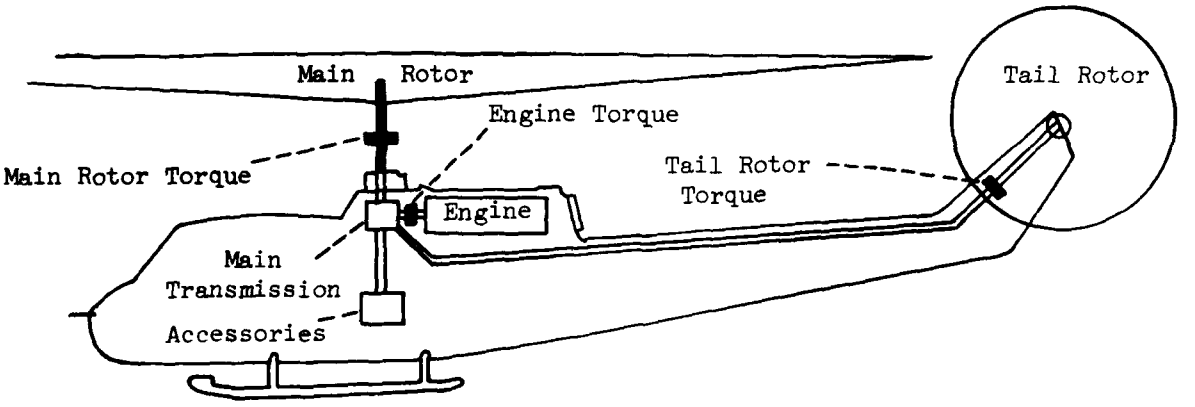

Typical Instrumentation Location For Power Required Determination

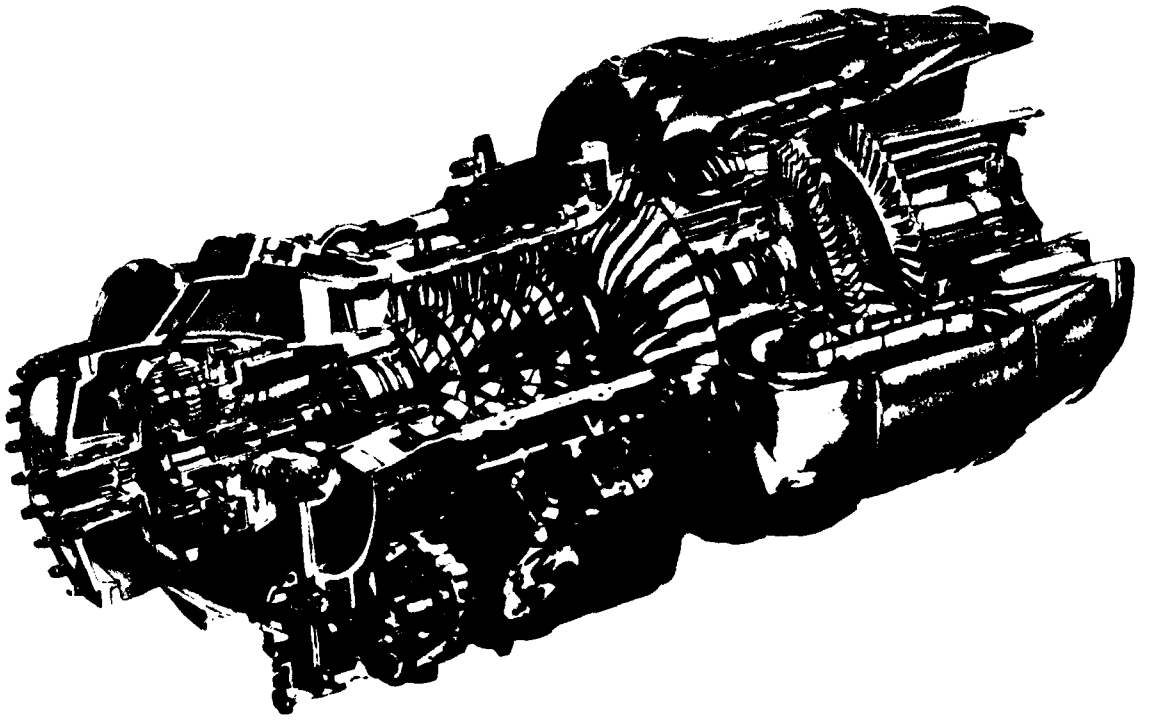

Cutaway of Lycoming T[illegible]

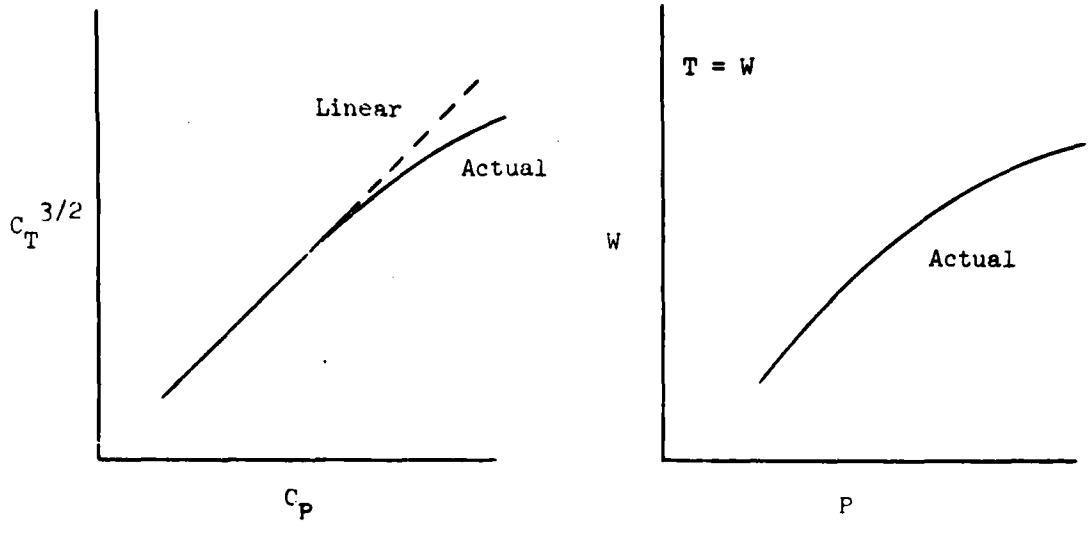

Figure 8
Generalized Hover Data

E. GROUND EFFECT

The energy of the wake from a propulsion system is ultimately dissipated by viscous mixing with the atmosphere, such that the wake is slowed and finally stops. In the case of a lifting system near enough to the ground, the wake may impinge on the ground with sufficient energy to produce a variety of phenomena called "ground effects". The effects of operating in the presence of ground effect can be generally grouped as:

(1) Operational - surface erosion or burning, noise generation, reduced visibility, and erosion or corrosion of aircraft parts (see Figure 10).

(2) Stability and control - changes in height and attitude control, and the creation of external disturbances (see Figure 11).

(3) Performance - exhaust gas reingestion and changes of the pressure field around the aircraft.

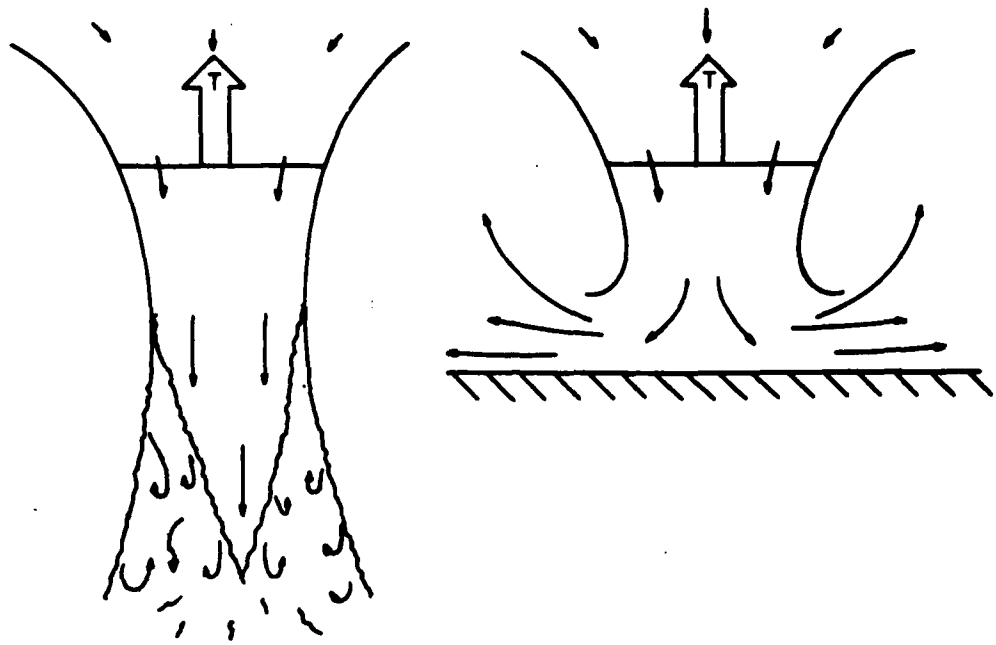

Figure 9
Ground Effect on Rotor Wake

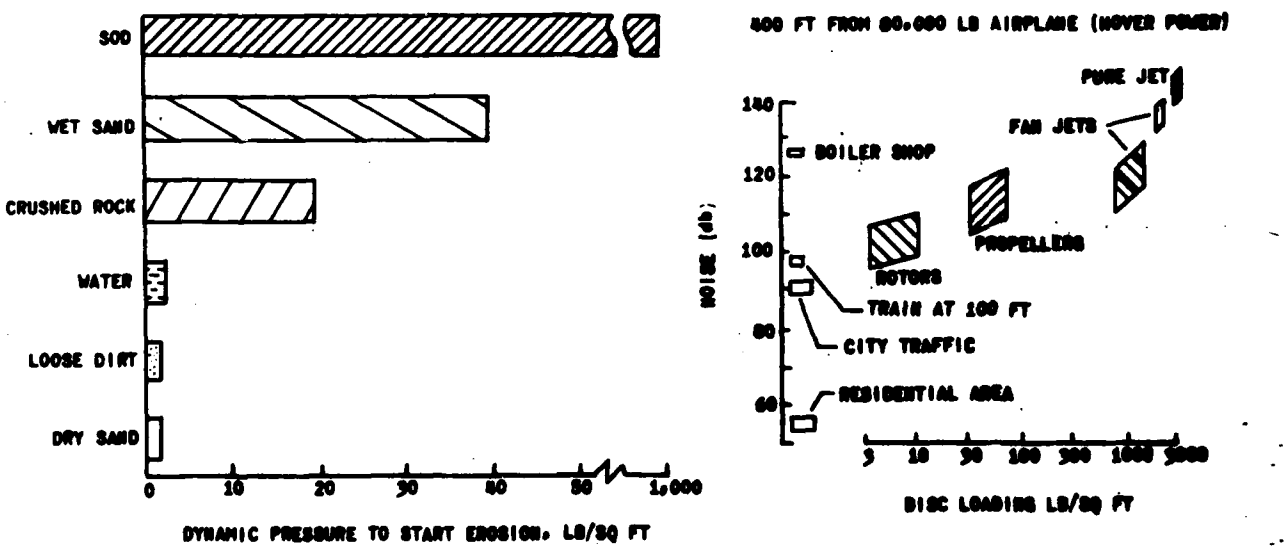

Figure 10
Ground Effects - Erosion and Noise

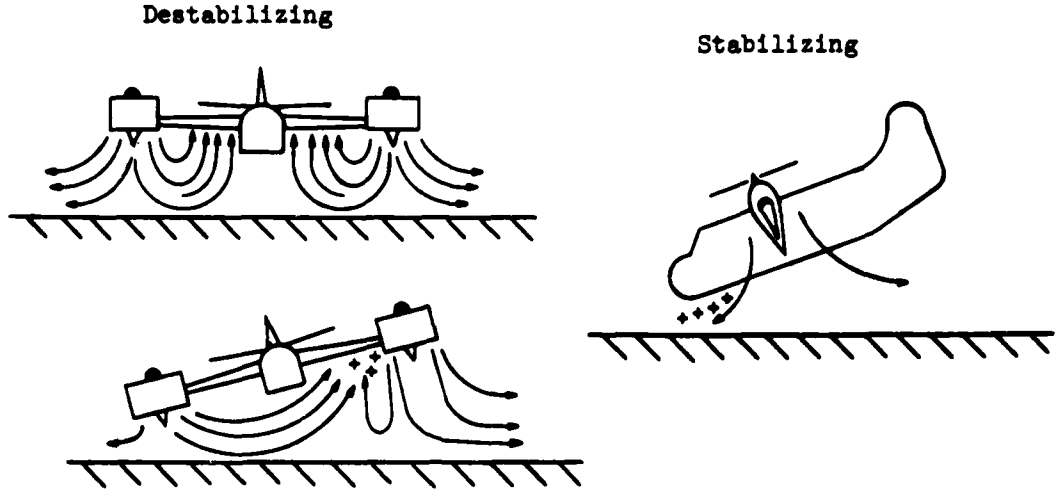

Figure 11
Ground Effects - Attitude Stability

Exhaust gas reingestion dillutes the air entering the engine with the products of combustion and reduces engine performance.

The changes in performance near the ground that result from the pressure field can be favorable or unfavorable depending on the type of vehicle. As the wake impinges on the surface, a region of greater than ambient pressure is created causing the deflection of the wake. The high pressure region is maintained by the centrifugal force (radial component of inertia force) of the air particles on the curved path.

From momentum analysis, the thrust produced by an actuator disc is $T = A_D(\Delta P)$. As the rotor approaches the ground, the pressure field below the disc provides an additional ΔP on the disc which produces more thrust at a constant power, or reduces the power required at a constant thrust.

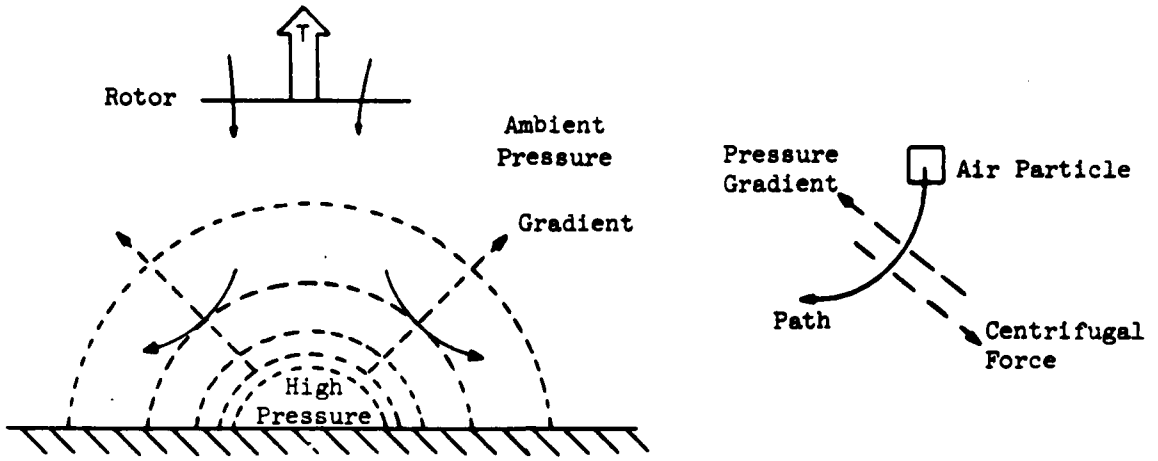

Figure 12
Ground Effect - Pressure Field

The effect becomes more pronounced as the rate of turning increases, that is, as the ratio of height to rotor diameter decreases. An approximate ratio of the power required to produce a certain thrust for a helicopter in ground effect (IGE) to that required out of ground effect (OGE) and the effect on hover performance are shown in Figure 13. A more rigorous analysis considers the fact that this power correction should involve only induced effects which would influence the size of the correction and the height above which no correction is necessary (OGE).

The approximate variation in thrust produced at constant power for a jet in a flat plate is compared to that of a rotor in Figure 13 to show the distinct difference and the effect on the height stability of each type.

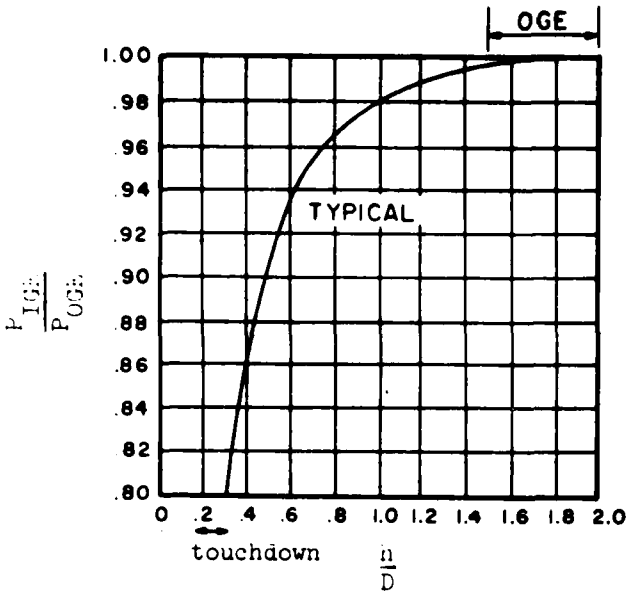

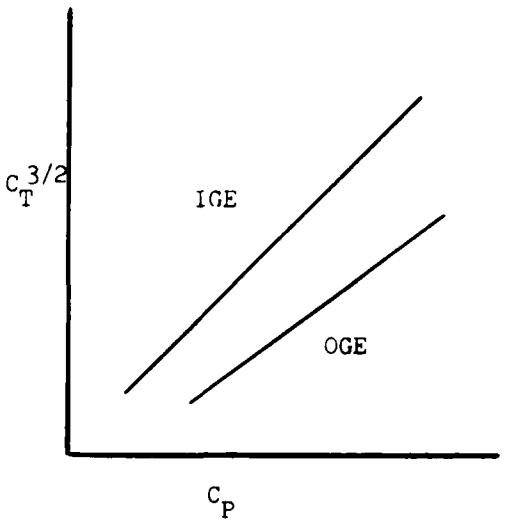

P_{IGE} - Power required in ground effect

P_{OGE} - Power required out of ground effect

h - Rotor height above ground, ft

D - Rotor diameter, ft

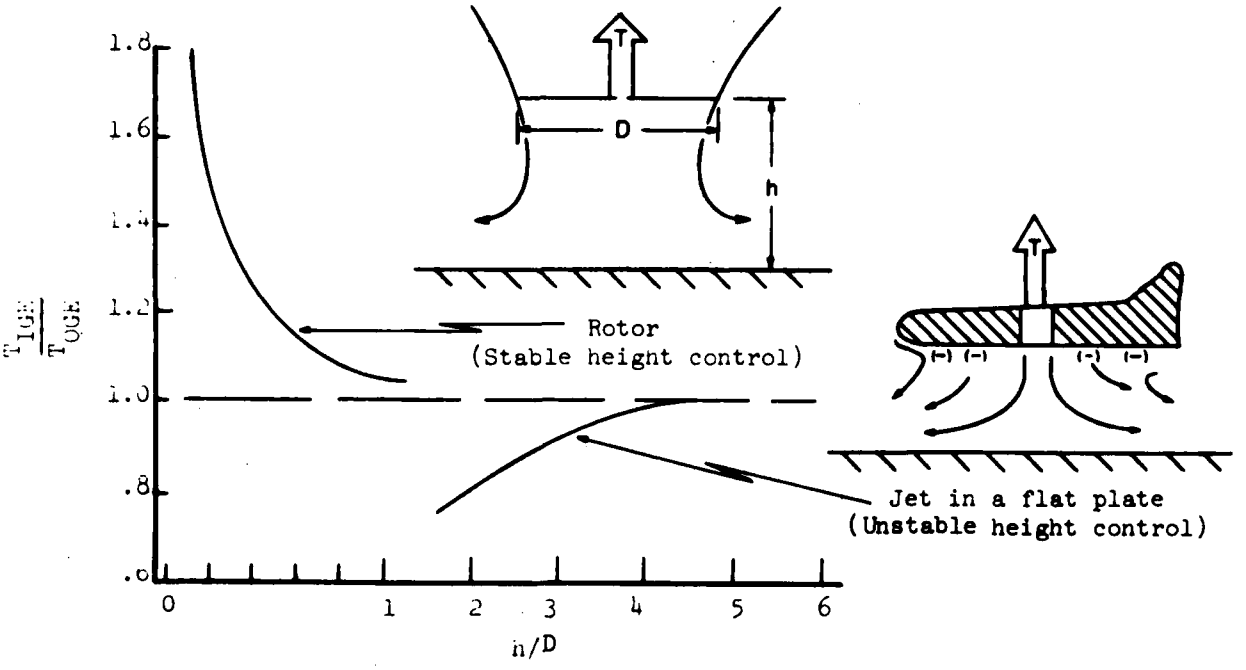

Figure 13
Ground Effect - Change in Thrust and Power

F. FIGURE OF MERIT

The efficiency of a propeller or rotor, η_p, usually is defined by the ratio of the time rate of doing useful work to the power input, or:

$$\eta_p \equiv \frac{\text{power output}}{\text{power input}}$$

A hovering rotor certainly performs a useful task, but accomplishes no useful work and, thus, it's efficiency is zero by the above standard.

To evaluate the relative performance of hovering rotors another measure is required. One method is a comparison based on the figure of merit, M', which is defined as the ratio of the minimum possible power required to produce the thrust, P', to the actual power required, P:

$$M' \equiv \frac{P'}{P}$$

The minimum possible power required is defined as that required by the ideal actuator disc of simple momentum analysis and is:

$$P' \equiv Tv_i = T\sqrt{\frac{T}{2\rho A_D}}$$

Thus, the figure of merit can be expressed as:

$$M' = \frac{T}{P}\sqrt{\frac{T/A_D}{2\rho}}$$

or, upon multiplying and dividing by $\rho A_D(\Omega R)^3$, the figure of merit can be expressed in terms of non-dimensional coefficients as:

$$M' = 0.707\,\frac{C_T^{3/2}}{C_P}$$

The significance of the figure of merit to hover performance is best seen by rearranging the equation:

$$\frac{T}{P} = M' \sqrt{\frac{2\rho}{T/A_D}}$$

For a particular disc loading ($T/A_D \approx W/A_D$) and density, the thrust loading (T/P, the pounds of thrust produced per horsepower) increases directly with figure of merit. Thus, the higher the figure of merit, the less power required to hover with a given disc loading.

The relationship between disc loading, power loading, and figure of merit is shown in Figure 14.

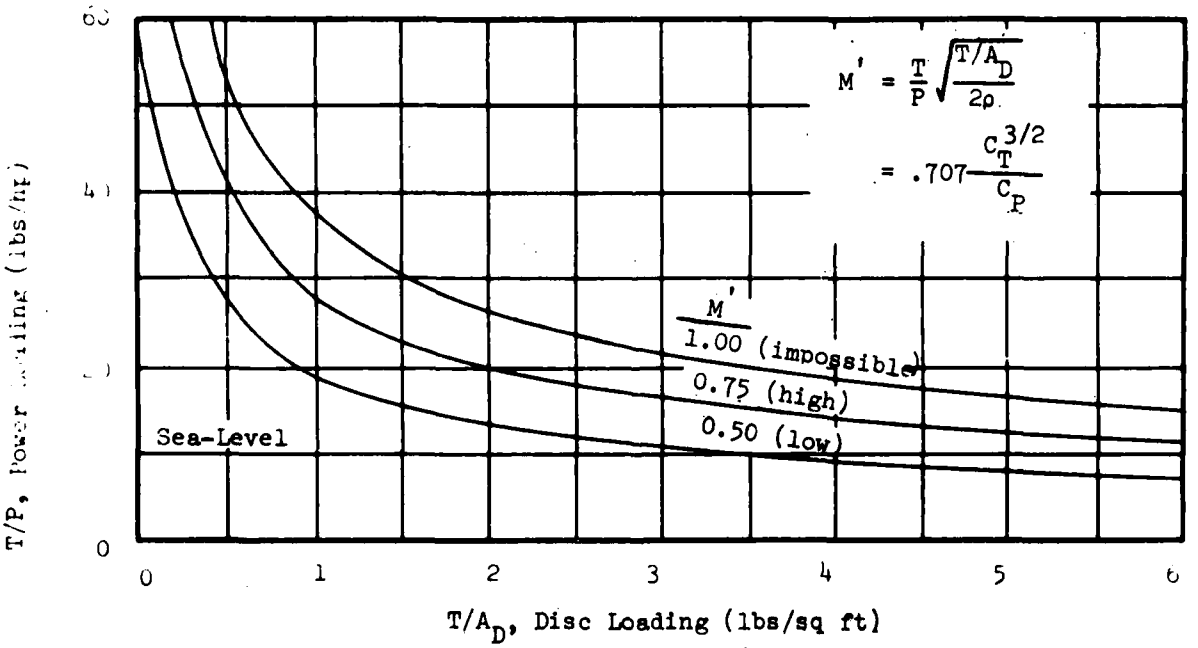

Figure 14
Figure of Merit

The ideal rotor power required to hover will be less than the actual (thus the figure of merit is a number less than unity) for two reasons. First, profile power is not considered and, second, the simple momentum analysis underpredicts the induced power because of losses incurred in a real situation.

Considering, for a moment, a rotor with profile drag but with induced velocity which does not vary with radius, the figure of merit is:

$$M' = \frac{P_i'}{P_i' + P_o} \qquad \text{if} \quad v_i \neq f(r)$$

which can be written in coefficient form as:

$$M' = \frac{\frac{C_T^{3/2}}{\sqrt{2}}}{\frac{C_T^{3/2}}{\sqrt{2}} + \frac{1}{8}\sigma_R \bar{C}_{d_o}} \qquad \text{if} \quad v_i \neq f(r)$$

For a particular rotor solidity (σ_R) and profile drag coefficient ($\bar{C}_{d_o}$), the figure of merit increases with increasing C_T. The reason being that as C_T increases and the induced power increases, the profile power becomes a relatively smaller portion of the denominator if $\bar{C}_{d_o} = \phi$ and the figure of merit approaches unity. This variation, which is not entirely typical of actual rotors, is shown in Figure 15. For an actual rotor, the distributing of induced velocity, which may vary with C_T, is not uniform and thus the figure of merit is less than that associated with uniform induced velocity. Furthermore, the increase of M' with C_T is limited

because at very high values of C_T the rising C_{d_o} will ultimately cause a reduction in figure of merit (see Figure 15).

Ground effect was shown to cause a reduction in power required to produce a given thrust and, therefore, will cause an increase in the figure of merit at a given C_T. The general effect is also shown in Figure 15.

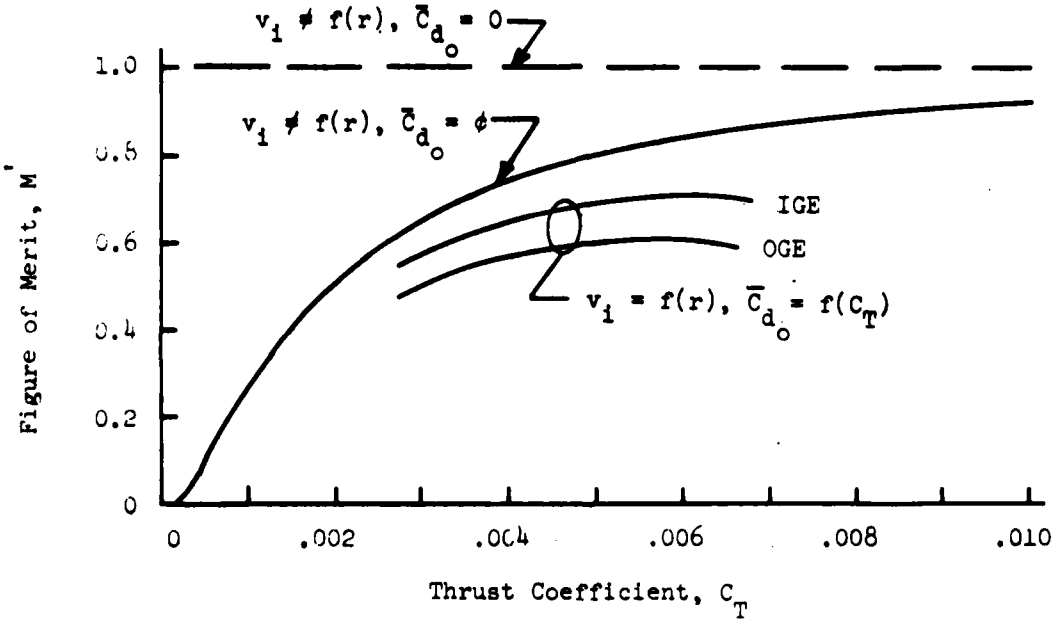

Figure 15
Effect of Thrust Coefficient on Figure of Merit

The figure of merit can be useful in making estimates of hovering performance. For instance, if enough information is known about a new design to establish the disc loading or the power loading, the other one can be optimistically estimated by assuming $M' = 1.0$. A more realistic estimate could be made by choosing a figure of merit more typical of machines of design similar to the one being analyzed.

The acutal value of the figure of merit depends on the physical design of a particular rotor and on the thrust coefficient at which it is operating. Values of M' can be generally classified as:

$M' = 1.0$, impossible (ideal)

$M' = .75$, good

$M' = .50$, poor

The value is somewhat meaningless as a measure of rotor performance because other design criteria may compromise the hover performance. Also, the figure of merit is really only a measure of the efficiency with which the rotor produces induced velocity, with no regard for the magnitude of the induced velocity. For example, consider a rotor design where the tip speed (ΩR), the average lift coefficient ($\bar{C}_\ell$) and the thrust ($T \approx W$) are prescribed values. For this case, increasing the disc loading may improve the figure of merit by operating the blades at a higher C_T, but the total power required to hover has increased (i.e., the power loading has decreased).

The fact that one rotor has a higher figure of merit than another is not sufficient to establish its relative superiority.

III. VERTICAL CLIMB ANALYSIS

The analysis of the helicopter in a vertical climb is a simple extension of hover analysis and although directed primarily at the main rotor, there may well be significant effects on the mechanical efficiency, η_m, and parasite drag which should be considered. The value of η_m changes as airspeed increases from zero due to decreases in tail rotor power required.

In hover, as in a stabilized climb, the main rotor thrust is equal to the aircraft weight plus airframe parasite drag resulting from rotor downwash. For small rates of climb, the parasite drag is essentially equal to that in hover, but may increase significantly at high rates of climb.

For simplicity, mechanical efficiency is assumed constant and parasite drag is assumed zero for the development of equations to follow.

A. ENERGY ANALYSIS

If the helicopter has power available in excess of that required to hover, this excess power may be utilized to produce climbing flight and change the potential energy of the helicopter. The excess power that is available to the main rotor in hover, ΔRSHP, is easily determined from hover tests as:

$$\Delta RSHP = RSHP_{avail} - RSHP_{req}$$

The power required to change the potential energy of a given weight, W, at a certain rate is:

$$P_{\Delta PE} = W\frac{dh}{dt}$$

This is simply the power that would be required to hoist the weight at a given rate. It is seen that corresponding to a certain excess rotor shaft horsepower in hover there is a specific climb rate which can be calculated as:

$$V' = \frac{\Delta RSHP(33000)}{W}$$

V' = uncorrected rate of climb (ft/min)

or, in terms of engine shaft horsepower:

$$V' = \frac{\Delta ESHP(\eta_m)33000}{W}$$

The uncorrected rate of climb, V', is the rate which would be produced only under the following conditions:

(1) If the main rotor induced power required is the same in the climb as in hover.

(2) If the main rotor profile power required is the same in the climb as in hover.

(3) If there is no loss in transmitting the excess rotor shaft horsepower to the air.

None of the above conditions are, in fact, true and as a consequence the uncorrected rate of climb, V', is not a realistic prediction of actual climb performance. However, corrections can be determined and applied to the uncorrected rate of climb, thus allowing closer prediction of true climb performance. To better understand what affects climb performance, the rotor in axial flight should be examined by momentum and blade element analyses.

B. MOMENTUM ANALYSIS

To determine the approximate effect of vertical velocity on the induced power of the main rotor, simple momentum analysis is used (recall the restrictive simplifying assumptions discussed on page II-10). An expression for the thrust produced by the actuator disc, T_v, in the presence of vertical velocity, V_v, is:

$$F = \dot{m}\Delta V$$

$$T_v = \rho A_D (V_v + v_{i_v})(2v_{i_v})$$

where $(V_v + v_{i_v})$ is the resultant flow rate through A_D. Rearranging

$$\frac{T_v}{2\rho A_D} = v_{i_v}(V_v + v_{i_v})$$

where V_v = corrected rate of climb

v_{i_v} = induced velocity in climb

Once the rate of climb is stabilized (vertical acceleration is zero), assuming parasite drag to be zero (a restrictive assumption the consequence of which will be observed), $T = W$ and $\frac{T_v}{2\rho A_D} = \frac{W}{2\rho A_D} = v_i^2$ where v_i is the induced velocity in hover. The above shows that the induced velocities in hover and climb are related by the rate of climb:

$$v_i^2 = v_{i_v}^2 + v_{i_v} V_v$$

or $$v_{i_v} = \sqrt{V_v/2^2 + v_i^2} - V_v/2$$

The resulting decrease in induced velocity in the presence of vertical velocity is obvious from the basic momentum equation $F = \dot{m}\Delta V$. Because a natural flow rate through the disc is established due to the vertical motion of the disc, less change in velocity need be imparted to the air to produce a given thrust.

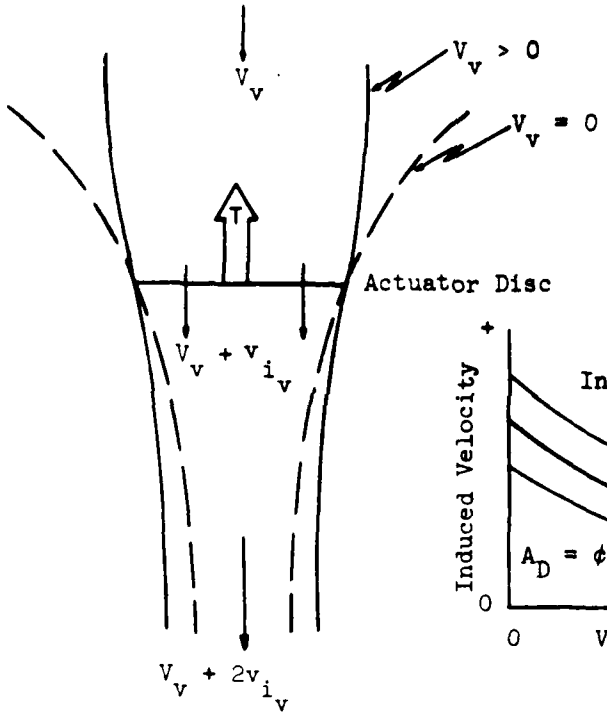

Figure 1
The Actuator Disc in Axial Flight

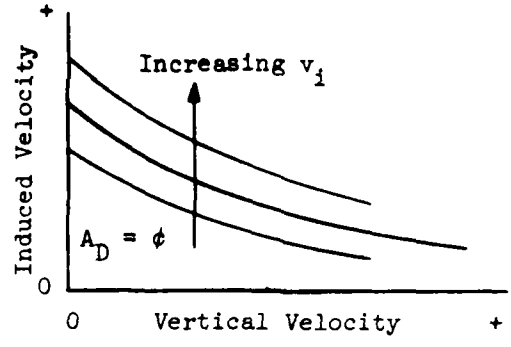

Figure 2
Variation of Induced Velocity

Note that the variation of induced velocity with vertical velocity depends on the value of induced velocity in hover (v_i) as shown in Figure 2. If the equation is divided by v_i a non-dimensional velocity ratio is produced which is dependent only on a non-dimensional vertical velocity:

$$\frac{v_{i_v}}{v_i} = -\frac{V_v/v_i}{2} + \sqrt{\left(\frac{V_v/v_i}{2}\right)^2 + 1}$$

where: $\frac{v_{i_v}}{v_i} \equiv$ non-dimensional induced velocity

$\frac{V_v}{v_i} \equiv$ non-dimensional vertical velocity

This form of the equation produces a single curve as shown in Figure 3.

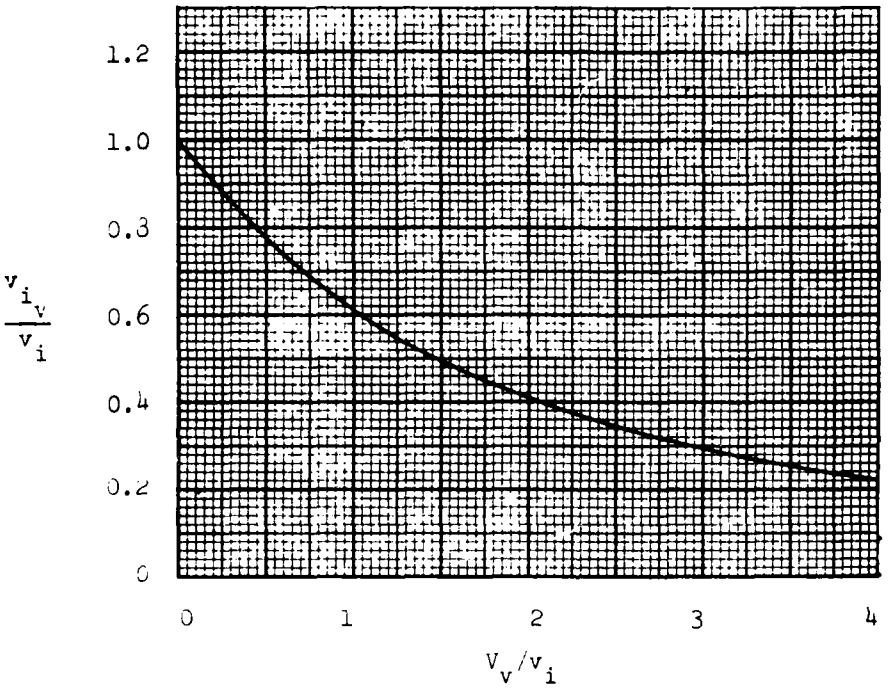

Figure 3
Non-Dimensional Induced Velocity in Climb

The gradient of the curve is - 1/2 at zero rate of climb implying relatively large reductions of induced power associated with small climb rates.

The power available to the main rotor is selected by the pilot and can be expressed as: $P_{avail} = P_{req} + P_{\Delta PE}$

where $P_{\Delta PE}$ is the power which can be used to produce a rate of climb

or $P_{avail} = P_p + P_o + P_i + P_{\Delta PE}$

Now, the predictable change in induced power developed above provides a means of making a correction to the power available to climb.

Considering a helicopter with a certain amount of power available:

$$P_{a_{hover}} = P_{a_{vert}}$$

$$P_{p_h} + P_{o_h} + P_{i_h} + P_{\Delta PE_h} = P_{p_v} + P_{o_v} + P_{i_v} + P_{\Delta PE_v}$$

Assuming $P_{p_h} = P_{p_v}$ and $P_{o_h} = P_{o_v}$ then

$$P_{i_h} + P_{\Delta PE_h} = P_{i_v} + P_{\Delta PE_v}$$

Expressing each excess power in terms of the vertical velocity that could be produced, and the induced power in terms of the induced velocity, then for a stabilized climb ($T \approx W$) considering ideal induced power:

$$W(v_i + V') = W(v_{i_v} + V_v)$$

Recall that v_i, v_{i_v} and V_v are related:

$$v_i^2 = v_{i_v}^2 + v_{i_v} V_v$$

Solving the two equations to eliminate v_{i_v}, which is unknown, results in the climb correction factor:

$$\frac{V_v}{V'} = 1 + \frac{1}{V'/v_i + 1}$$

where: $v_i \approx \sqrt{\frac{W}{2\rho A_D}}$, ideal hover induced velocity (known)

$V' = \frac{\Delta ESHP(\eta_m)33000}{W}$, uncorrected rate of climb (known)

V_v, corrected rate of climb (desired).

A plot of the climb correction factor is shown as Figure 2.

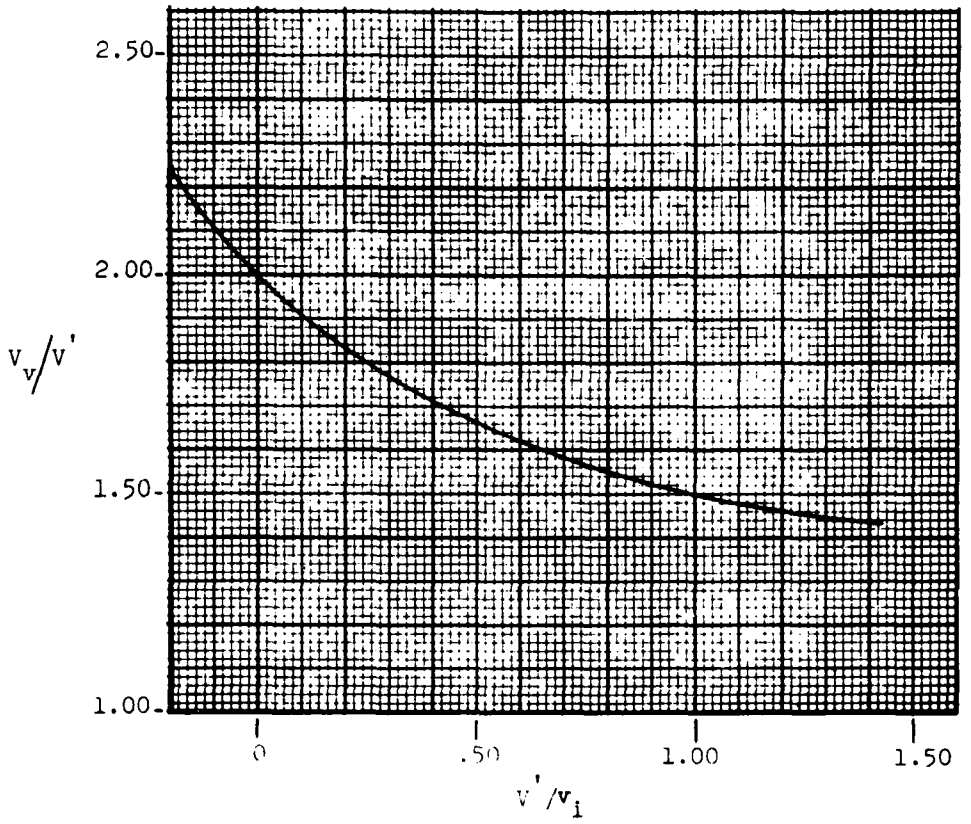

Figure 2
Vertical Climb Correction Factor

The induced power required to produce a certain thrust is less in climbing flight than in hover, and thus for a given engine power there is more excess power to produce the change in potential energy once the rotor is moving vertically than that observed in hover. The rate of climb calculated from hover excess power (the uncorrected rate of climb, V') can be

NAVY

corrected for the change in induced power by multiplying V' by the climb correction factor, V_v/V', obtained from Figure 2. Typical variations of both the corrected and uncorrected rates of climb are shown versus ΔESHP in Figure 3. It is seen that V' is considerably less than V_v and is essentially a linear function of ΔESHP if the variation of η_m is small.

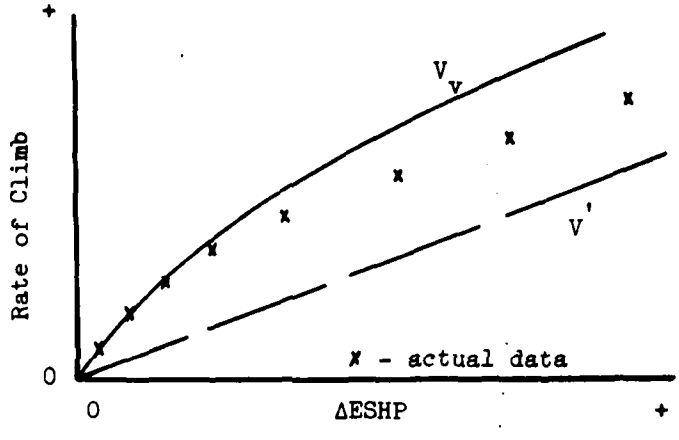

Figure 3
Variation of Rate of Climb with Excess Power

Notice that V_v is corrected only by considering an approximation to the change in induced power and the actual rate of climb will be less than the corrected rate due to:

(1) *Increase in parasite drag due to vertical velocity.*

(2) Imperfect transmission of excess power from rotor to air.

(3) Increases in profile drag, as observed in the blade element analysis.

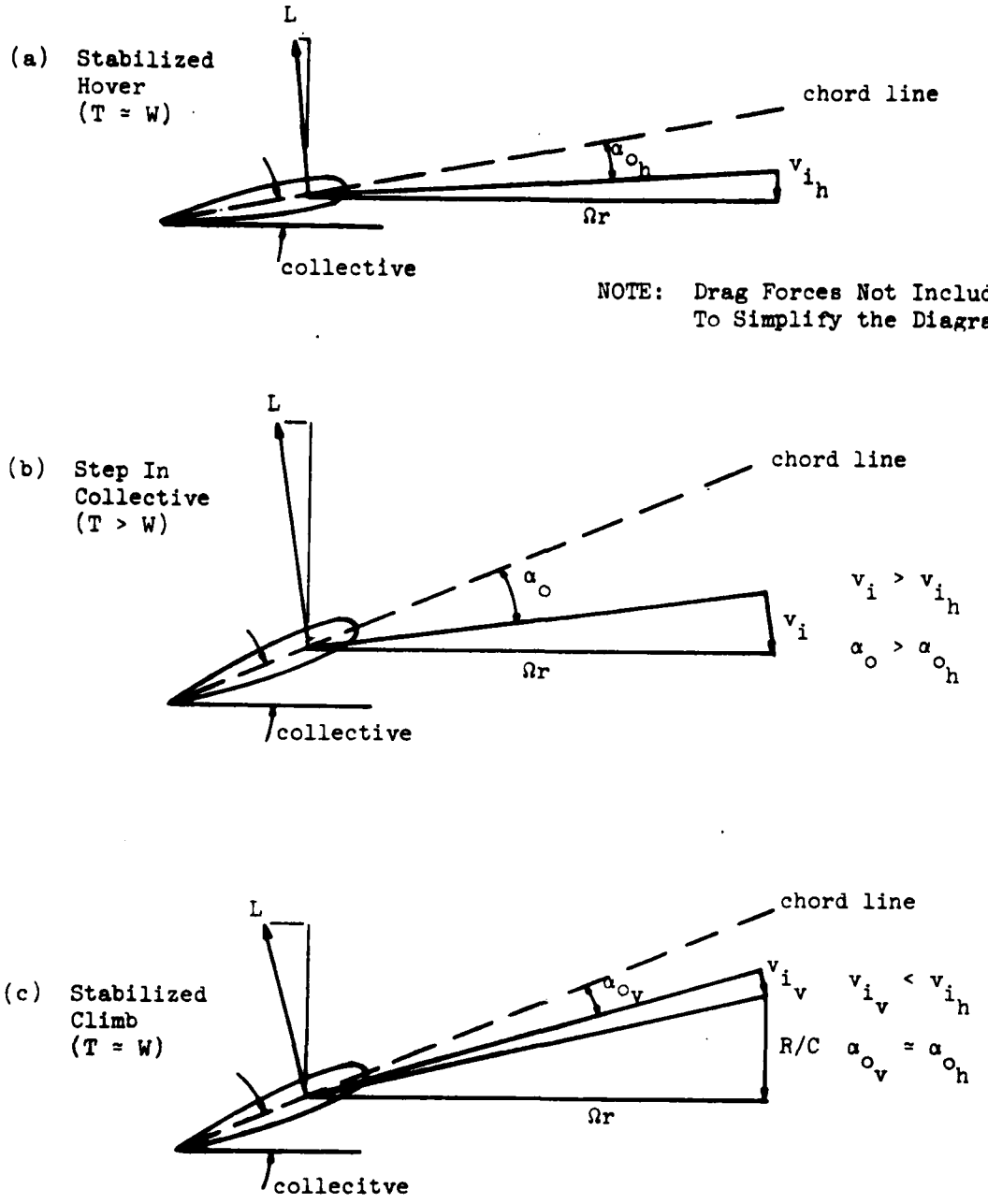

Figure 4
Blade Element in Hover and Vertical Climb

C. BLADE ELEMENT ANALYSIS

A typical blade element in hover is shown in Figure 4(a). If the blade pitch is increased from that required to hover, the blade section angle of attack is increased resulting in a larger aerodynamic reaction, increased lift, and increased induced velocity (Figure 4(b)). The unbalanced vertical force will cause the helicopter to accelerate upward thus producing a vertical velocity which must be added vectorially to the velocity due to rotation and the induced velocity to determine the element angle of attack. Thus, as the vertical velocity increases, the angle of attack decreases, decreasing the excess thrust and the acceleration. The vertical velocity will continue to increase, decreasing the angle of attack, until the excess thrust becomes zero and the rotor is in a stabilized climb, as shown in Figure 4(c). Momentum analysis showed that an increase in velocity of flow through the disc results in a given lift being produced with a smaller induced velocity. Although the decrease in the induced velocity results in a reduction in the induced power required, the effect of the climb velocity is to tip the lift vector such that there is an increase in the force component in the plane of rotation and thus an increase in the total power required in the climb.

Thus, the power required to produce a specified vertical force is greater in a sustained climb than in hover. The consequence of descent is considered in the Autorotation Section.

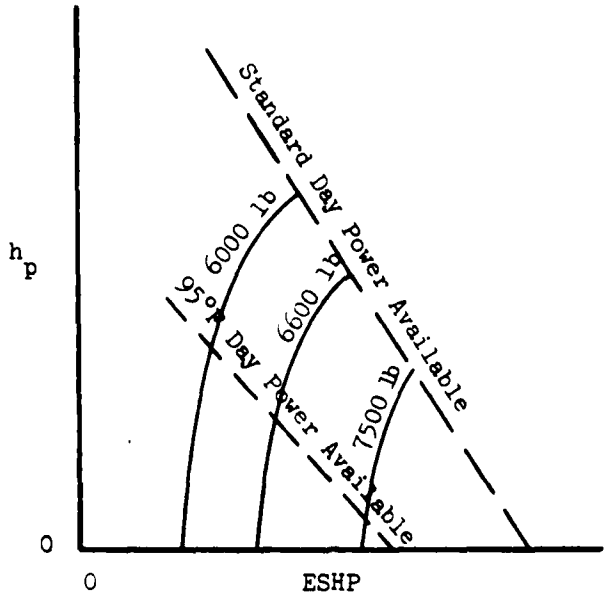

Figure 5
Variation of Excess Power

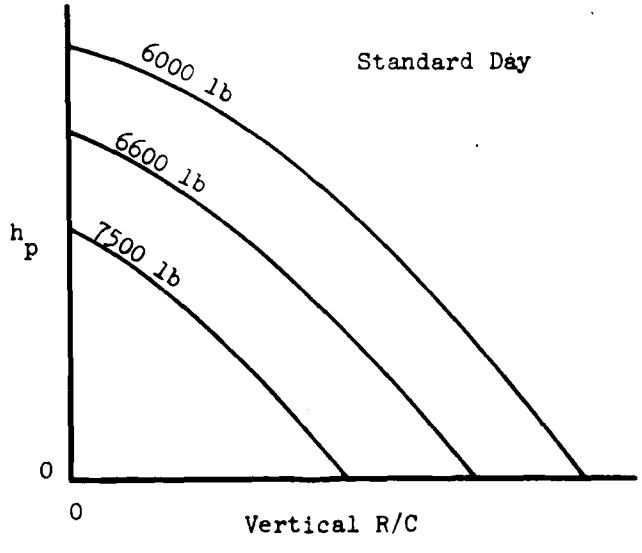

Figure 6
Variation of Vertical Rate of Climb

D. RATE OF CLIMB

The rate of climb capability of a helicopter has been shown to be related to the excess power in hover and, therefore, any variation in the power available (engine characteristic) or power required (airframe characteristic) will directly affect the climb performance.

Engine analysis shows the engine shaft horsepower available to be adversely affected by decreasing atmospheric density such that the power available is less at altitude than at sea-level, and, at a particular pressure altitude, is less on a hot day than on a cold day. These effects are shown in Figure 5 for a typical installation.

For a given helicopter, variations in power required to hover are due primarily to changes in induced power requirements. Results of momentum analysis show the induced power required will increase at higher altitudes and, at a particular altitude, will increase directly with the helicopter gross weight. These effects on power required are also displayed in Figure 5. Comparing power available and power required to hover at any altitude describes the excess power in hover and locates the hover ceiling, the altitude at which the excess power becomes zero.

The variation of excess power with altitude and gross weight will affect vertical climb performance, the results of which will be similar to Figure 6.

MARINES

IV. FORWARD FLIGHT ANALYSIS

As the helicopter proceeds from hover into forward flight, the total power requirement changes significantly due to the effect of translational velocity on the rotors and due to the variation of parasite drag with forward flight speed. A rigorous analysis of the rotor in forward flight is extremely difficult due to the velocity variation over the disc and is not warranted here; however, the major consequences of forward flight can be observed through relatively simple approximate solutions.

The total power required in forward flight is the sum of the power to overcome the following:

(a) Main rotor induced power

(b) Main rotor profile power

(c) Fuselage parasite power

(d) Miscellaneous power, including tail rotor power and mechanical losses.

The effect of forward flight on each of the above is discussed in the following sections.

A. INDUCED POWER

In hover, the total flow through the rotor is entirely induced and thus variations in induced velocity cause proportionate changes in the induced power required. As forward flight speed increases, the mass flow rate through the rotor increases due to its translation and the change in velocity required to produce a certain thrust, induced velocity, decreases.

Predicting the induced power requirements of the main rotor in forward flight becomes a more complicated problem than in hover and no theory

exists which enables the exact calculation of the induced velocity distribution over the rotor disc. Simple momentum theory can be used to estimate the variation of induced velocity and the effect of forward flight on induced power by considering the variation of an induced velocity which is the average over the disc, as was done for hover.

For momentum analysis, the mass flow affected by the rotor can be conveniently visualized, as shown by aerodynamic theory, to be that contained in a circular stream tube the diameter of which is that of the rotor (see Figure 1). In this analogy, the entire stream tube is experiencing the same induced velocity, v_{i_f}.

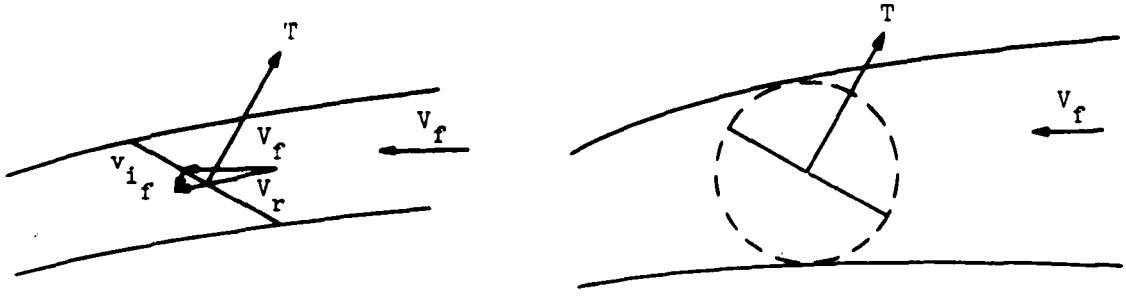

Figure 1
Rotor Stream Tube in Forward Flight

A velocity and force vector diagram of the rotor as visualized in forward flight (neglecting any vertical drag due to downwash) is shown in Figure 2. The vertical component of the induced velocity, v_{i_v}, is that required to produce a vertical force to support the weight of the aircraft, W.

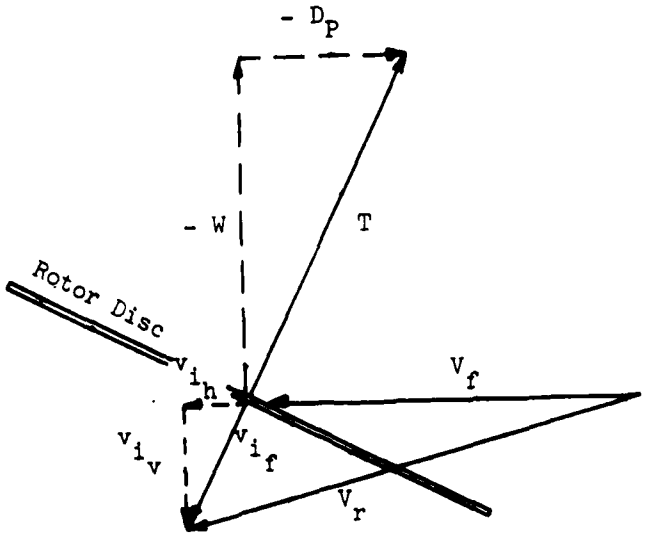

Figure 2
The Rotor as Visualized in Forward Flight

The power required to produce this component of induced velocity is defined here as the induced power in forward flight and will be analyzed by momentum analysis. The horizontal component of the induced velocity, v_{i_h}, is that required to produce a horizontal force to overcome the parasite drag of the aircraft and will be accounted for separately in the parasite power analysis. Thus, the momentum analysis of induced power is concerned only with the power required to produce a force opposite to W, and with the vertical component of the induced velocity, v_{i_v}.

As before, Newton's Law is used to relate the vertical force to the vertical induced velocity:

$$W = \rho A_D V_r \left(2 v_{i_v}\right)$$

where V_r is the resultant velocity through the rotor disc and can be expressed as:

$$V_r^2 \cong V_f^2 + v_{i_v}^2$$

Figure 2 shows that the above equation for V_r is exact only when D_p/W is zero or when v_{i_f} is equal to zero, but the error in the calculation of V_r will be small when $D_p/W \ll 1$ (i.e., at low forward flight speeds) and when $v_{i_f} \ll V_f$ (i.e., at high forward flight speeds).

From Newton's Law:

$$W = \rho A_D V_r \left(2v_{i_v}\right)$$

or

$$V_r v_{i_v} = \frac{W}{2\rho A_D} \cong v_i^2$$

and thus

$$v_{i_v} = \frac{v_i^2}{V_r}$$

showing the decrease with forward flight speed of the induced velocity required to support the aircraft weight.

To better display the dependence of v_{i_v} on forward flight speed, the approximate relationship previously defined between V_r and V_f is used, producing a quadratic equation in $v_{i_v}^2$, the solution of which is:

$$v_{i_v}^2 = -\frac{V_f^2}{2} + \sqrt{\left(\frac{V_f^2}{2}\right)^2 + v_i^4}$$

where only the positive radical has significance.

The effect on the relationship of the induced velocity in hover, v_i, can be eliminated to obtain a more general (non-dimensional) expression:

$$\frac{v_{i_V}}{v_i} = \left[-\frac{V_f^2/v_i^2}{2} + \sqrt{\left(\frac{V_f^2/v_i^2}{2}\right)^2 + 1} \right]^{1/2}$$

This variation is displayed graphically as Figure 3.

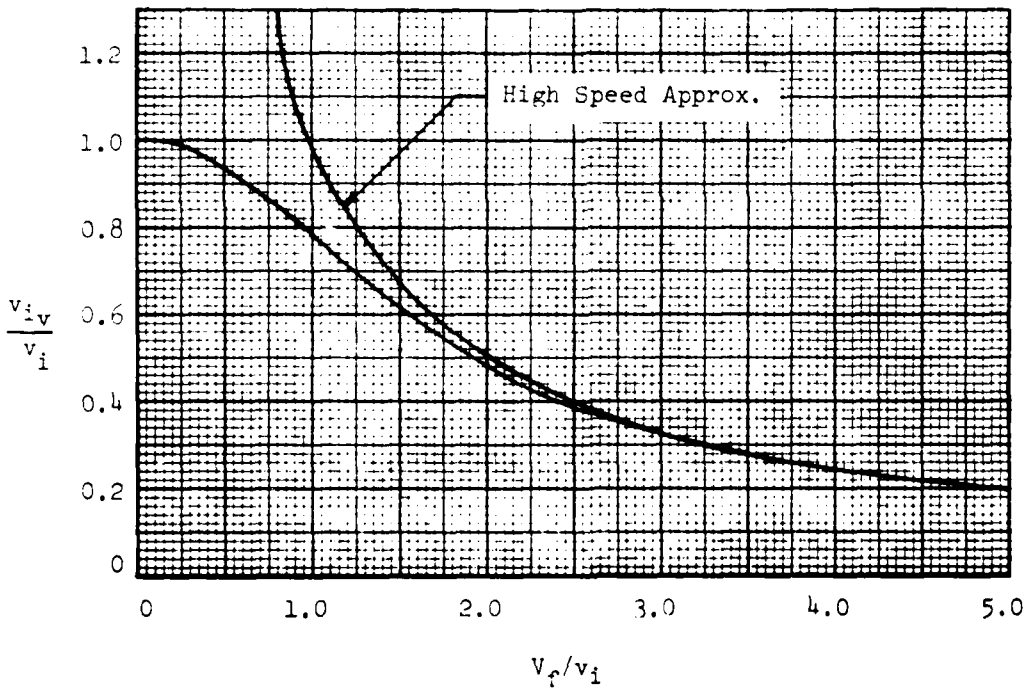

Figure 3
Effect of Forward Flight on Induced Velocity

The power required to support the weight of the aircraft, induced power, is the product of weight and induced velocity. The ratio of the induced power in forward flight, P_{i_f}, to that required in hover, P_i, is:

$$\frac{P_{i_f}}{P_i} = \frac{Wv_{i_v}}{Wv_i} = \frac{v_{i_v}}{v_i}$$

Thus, Figure 3 also represents the variation of the induced power requirement with forward flight speed, within the limitations of the analysis. Even though the simple momentum analysis underpredicts the induced power requirements (recall the restrictive assumptions), the application here is to predict variations or ratios which will be quite accurate.

At high forward flight speeds, momentum considerations indicate that the induced velocity will become very small, or:

$$V_r \simeq V_f$$

so that

$$v_{i_v} = \frac{v_i^2}{V_r} \simeq \frac{v_i^2}{V_f}$$

recalling that

$$v_i^2 \equiv \frac{W}{2\rho A_D}$$

the induced power required at high forward flight speed becomes:

$$P_{i_f} = Wv_{i_v} \simeq \frac{W^2}{2\rho A_D V_f}$$

Aerodynamic analysis of a fixed wing with uniform downwash (e = 1) shows the induced power to be:

$$P_i = \frac{W^2 V_f}{\pi ARqS} = \frac{W^2}{\frac{1}{2}\rho\pi b^2 V_f}$$

where b is the wing span. This result is the same as that for a rotary wing of the same span and with uniform downwash. This high speed approximation

shows that the induced power requirement of the rotary wing behaves like that of a fixed wing at high forward flight speeds, that is, decreases hyperbolically with increasing speed. The similarity fails at low forward flight speeds where the fixed wing theory indicates increasing induced power requirements, which is limited aerodynamically by stall, as speed decreases whereas the rotary wing induced power approaches that required in hover (see Figure 3).

B. PROFILE POWER

Having considered the influence of forward flight on the induced power of the main rotor by momentum analysis, blade element analysis is once again used to analyze the variation in profile power.

It should be emphasized that in the profile power analysis to follow, the section profile drag coefficient is replaced by an average coefficient ($\bar{C}_{d_o}$), as was done in hover analysis. If calculations are performed using a $\bar{C}_{d_o}$ based on relatively low angles of attack and sub-critical mach numbers, the evaluation may be grossly in error for other conditions of operation such as may occur in forward flight (see Power Corrections Section).

For small induced angles, the element profile drag force lies essentially in the rotor plane of rotation and the profile power required for "b" blades can be expressed as

$$P_o = b\int_o^R (dD_o)V_e = b\int_o^R C_{d_o} \frac{1}{2}\rho V_e^3 c\,dr$$

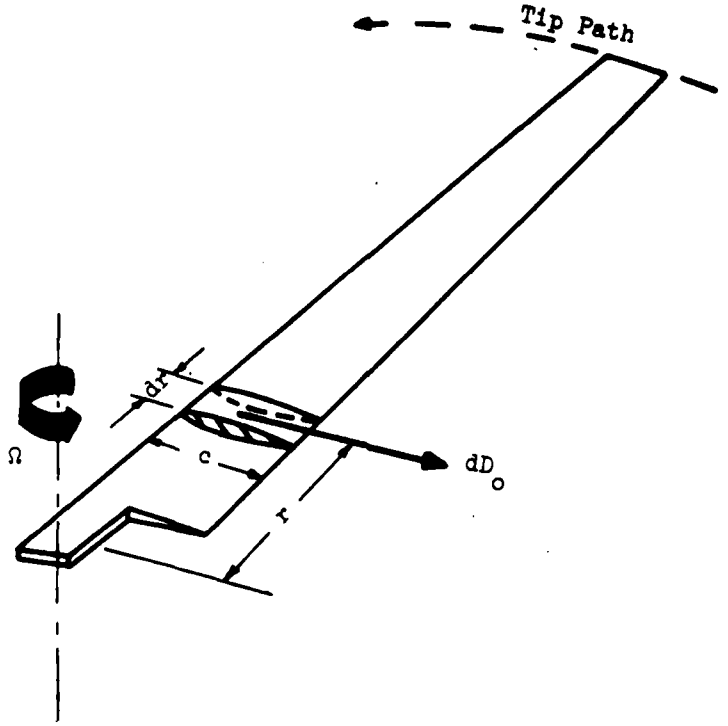

Figure 4
Rotor Blade Element Profile Drag

In hover, the element velocity (V_e) is simply the linear velocity due to rotation, for small induced angles, and is

$$V_e = \Omega r$$

Thus the profile power in hover is

$$P_o = \frac{1}{8}\sigma_R \bar{C}_{d_o} \rho A_D (\Omega R)^3$$

In forward flight, the element velocity vector ($\vec{V_e}$) is the resultant of the velocity due to rotation and the forward flight velocity, V_f,

$$\vec{V_e} = \vec{\Omega r} + \vec{V_f}$$

which results in a cyclic variation of element velocity with respect to the air mass as shown in Figure 5 for the blade tip, as an example.

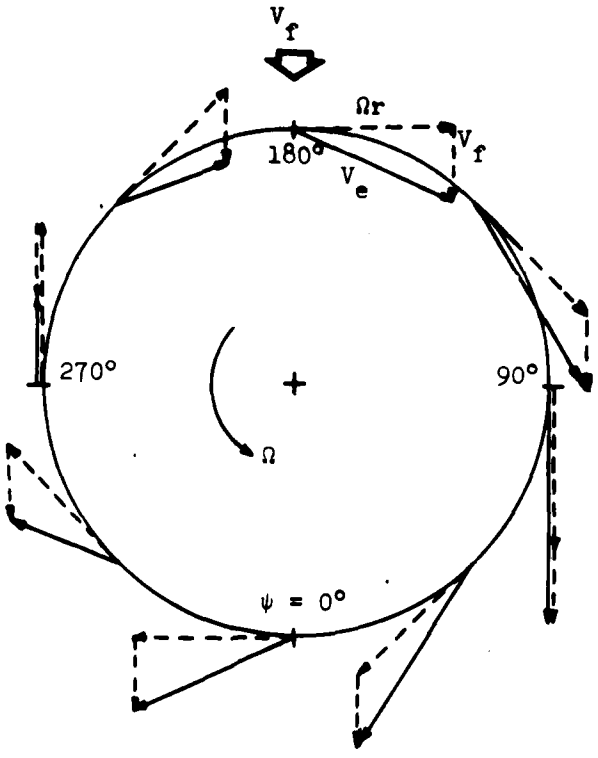

Figure 5
Velocity of Air Relative to Rotor Tip

The torque created about the rotor shaft results from the profile drag forces produced by the component of $\vec{V}_e$ normal to the rotor blade (chordwise). For this reason, the element velocity considered for profile power analysis is the chordwise component:

$$V_e = \Omega r + V_f \sin \psi$$

where ψ is the blade azimuth angle measured in the direction of rotor rotation from downwind (see Figure 6). The influence of the component of V_e parallel to the rotor blade (spanwise) will be considered later.

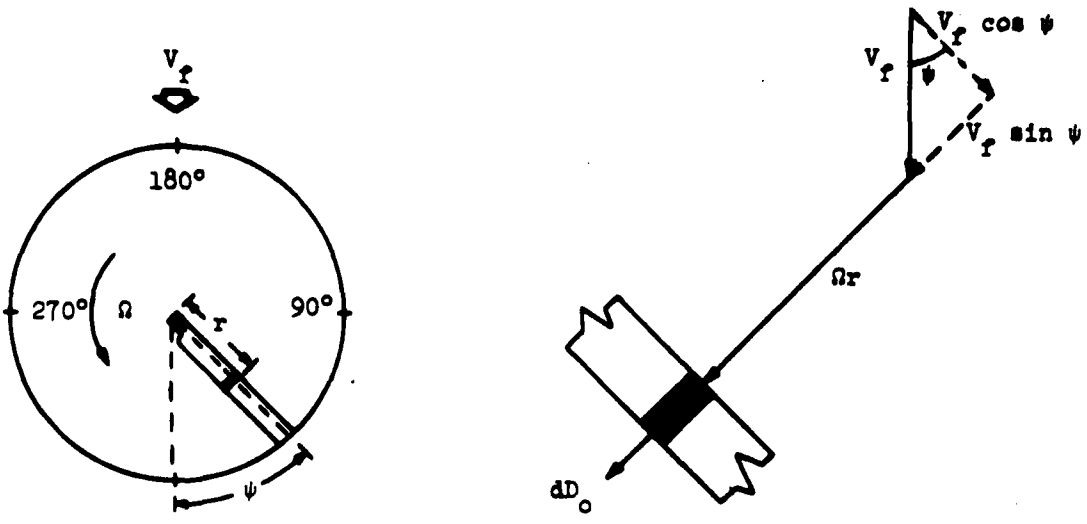

Figure 6
Element Chordwise Velocity

The profile power of a given element is

$$dP_{o_f} = dD_o V_e = C_{d_o} \frac{1}{2} \rho V_e^3 c dr$$

$$= C_{d_o} \frac{1}{2} \rho (\Omega r + V_f \sin \psi)^3 c dr$$

Notice that as a given element changes azimuth, the power to overcome profile drag changes. Considering the profile drag coefficient constant, the power required to drive an element varies directly as the cube of velocity and thus the element profile power varies with azimuth (see Figure 7). The average power required around the azimuth for a single element can be expressed as

$$d\bar{P}_{o_f} \equiv \frac{1}{2\pi} \int_o^{2\pi} dP_{o_f} d\psi$$

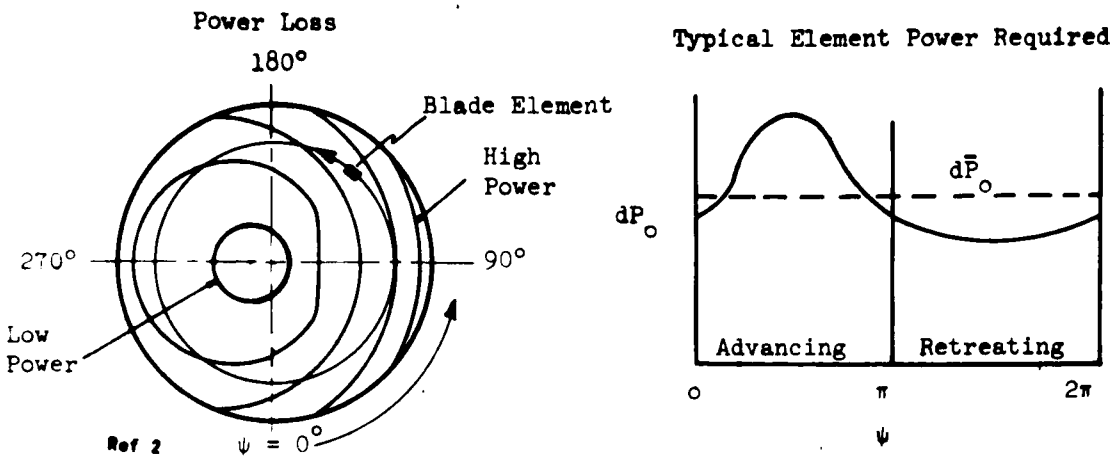

Figure 7
Variation of Profile Power Required with Azimuth

and the profile power of the entire rotor with "b" blades is

$$P_{o_f} = b\int_o^R d\bar{P}_{o_f} = \frac{b}{2\pi}\int_o^R\int_o^{2\pi} dP_{o_f}\, d\psi$$

$$P_{o_f} = \frac{b}{2\pi}\int_o^R\int_o^{2\pi} C_{d_o}\frac{1}{2}\rho(\Omega r + V_f \sin\psi)^3 c\, dr\, d\psi$$

Evaluation of this integral produces the main rotor profile power required:

$$P_{o_f} = \frac{1}{8}\sigma_R \tilde{C}_{d_o}\rho A_D(\Omega R)^3(1 + 3\mu^2)$$

where

$$\mu \equiv \frac{V_f}{\Omega R}$$

The profile power in forward flight is seen to increase with the tip speed ratio squared over that for hover. This increase can be expressed in percent of hover profile power, P_o, as

$$\frac{P_{o_f}}{P_o} = 1 + 3\mu^2$$

However, this analysis has been oversimplified and a more accurate estimate of the rotor power required must consider the items discussed in the following paragraphs.

Rotor H-Forces

The dissymmetry of local velocity on the rotor in forward flight shown in Figure 5 causes a corresponding variation in local drag force. For convenience, the local velocity is resolved into chordwise and spanwise components and the drag force due to each component is considered separately.

The H_1 force is a consequence of the chordwise velocity component and represents the summation of element profile drag forces parallel to the blade chord. In hover the H_1 force is zero but in forward flight, because of a lack of symmetry of the chordwise velocities, there is a difference in the advancing (high velocity) and the retreating (low velocity) blade chordwise drag forces (see Figure 8a). This asymmetrical variation of the chordwise profile drag force in forward flight results in two effects: (1) An increased torque requirement, which cause a power requirement of $P_o (\mu^2)$, and ; (2) The generation of a rotor hub sheer force, H_1, which has associated with it, a power requirement of $P_o (2\mu^2)$.

The H_1 force is a result of viscous drag due to chordwise flow. This flow was considered in determining the rotor profile power in forward flight and resulted in an increased power required from both of the above effects, or:

$$P_{o_f} = P_o(1 + 3\mu^2)$$

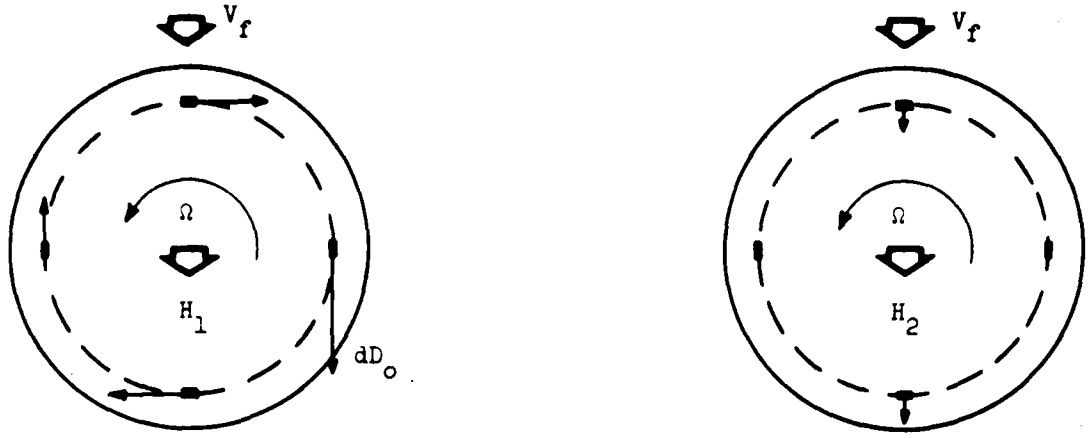

Figure 8
Rotor H Forces

The H_2 force is a result of viscous drag due to the spanwise (radial) flow and was neglected in the determination of profile power. The consequence of this flow is the generation of an additional rotor shear force in the downstream direction (see Figure 8b) and an associated increase in power required due to forward flight of approximately 55%. This effect can be included by expressing the profile power in forward flight as

$$P_{o_f} = P_o(1 + 4.65\mu^2)$$

Region of Reverse Flow

The blade element chordwise velocity is

$$V_e = \Omega r + V_f \sin \psi$$

On the retreating side (ψ from 180° to 360°) the two components subtract such that there exist a region where the local velocity is reverse, or

from the rear of the airfoil section (see Figure 9). The radius at which

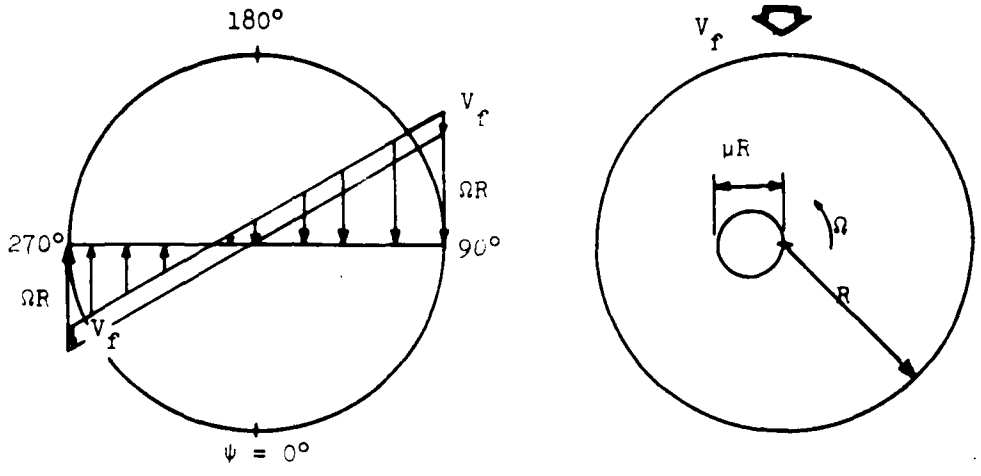

Figure 9
Region of Reverse Flow

the resultant is zero, r_o, represents the boundary of the reverse flow region and can be determined by setting V_e equal zero:

$$r_o = - \frac{V_f}{\Omega} \sin \psi$$

or, in percent of rotor radius,

$$\frac{r_o}{R} = - \mu \sin \psi$$

Thus, the reverse flow region is contained in a circular area on the retreating blade side. The percent of the blade experiencing reverse flow at 270° azimuth is equal to the tip speed ratio, μ.

The actual flow situation that exists in and around the reverse flow region is quite complex considering the aerodynamics of the section

in reverse and the large excursions in local angle of attack which will occur.

To estimate the effect of reverse flow on profile power, recall that the element power is a function of element velocity cubed so that in the region where the local velocity is negative, the power required would be negative (i.e., the blade is being driven by the drag force). Because no effort was made to avoid this negative power region in the power integral, the solution previously derived considered the blade to be as effective in extracting power from the air when in reverse flow as in adding power to the air when in forward flow. The amount of negative power required which the integration inherently considered can be evaluated by integration of the reverse flow region and is $P_o\ (3/8\ \mu^4)$. This term is obviously a very small portion of the profile power expression and, therefore, power corrections are seldom applied for reverse flow.

The resulting expression for profile power in forward flight, considering no correction to the reverse flow region, is:

$$P_{o_f} = \frac{1}{8}\sigma_R \bar{C}_{d_o} \rho A_D (\Omega R)^3 (1 + 4.65\mu^2)$$

C. PARASITE POWER

As the helicopter proceeds into forward flight, drag forces are created on the fuselage, rotor mast and hub, gear, etc, due primarily to base pressure drag and, to a smaller extent, to skin friction drag. For a helicopter, this aerodynamic drag must be overcome by the main rotor and must be considered in determining main rotor power required.

The parasite drag can be expressed as:

$$D_p = C_{D_p} qS$$

where S is the chosen reference area and C_{D_p} is the parasite drag coefficient. The value of C_{D_p} for a particular full-scale configuration and reference area depends primarily on fuselage attitude with respect to the freestream. Consider an example of an object experiencing a parasite drag, D_p, at a dynamic pressure, q. The drag coefficient to define this situation depends on the choice of reference area, which choice may be quite arbitrary since the parasite drag is not entirely dependent upon any particular body area. Once a reference area is chosen there is a unique drag coefficient but what is really specified by the physical situation is the product of C_D and S. To avoid this quandry of choice of reference area and the dependence of C_D on that choice, the equivalent flat plate area, f, is often used, where

$$f \equiv C_{D_p} S = \frac{D_p}{q}$$

The value of f for a particular machine will vary depending on the free-stream direction. Once f is defined by model or full-scale testing the parasite drag coefficient corresponding to any convenient reference area, S, can be determined:

$$C_{D_p} = \frac{f}{S}$$

If the reference area chosen is disc area: $D_p = C_{D_p} qA_D$.

The induced power analysis presented in Section IVA considered only the vertical component of induced velocity, v_{i_v}, in the determination of induced power. The horizontal component, v_{i_h} (see page IV-3), results from the requirement to provide a horizontal force to overcome parasite drag for equilibrium flight. The relative importance of the horizontal induced effects can be considered by applying simple momentum analysis along the horizontal axis:

$$\dot{m}\Delta V = F$$

$$\rho A_D V_r (2v_{i_h}) = D_p = C_{D_p} \frac{1}{2} \rho V_f^2 A_D$$

where the parasite drag coefficient has been based on the rotor disc area. Solving for v_{i_h}:

$$v_{i_h} = \frac{C_{D_p}}{4} \frac{V_f^2}{V_r}$$

The velocity V_r is the resultant through the disc and for high speed ($v_{i_v} \to 0$)

$$V_r \approx V_f + v_{i_h}$$

Eliminating V_r from the above equations produces a quadratic equation in v_{i_h}, the solution of which is:

$$v_{i_h} = \frac{1}{2}(\sqrt{C_{D_p} + 1} - 1)V_f$$

This shows that although v_{i_h} increases with forward flight speed, for most helicopters $C_{D_p} < .04$ and, therefore, $v_{i_h} < .01\ V_f$.

The power required to create a force equal to D_p is:

$$P_p = D_p(v_{i_h} + V_f)$$

and at high speed, where $V_f >> v_{i_h}$:

$$P_p \simeq D_p V_f$$

Thus, the parasite power term can be expressed as:

$$P_p = C_{D_p} q A_D V_f = \frac{1}{2}\rho V_f^3 C_{D_p} A_D$$

or

$$P_p = f q V_f = \frac{1}{2}\rho V_f^3 f$$

D. MISCELLANEOUS POWER

The previous paragraphs have discussed power which the engine must provide to the main rotor shaft (RSHP). In addition, the total engine shaft shorsepower (ESHP) must be sufficient to supply power to the tail rotor and accessories as well as, to overcome transmission losses. The power required in excess of RSHP is referred to as miscellaneous power and is expressed in percent of ESHP as $1 - \eta_m$, where $\eta_m \equiv$ RSHP/ESHP.

The power required to drive the accessories remains fairly constant with normal system loads, where as the transmission load remains a fairly constant percent of RSHP.

The major consequence of forward flight on the tail rotor is the reduction of the tail rotor induced power required to produce a given thrust, as observed previously for the main rotor. Therefore, the tail rotor power required to balance a certain main rotor torque will decrease

with increasing forward flight speed and result in an increase in mechanical efficiency.

E. TOTAL POWER REQUIRED

The total engine power required (P_E) for equilibrium in forward flight is the main rotor power (P_{MR}) plus the miscellaneous power or, in terms of mechanical efficiency,

$$P_E = \frac{1}{\eta_m} P_{MR}$$

The main rotor power is the summation of the induced, profile and parasite power:

$$P_{MR} = P_i + P_o + P_p$$

From the expressions developed above:

$$P_{MR} = \frac{W^2}{2\rho A_D V_f} + \frac{1}{8}\sigma_R \bar{C}_{d_o} \rho A_D (\Omega R)^3 (1 + 4.65\mu^2) + \frac{1}{2}\rho V_f^3 f$$

where the high speed approximation for induced power has been used. This variation, including the miscellaneous power, is shown in Figure 10. Note the failure of the high speed approximation at low speeds.

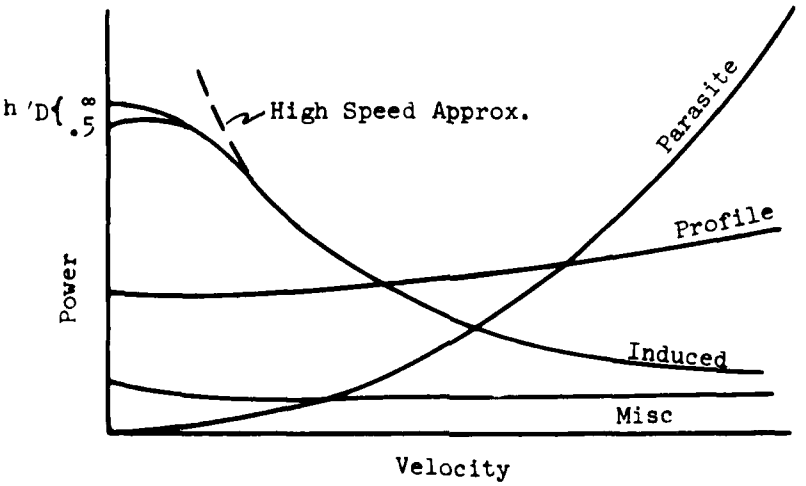

Figure 10
Power Required in Forward Flight

Ground effect, which varies as a function of h/D, is apparent in the power required to hover. As the helicopter proceeds into forward flight, the rotor wake strikes the ground at a angle behind the helicopter and the ground effect diminishes.

To express the power required in terms of the non-dimensional coefficients, the above equation is divided by $\rho A_D(\Omega R)^3$:

$$C_{P_{MR}} = \frac{C_T^2}{2\mu} + \frac{1}{8}\sigma_R \bar{C}_{d_o}(1 + 4.65\mu^2) + \frac{1}{2}C_{D_p}\mu^3$$

For a particular helicopter, the following are constant (with limitations):

$\sigma_R \equiv \frac{bc}{\pi R}$

$\bar{C}_{d_o}$ - (will vary at high section angle of attack or Mach number)

C_{D_p} - (depends on attitude and external configuration)

Within the limitations mentioned above: $C_P = f(C_T, \mu)$

and forward flight power required data can be generalized as shown in Figure 11.

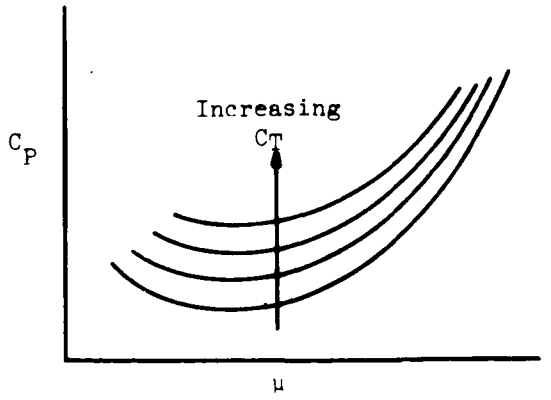

Figure 11
Forward Flight Generalized Power Required

F. FORWARD FLIGHT CLIMBS

The effect of vertical climb and forward flight on the induced velocity, and thus on induced power, have been individually examined by simple momentum theory. By a similar development, the induced power variation can be approximately determined for an actuator disc subjected to both forward flight velocity (V_f) and vertical velocity (V_v). From simple momentum analysis, assuming the vertical force produced by the disc is equal to the aircraft weight (neglecting vertical drag):

$$W = \rho A_D V_r (2 v_{i_v})$$

where v_{i_v} is the vertical component of induced velocity at the disc and

$$V_r \equiv \sqrt{V_f^2 + (V_v + v_{i_v})^2}$$

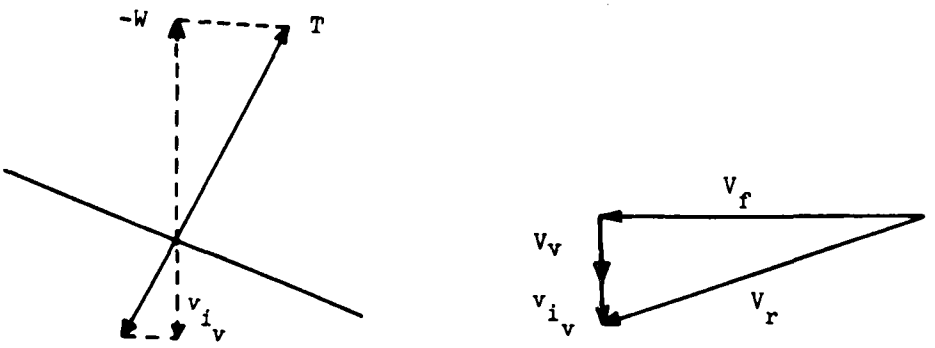

Figure 12
Actuator Disc In Forward Flight Climb

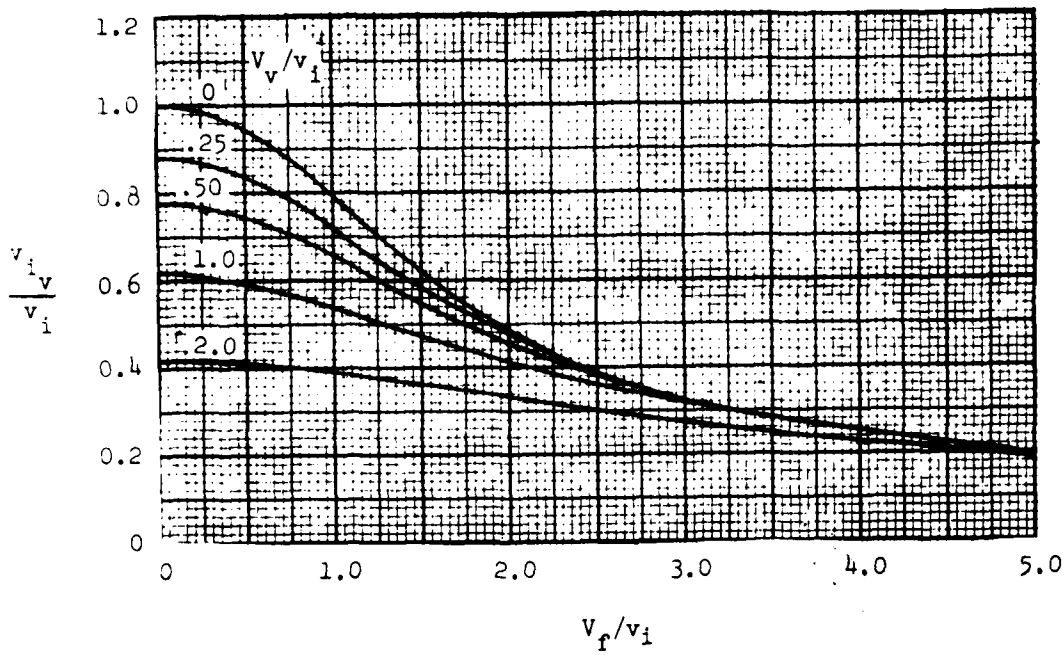

Figure 13
Induced Velocity in Forward Flight Climb

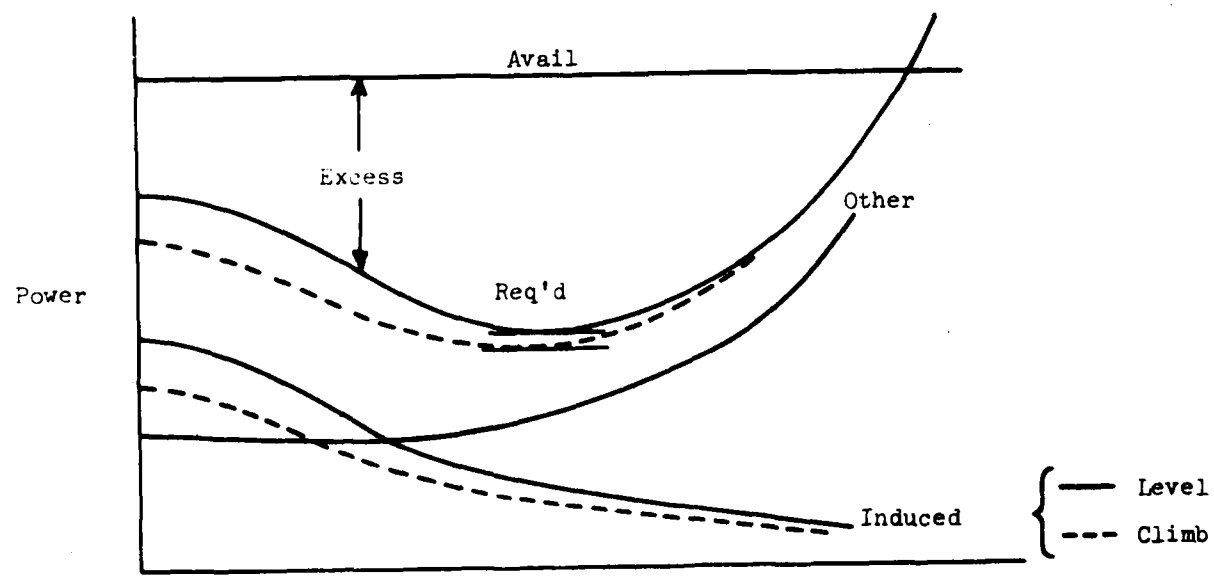

Figure 14
Excess Power in Forward Flight Climb

Using these relationships and recalling that the induced velocity in the absence of any translational velocity (hover) is

$$v_i \equiv \sqrt{\frac{W}{2\rho A_D}}$$

produces the following:

$$v_i^2 = v_{i_v} \sqrt{V_f^2 + (V_v + v_{i_v})^2}$$

which can be rearranged into non-dimensional form as

$$\frac{v_i}{v_{i_v}} = \sqrt{\left(\frac{V_f}{v_i}\right)^2 + \left(\frac{V_v}{v_i} + \frac{v_{i_v}}{v_i}\right)^2}$$

The reduction of induced velocity as a result of climbing can be compared to the level flight results as shown in Figure 13. Assuming the vertical force equal to the weight, the above ratio is also that of the induced power. Considering a specified amount of maximum power available, the power available to climb will be more than the excess power in level flight (as was also observed in the vertical climb analysis) the difference being most significant at low forward speeds. This effect is shown in Figure 14 which considers only induced power to vary with climb speed and also shows that the speed for maximum power to climb changes because of this effect. If the reduction of induced power is sizable, the forward speed for maximum rate of climb will be significantly slower than that for maximum excess power in level flight.

The equation derived for induced velocity ratio is that of a circle, the center of which is at

$$\frac{V_v}{v_i} = -\frac{v_{i_v}}{v_i}, \qquad \frac{V_f}{v_i} = 0$$

and of radius v_i/v_{i_v} suggesting another method to conveniently show the variation. These idealized circles are shown in Figure 15 for various induced velocity ratios and will be compared to empirical results later (see Power Correction Section). Figure 15 provides a simple manner to determine the variation of induced velocity and thus induced power as predicted by the idealized simple momentum analysis.

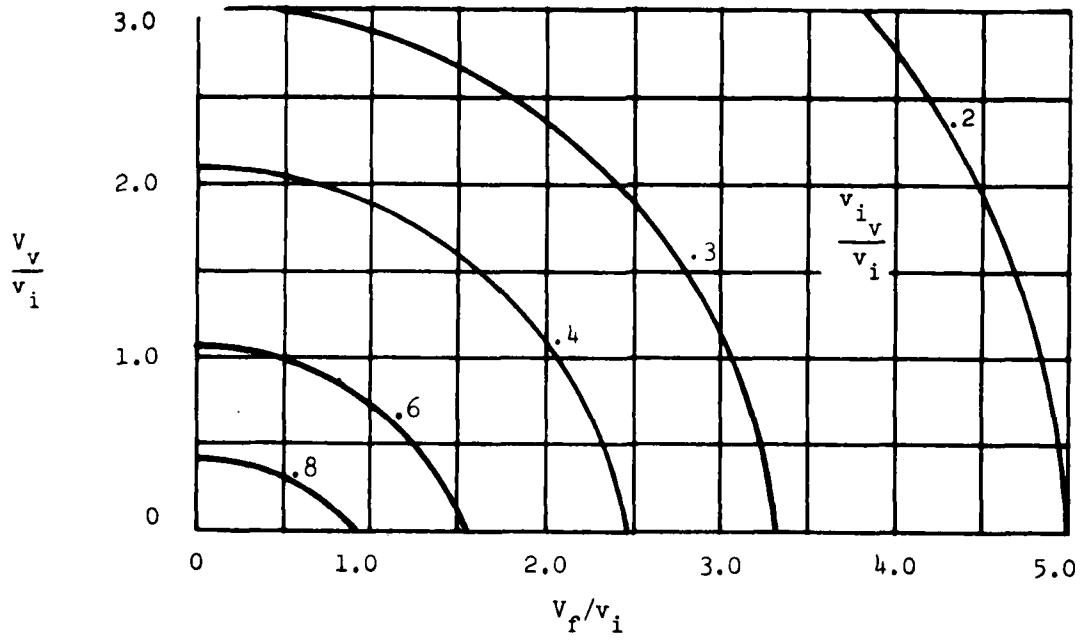

Figure 15
Idealized Variation of Induced Velocity

V. DESCENT AND AUTOROTATION

In each of the flight conditions considered previously, engine power has been required to drive the rotor against the aerodynamic forces generated in the plane of rotation by the lifting rotor. If engine power were not available to apply torque to the main rotor, RPM could not be maintained. Under certain descent conditions the lifting rotor can be driven in rotation and the RPM can be self-sustained (autorotation) by aerodynamic forces on the blades in much the same manner by which airspeed is maintained for a fixed wing aircraft in a power-off descent. Because autorotative flight provides a means of descending in the event of engine failure, the helicopter transmission is so constructed that the rotor is "free wheeling" and does not drive the engine. However, power must be supplied by the rotor to overcome frictional losses and to drive the tail rotor and accessories.

To simplify the analysis the rotor is first considered in axial flight, which avoids the dissymmetry of conditions on the disc associated with translational flight. Also, it is recognized that the usual rates of descent are much smaller than the rotor blade tip speed so that, as an approximation, the local velocity on the blade is essentially that due to rotation.

A. ENERGY ANALYSIS

In autorotation, when no engine power is available, the power supplied to the main rotor must result in an equivalent reduction of

either the potential energy of the helicopter (descent) or the kinetic energy of the rotor (decreasing RPM). During a constant RPM descent the power required is equal to the time rate of change of potential energy:

$$P = \frac{d(PE)}{dt} = W \frac{dh}{dt} = W V_v$$

or, the rate of descent (V_v) is: $V_v = \frac{P}{W}$

The main rotor power required can be approximated as:

$$P_{MR} = \frac{1}{8} \sigma_R \bar{C}_D \rho A_D (\Omega R)^3$$

where $\bar{C}_D$ is the average three dimensional drag coefficient composed of both profile and induced effects. If the fuselage vertical drag is neglected as being small, thrust is equal to weight for a constant rate of descent and

$$W = T = \frac{1}{6} \sigma_R \bar{C}_L \rho A_D (\Omega R)^2$$

Solving for the rotor tip speed for equilibrium produces:

$$\Omega R = \sqrt{\frac{6W}{\sigma_R \bar{C}_L \rho A_D}}$$

Using the expressions for P_{MR} and ΩR, the rate of descent is

$$V_v = \frac{P}{W} = \frac{\bar{C}_D}{8} \left(\frac{6}{\bar{C}_L}\right)^{3/2} \sqrt{\frac{W/\rho}{\sigma_R A_D}}$$

or, for a particular rotor,

$$V_v = \phi \frac{\bar{C}_D}{\bar{C}_L^{3/2}} \sqrt{\frac{W}{\sigma}}$$

For a given gross weight and density altitude, the rate of descent varies inversely with the ratio of $\bar{C}_L^{3/2}$ to $\bar{C}_D$, which is a function of the blade angle of attack. The aerodynamic relationships are best seen by blade element analysis.

B. BLADE ELEMENT ANALYSIS

This analysis approaches the problem by examining a discrete element, or section, of the rotor blade. Although local flow conditions, blade geometry and aerodynamic forces may well change with radial position, the general situation can be presented by analyzing an "average" blade element which may be thought of as representing the average conditions across the blade.

The conditions under which the rotor must operate for self-sustained RPM can be determined by observing the origin of the forces in the plane of rotation. In hover, for instance, the velocity of the air approaching the blade is in the plane of rotation and produces the resultant aerodynamic force R which is not normal to the velocity because of : (1) induced effects producing induced drag, and (2) viscous effects producing profile drag. The inclination of R with respect to the rotor plane of rotation produces a component of R in that plane and in this case, a decelerating torque must be overcome by the engine to sustain RPM.

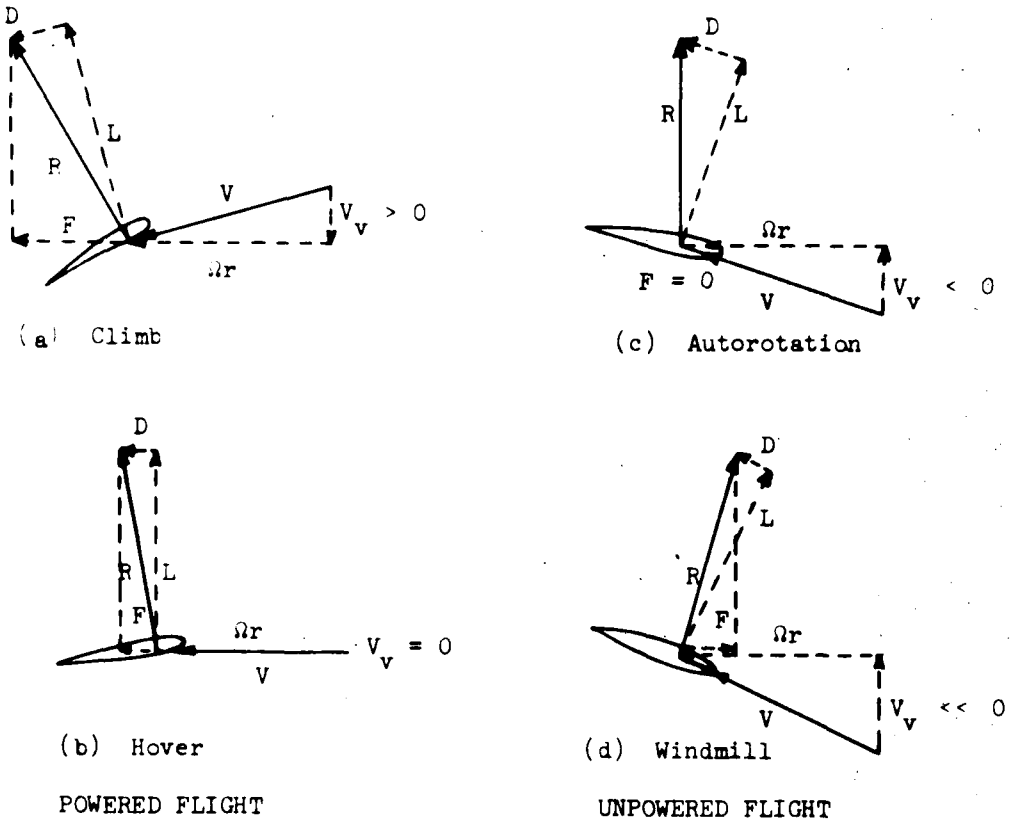

Figure 1
Axial Flight States of the Rotor

Next, consider a vertical climb. The change in direction of the velocity approaching the blade changes the direction of R in a corresponding manner such that the component of R in the plane of rotation increases, explaining the increase in power required to climb. On the other hand, if the rotor descends R is tipped forward as the descent velocity increases, reducing the power required and ultimately, at a high enough descent rate, producing a component in the plane of rotation which will actually make power available from the windmilling rotor.

Autorotation is the state at moderate rates of descent when the resultant aerodynamic reaction, as an average across the blade, is normal to the rotor plane of rotation and the rotor is in equilibrium with zero power required. In stabilized autorotation, the resultant aerodynamic force of the average blade element is normal to the plane of rotation. Actually, the local angle of attack changes across the blade because of the variation in Ωr, resulting in the sections of the blade near the hub producing "driving" forces in the plane of rotation (windmilling) and sections near the tip have "dragging" forces in the plane of rotation (absorbing the power made available by the inboard sections). This variation is shown in Figure 2.

The inclination of the resultant aerodynamic force with respect to the rotor's plane of rotation is dependent upon: (1) the angle at which the velocity is approaching the rotor disc, ϕ, and (2) the angle between a normal to the velocity and the resultant force, ϕ'.

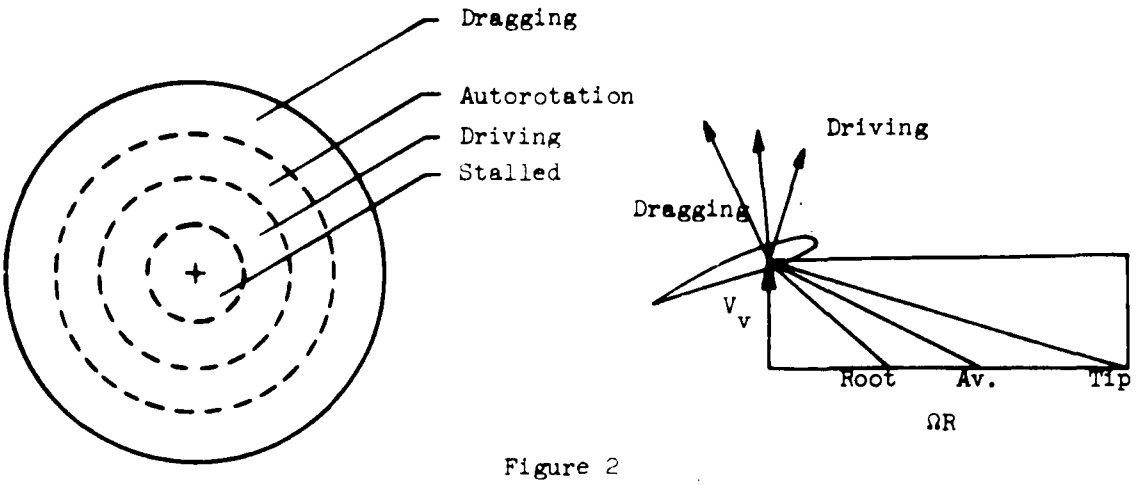

Figure 2
Rotor Blade Froces In Autorotation

The angle ϕ is referred to as the inflow angle (not considering induced velocity) and can be expressed as:

$$\tan \phi = \frac{V_v}{\Omega r} \qquad \text{or} \qquad \phi \cong \tan^{-1} \frac{V_v}{\Omega r}$$

Defining lift as the component of the resultant aerodynamic force normal to the velocity and drag as the component (including induced drag) parallel to the velocity, then

$$\tan \phi' = \frac{D}{L} = \frac{C_D}{C_L} \qquad \text{or } \phi' = \tan^{-1} \frac{C_D}{C_L}$$

It can be seen, geometrically, that the magnitude and direction of the in-plane component of R is dictated by the relative size of ϕ and ϕ' (see Figure 3).

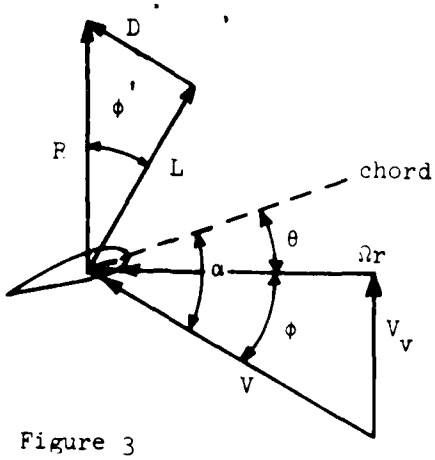

Figure 3
Blade Element In Equilibrium

From the above it can be concluded that:

(1) If $\phi' = \phi$ the resultant force has no component in the plane of rotation and the RPM will remain constant.

(2) If $\phi' > \phi$ the resultant force will have a component in the plane of rotation which will cause a decrease in RPM.

(3) If $\phi' < \phi$ the component in the plane of rotation will cause an increase in RPM.

The angle ϕ' is dictated by the rotor blade lift-drag ratio (L/D) which is a function of blade angle of attack (see Figure 4).

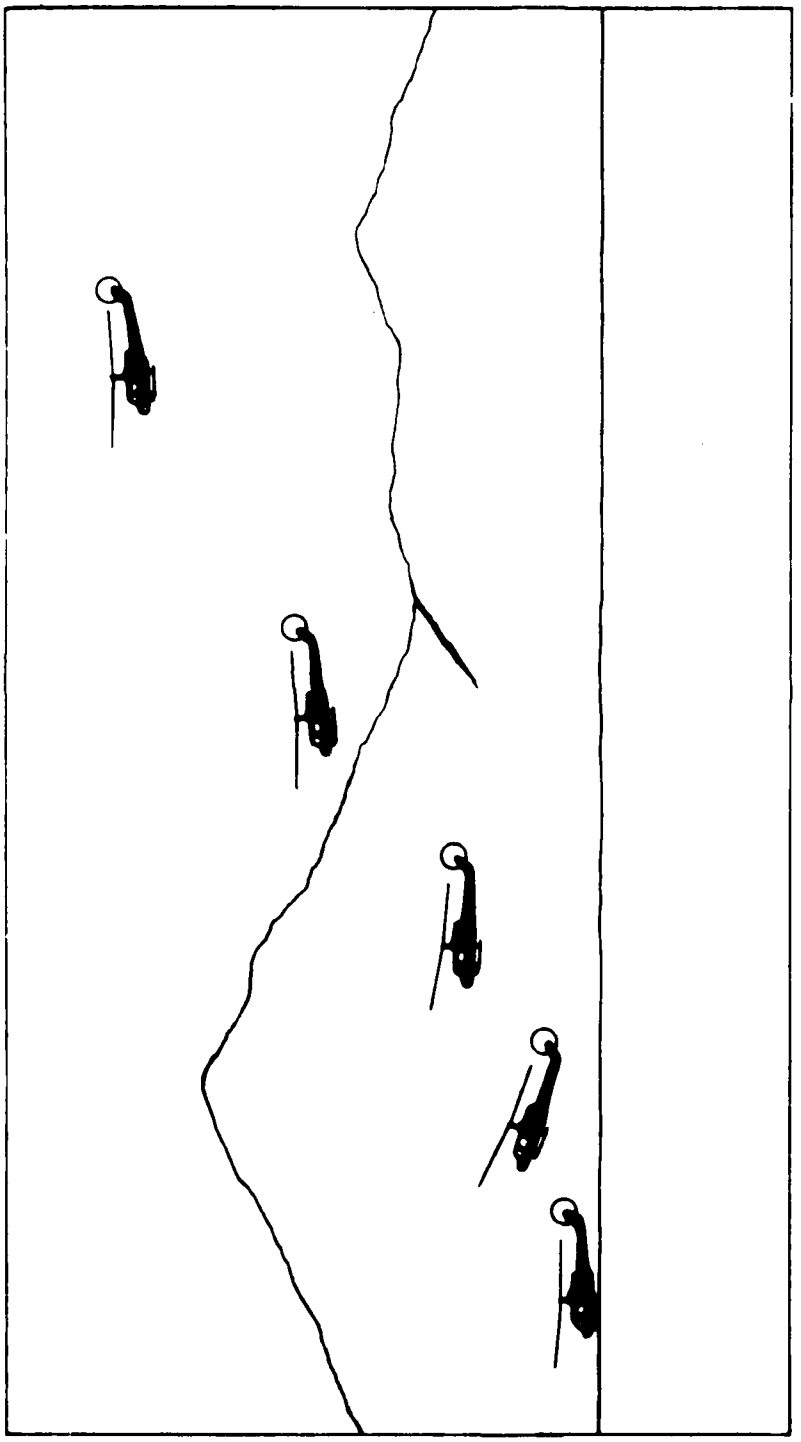

Profile of Typical Autorotative Descent and Flare

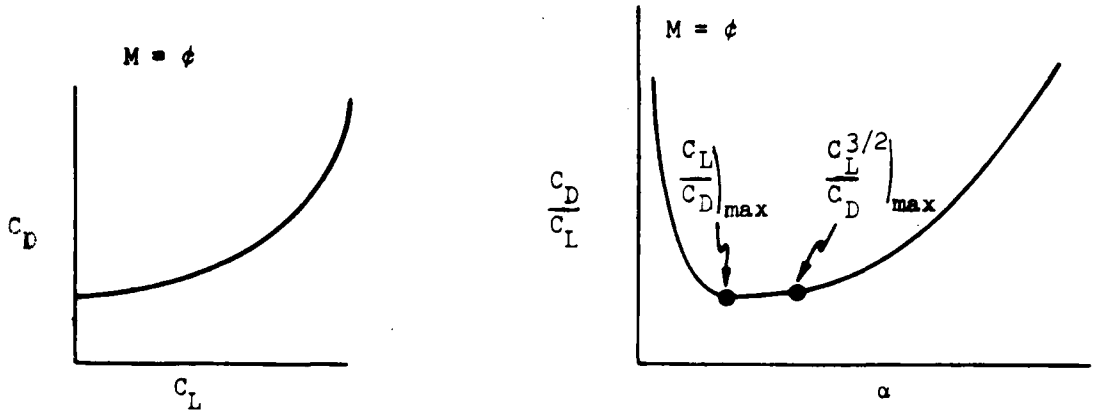

Figure 4
Typical Lift-Drag Ratio

The angle of attack is controlled, although somewhat indirectly, by the collective blade angle, θ, as indicated by the following relationships (see Figure 3):

$$\alpha = \theta + \phi$$

$$\phi = \phi' \text{ when stabilized}$$

$$\phi' = f(\alpha)$$

Therefore, in a stabilized autorotation, the collective pitch selected by the pilot dictates the angle of attack. Recall that energy analysis showed the rate of descent inversely proportional to the ratio $C_L^{3/2}/C_D$ which indicates that if descents are made at various collective settings, the rate of descent will vary and be a minimum for a given W/σ when the angle of attack is such that, as an average, the ratio of $C_L^{3/2}/C_D$ is a maximum.

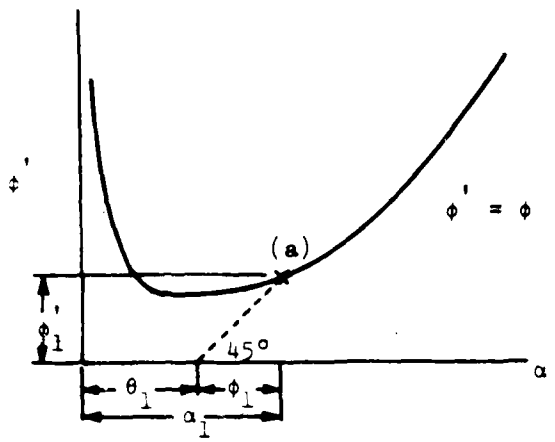

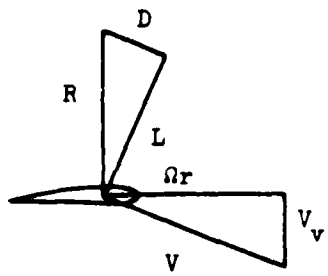

Stabilized at θ_1

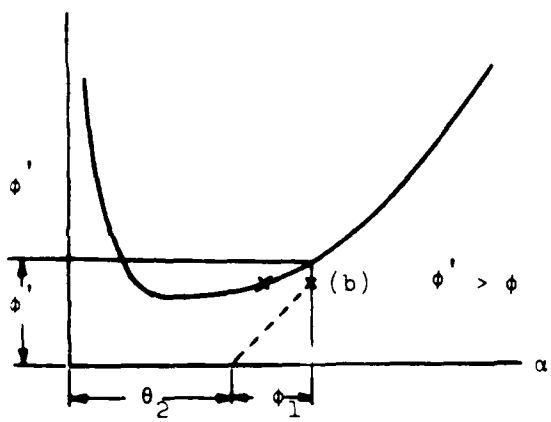

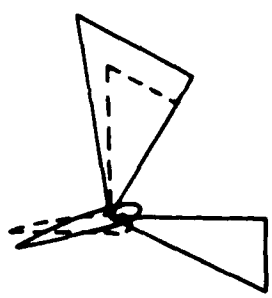

Step in Collective

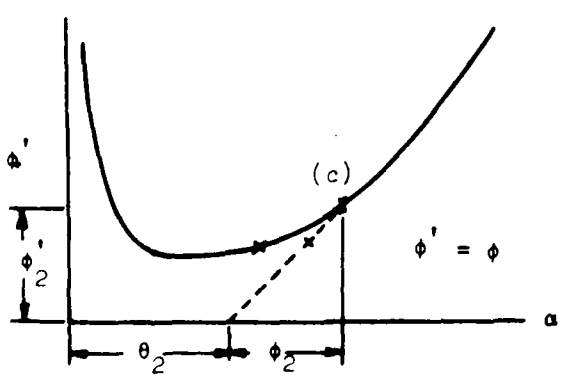

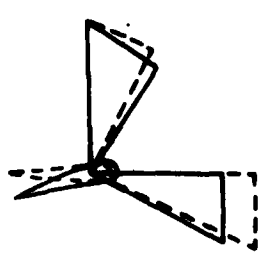

Stabilized at θ_2

Figure 5
Effects of Step in Collective

Next, consider the effect a change in collective has on the RPM during autorotation of a rotor initially stabilized at an angle of attack corresponding to point "a", Figure 5, for example. If conditions are stabilized, $\phi' = \phi$ which imposes that the pitch angle (θ) measured along the angle of attack scale and the point of operation on the L/D curve must lie on a 45° line, both axes being drawn to the same scale. If the collective angle is increased, the immediate consequence is a change in angle of attack and a different L/D (ϕ') with no changes in velocities (ϕ). Thus, a transient situation exists where $\phi' \neq \phi$, producing a force in the plane of rotation and causing the rotor RPM to change. If the step in collective causes a reduction in the lift-drag ratio ($\phi' > \phi$) the RPM will decrease (as shown in the example of Figure 5, whereas an increase in L/D ($\phi' < \phi$) will increase the RPM with maximum RPM occurring at maximum L/D.

The preceeding discussion has shown how the collective selected by the pilot controls the rotor angle of attack and the lift-drag ratio. Operation near $(C_L/C_D)_{max}$ produces maximum rotor RPM and near $(C_L^{3/2}/C_D)_{max}$ produces minimum rate of descent. It should be pointed out that the variation of C_L/C_D and $C_L^{3/2}/C_D$ versus angle of attack is relatively flat near the maximum value (see Figure 6) and therefore the rate of descent and RPM are not sensitive functions of collective position.

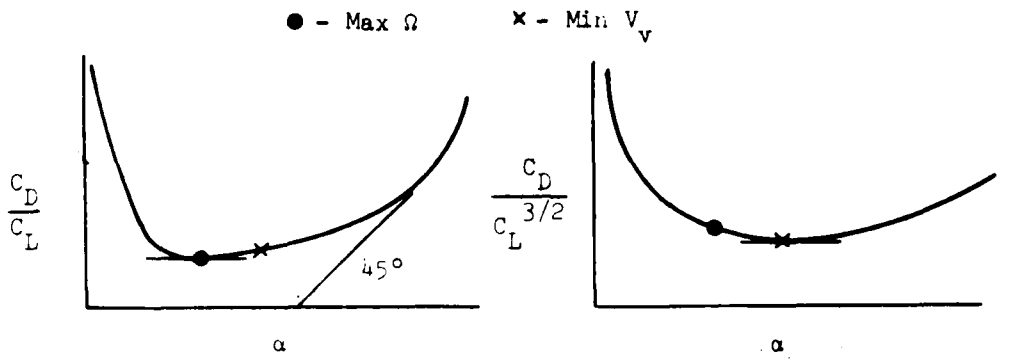

Figure 6
Typical Lift-Drag Variation

A final point of interest on the L/D curve is that at which the slope of the curve is unity (45°) because this represents the highest angle of attack for equilibrium in autorotation. It is important to note that for pitch angles below that associated with this angle of attack the autorotation is a stable phenomenon, that is, a disturbance which increases or decreases the rotor RPM changes ϕ and produces in-plane forces in such a manner as to return the RPM to the initial value. Above the point where the slope is unity, a decrease in RPM causes an increase in ϕ larger than that of the angle of attack, causing the rotor RPM to decrease further. Recovery from this condition would require a reduction in collective, however, this condition is usually instinctively avoided because of the low rotor speed and high rate of descent associated with operation at high angles of attack.

C. MOMENTUM ANALYSIS

Simple momentum analysis is useful to predict the variation of induced power with a reasonable degree of accuracy as long as a well defined continuous stream tube exists, proportional in size to the rotor disc. In hover and in vertical climbing flight the stream tube is accelerated as it passes through the disc and induced velocity is imparted to it (see Figure 7). In a vertical descent, the induced velocity is opposite to the direction of flow in the stream tube and decelerates the air relative to the disc. In the downstream wake (above the rotor in this case) the velocity of the stream tube has been decreased by twice the induced velocity. Thus, the concept of a continuous stream tube fails when the rate of descent is less than twice the induced velocity. This region where momentum analysis fails, defined here as the "vortex ring region", is difficult to analyze and will be discussed separately.

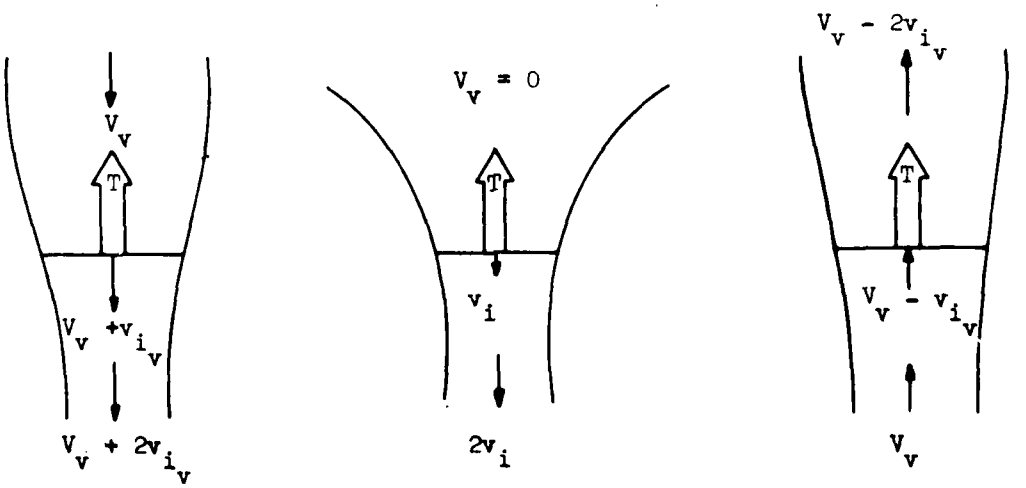

Figure 7
Momentum Analysis Axial Flight States

Considering a vertical descent velocity (V_v) greater than twice the induced velocity in the descent (v_{i_v}):

$$T = \dot{m}\Delta V = \rho A_D (V_v - v_{i_v})(2v_{i_v})$$

Equating thrust (T) to weight and using the expression previously developed for the induced velocity in hover (v_i):

$$v_i^2 = V_v\, v_{i_v} - v_{i_v}^2$$

This is a quadratic equation in v_{i_v}, the solution of which is

$$v_{i_v} = \frac{V_v}{2} - \sqrt{\left(\frac{V_v}{2}\right)^2 - v_i^2}$$

where only the negative radical has significance. In non-dimensional form:

$$\frac{v_{i_v}}{v_i} = \frac{V_v/v_i}{2} - \sqrt{\left(\frac{V_v/v_i}{2}\right)^2 - 1}$$

This variation of induced velocity in vertical descents is shown graphically in Figure 8 along with the solution obtained from vertical climb analysis. Excluding the vortex ring region, simple momentum theory defines a variation of induced effects with vertical velocity which is in good agreement with actual results obtained with rotors and propellers.

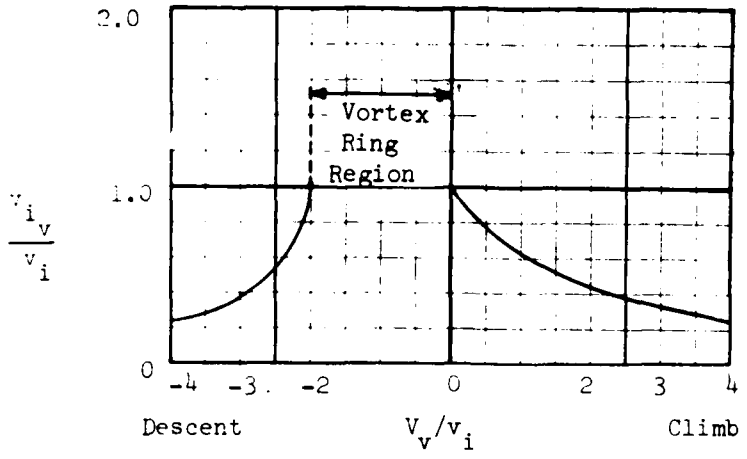

Figure 8
Induced Velocity Variation in Axial Flight

D. VORTEX RING REGION

The vortex ring region extends over the range of non-dimensional rates of descent from 0 to -2. In this region, where the rotor is settling into it's own slipstream, strong vortex action about the rotor can occur and ultimately the net flow through the rotor changes direction. In hover and climbing flight the flow passes through the rotor from above, whereas during descents at relatively high rates the flow passes through the rotor from below. To observe how this change takes place and how the vortex ring state is generated, the individual rotor blades and the wake must be examined with a downwash velocity distribution which is more realistic than that supposed by simple momentum theory.

The actual induced velocity in hover is not uniform across the span of the blade but varies from relatively large values near

the blade tip to zero near the hub (see Figure 9). Furthermore, in response to the high pressure underneath the lifting blade and the low pressures above, a circulatory flow (vortex) is established

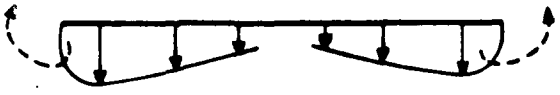

Figure 9
Actual Flow Through Hovering Rotor

around the blade tip path. (The effects these phenomena have on the performance of the hovering rotor are discussed in the Power Correction Section.) Actually, a sheet of vorticity is shed behind the blade across it's entire lifting span in response to spanwise pressure variations but the greatest concentration is near the blade tip.

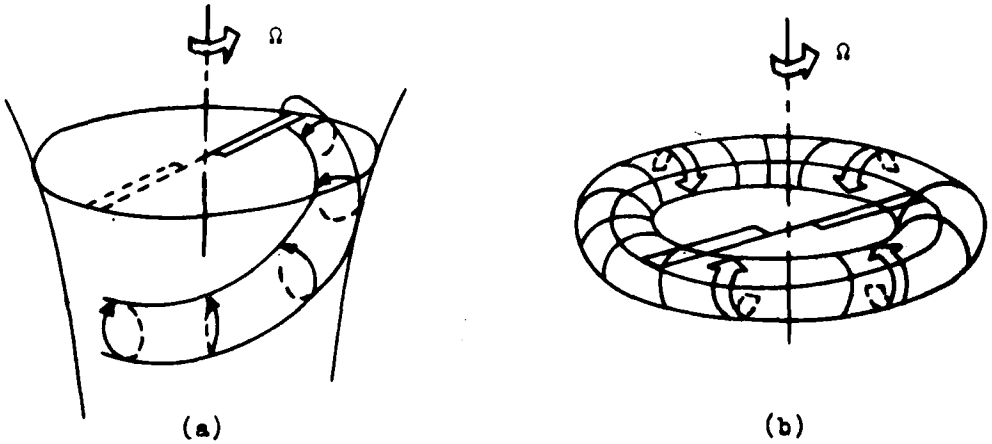

(a) Tip Vortex Trailing Downstream

(b) Vortex Ring State

Figure 10
Simplified Vortex Situation

In hover, the tip vortex (as well as the entire sheet) travels downstream from the blade initially at a speed equal to the induced velocity (see Figure 10a). If a rate of descent is established which is on the same order as the induced velocity, the rotor catches up with previously generated tip vorticity, adding new vorticity and generating a strong circulation (see Figure 10b). In this vortex ring state, as the intensity of the circulatory field is increased, the induced velocity and induced angle of attack increase, requiring higher collective pitch angles to produce lift for equilibrium. The large induced angles tip the resultant aerodynamic force back and create larger force components in the plane of rotation (see Figure 11). This increase in torque (power required) is the consequence of operating the blade with large inflow velocities much the same as in a vertical climb except the additional power is sustaining the circulatory field and the helicopter is actually descending (power settling). In this situation, applying power in an attempt to stop the descent intensifies the circulatory field and aggravates the situation.

Flow conditions in the vortex ring region are not steady and power predictions are mostly empirical. An average variation obtained from several technical reports is shown in Figure 12.

At high rates of descent the flow is fully established up through the rotor and momentum theory again applies, the conclusions of which have already been presented.

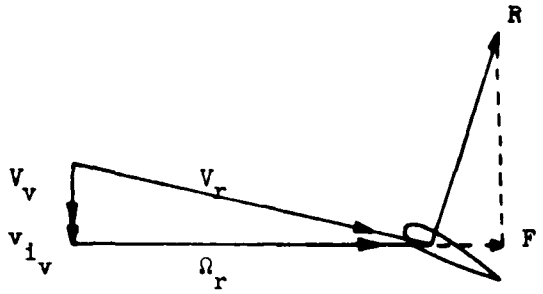

Climb

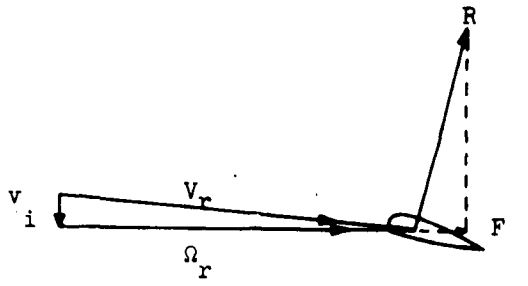

Hover

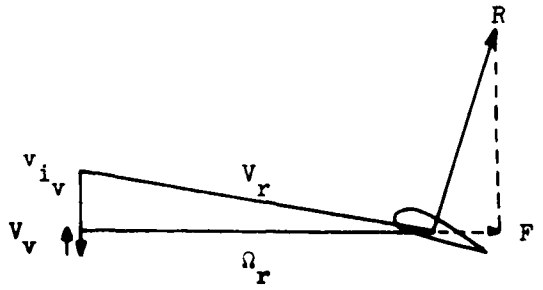

Vortex Ring

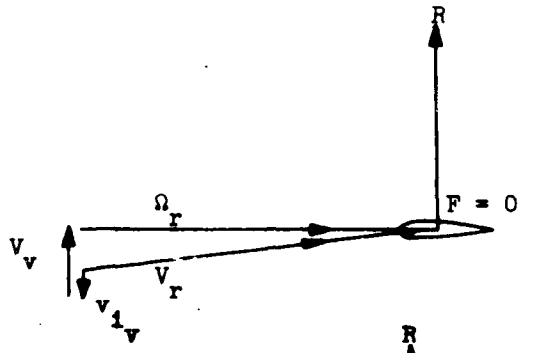

Auto

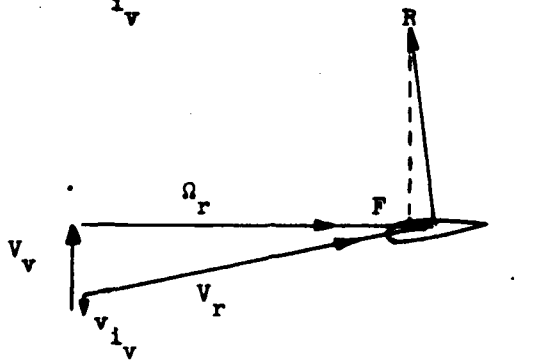

Windmill

Figure 11
Effect of Inflow Velocity

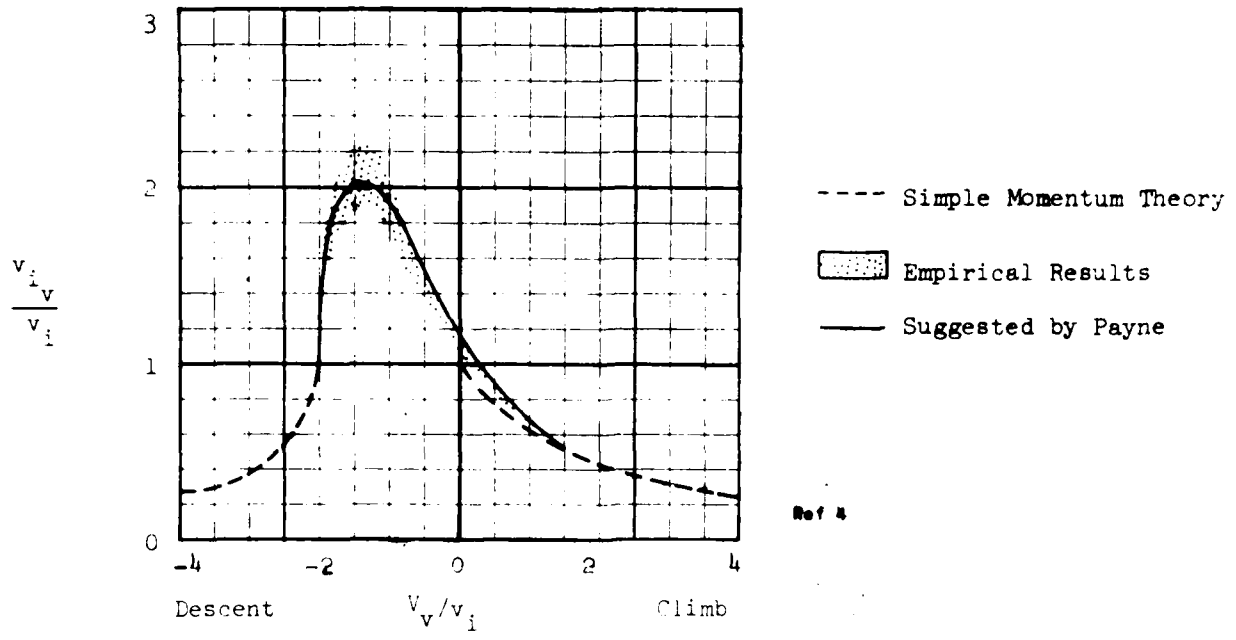

Figure 12
Empirical Induced Velocity in Vortex Ring Region

E. FORWARD FLIGHT

The energy analysis discussed previously relates the rate of descent to the power required, realizing that the power required to drive the rotor system is provided by a decrease in potential energy (descent) of the helicopter. Any change in power required is reflected in the rate of descent so that the reduction of power required occurring with increasing speed in the low speed range produces a corresponding reduction of the rate of descent in autorotation. Therefore, the variation of rate of descent with forward flight speed will be similar to the variation of power required in forward flight, displaying large reductions at moderate forward velocity. Because of this effect and other problems, such as those

associated with restricted visibility and settling into the rotor downwash, vertical autorotations are seldom done.

Except at low forward flight speeds, the vortex ring state is not encountered in forward flight because the rotor wake trails sufficiently far downstream of the rotor. The reason for this is that as forward velocity increases, even though induced velocity decreases, the flow rate through the rotor and the wake velocities increase. Also, the direction of the wake is skewed aft from a normal to the rotor disc. The wake skew angle is shown in Figure 13 for a horizontal attitude rotor in horizontal flight.

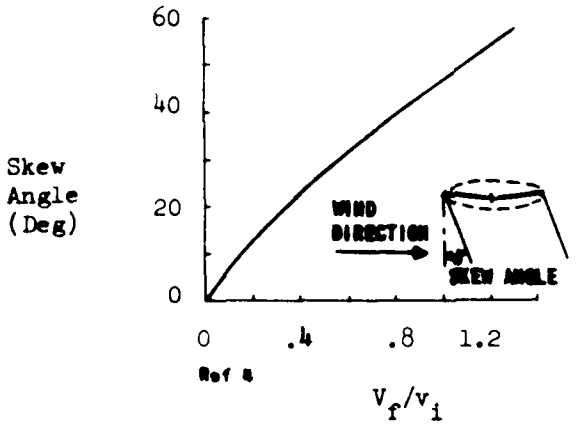

Figure 13
Rotor Wake Skew in Horizontal Flight

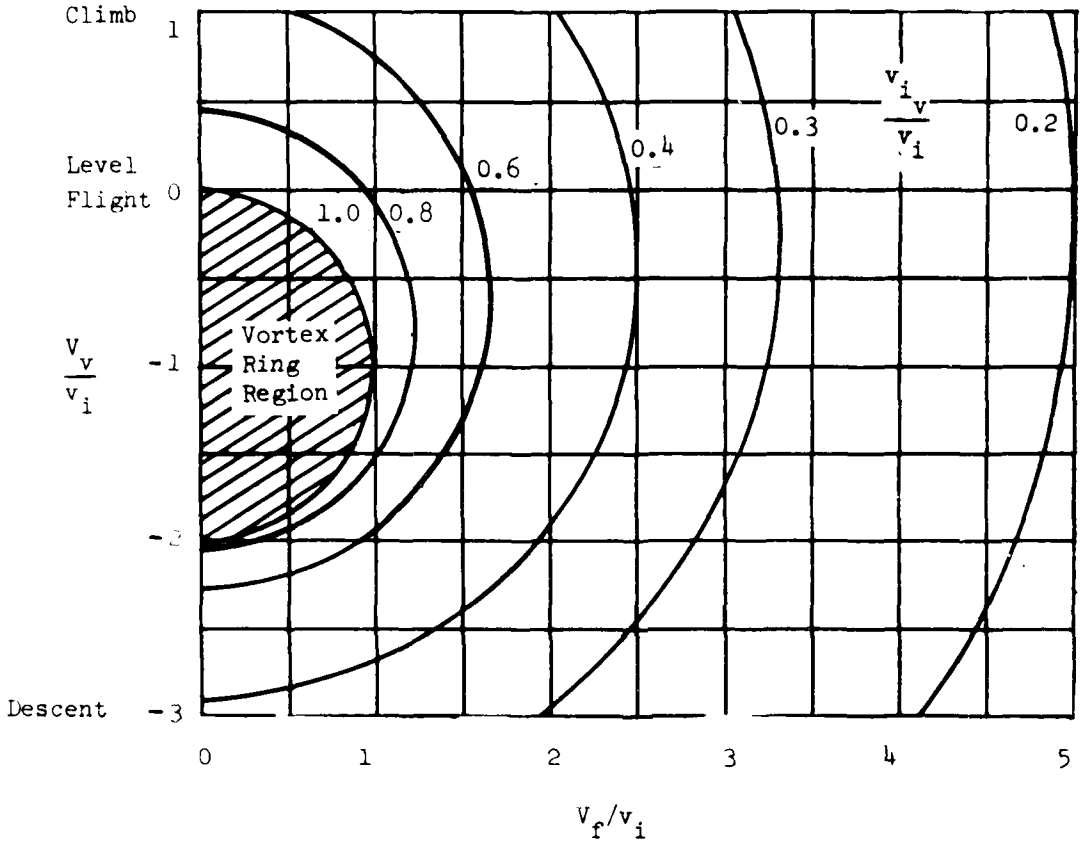

Figure 14
Induced Velocity in Forward Flight Descents

The boundary of the vortex ring region has been defined for axial flight to be between hover and a non-dimensional rate of descent of 2.0 wherein the rotor descends into it's wake. It is only in this region that the induced velocity (and thus induced power required) exceeds that in hover. The expression for non-dimension induced vleocity developed in the section on forward flight climb,

$$\frac{v_i}{v_{i_v}} = \sqrt{\left(\frac{V_f}{v_i}\right)^2 + \left(\frac{V_v}{v_i} + \frac{v_{i_v}}{v_i}\right)^2}$$

will reasonably well predict induced velocities in forward flight descents outside of the vortex ring region (see Figure 12). When using the above equation, a convenient manner to describe the vortex ring region is that where $v_{i_v}/v_i > 1.0$. This boundary is compared in Figure 15 to other boundaries obtained empirically.

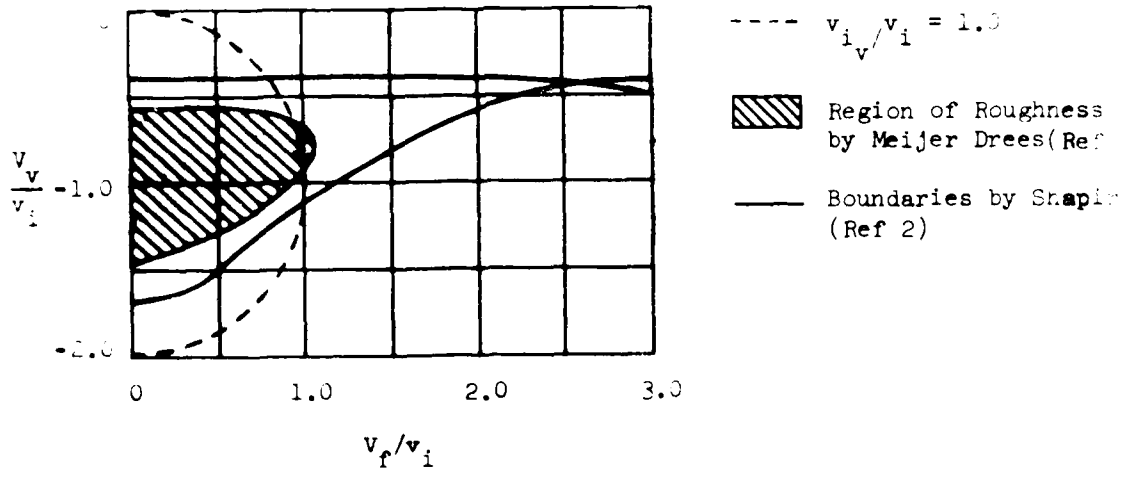

Figure 15
Vortex Ring Region

F. TRANSIENT PROBLEMS

Having considered the steady-state autorotative descents, some mention should be made of a few of the more significant aspects associated with entry into autorotation and the terminating landing flare.

Figure 16 shows a helicopter in forward flight, illustrating a relatively high blade pitch angle and the associated in-plane forces which must be balanced by engine power to the rotor shaft. In this situation, loss of engine power would result in a rapid decrease of rotor RPM to a value below the operating range with dire results.

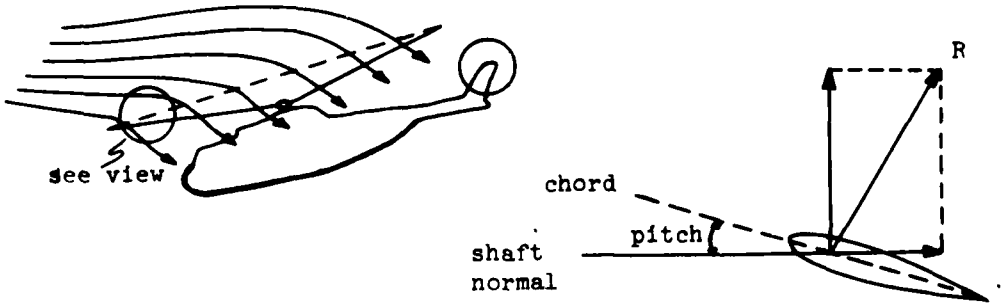

Figure 16
Steady State High Speed Situation
(High Collective)

The decay rate of rotor RPM can be easily approximated if it is assumed that the rotor blade angle of attack does not change. This represents a situation where, following power loss, the pilot takes no corrective action and the time interval of interest is short enough that there is no appreciable change in the aircraft velocity vector. For a constant blade angle of attack, C_p is essentially constant

and can be written as:

$$C_P = \frac{Q\,\Omega}{\rho A_D (\Omega R)^3} = \phi$$

where Q is the main rotor torque, and Ω is the angular velocity. For a given density, then, torque and RPM are related:

$$\frac{Q}{Q_o} = \left(\frac{\Omega}{\Omega_o}\right)^2$$

Also, Newton's law can be used to express the angular acceleration of the rotor in response to torque as:

$$\frac{d\Omega}{dt} = -\frac{Q}{I_R}$$

where I_R is the rotor moment of inertia about the axis of rotation. Combining both equations produces the following differential equation:

$$dt = -\frac{I_R \Omega_o^2}{Q_o}\,\frac{d\Omega}{\Omega^2}$$

where the subscript o is used to signify initial conditions. If initial time is taken as zero, the integral solution is

$$t = \frac{I_R \Omega_o^2}{Q_o}\left(\frac{1}{\Omega} - \frac{1}{\Omega_o}\right)$$

or

$$t = \frac{I_R \Omega_o}{Q_o}\left(\frac{\Omega_o}{\Omega} - 1\right)$$

where t is the time elapsed between Ω_o and Ω.

Stipulating, for example, that the tolerable loss of rotor RPM is 20 % of the initial value ($\Omega = .8\Omega_o$), the time required for the rotor to decelerate to a critical condition is:

$$t_{.8\Omega_o} = 0.25 \frac{I_R \Omega_o}{Q_o}$$

This illustrates the dependence of the decay time on the rotor angular momentum at the time engine power is lost ($I_R \Omega_o$) and on the torque the engine was supplying (Q_o). The variation is shown graphically in Figure 17.

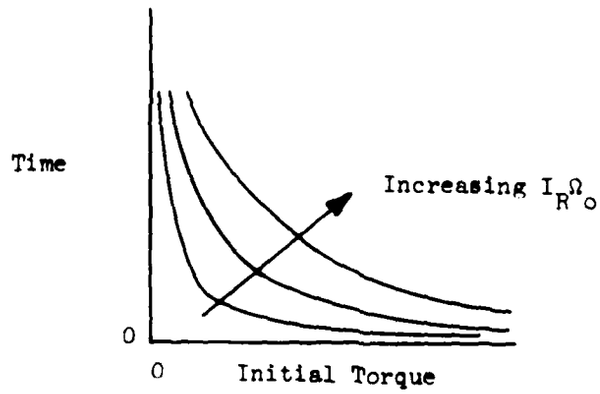

Figure 17
Computed Time For 20% Loss In Rotor RPM

To avoid this rapid loss of RPM, action must be taken by the pilot. Lowering the collective control reduces the pitch angle of the rotor blades accomplishing two things of primary importance:

(1) The aerodynamic forces in the plane of rotation, which are decelerating the rotor, are decreased (see Figure 18).

(2) The rotor thrust is reduced and a descent commences, which is necessary to establish autorotation (see Figure 19).

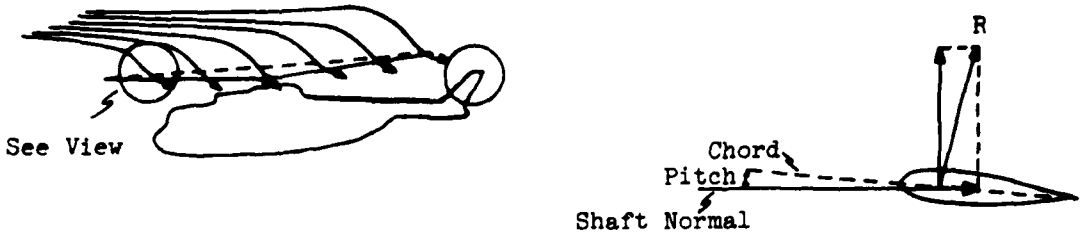

Figure 18
Transient High Speed Situation
(Low Collective)

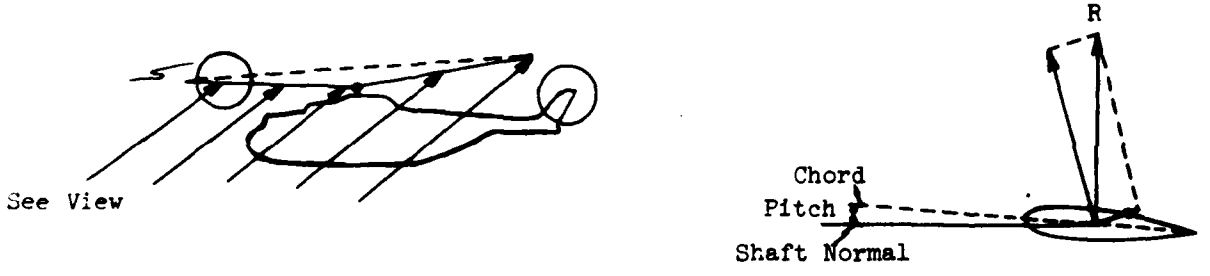

Figure 19
Steady State Autorotation
(Low Collective)

After stabilized autorotation has been established and the helicopter approaches the ground, forward velocity and descent rate are of extreme interest because those usually associated with good performance in stabilized autorotation are excessive for touchdown. Both problems are alleviated by the pilot's action of applying aft stick and thereby

"flaring" the rotor, or tipping it back. Not only is the rotor thrust tipped aft which tends to reduce the forward velocity but the flare also increases the angle of attack on all blade elements producing a larger vertical force and slowing the descent rate. This increase in angle of attack also tips the blade element resultant aerodynamic forces forward tending to increase RPM. During this flare maneuver, the kinetic energy due to forward motion of the helicopter is being utilized to drive the rotor.

If more rotor lift is desired near the ground, the blade pitch angles can be increased collectively, the necessary power supplied by the rotational kinetic energy with a sacrifice of RPM. Obviously this requires some technique to coordinate the RPM decay with touchdown.

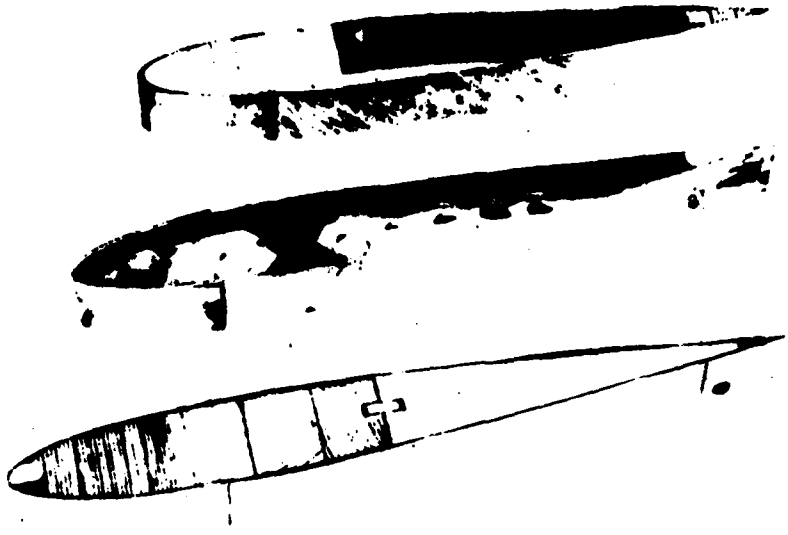

SECTIONS OF TYPICAL WOODEN ROTOR BLADES

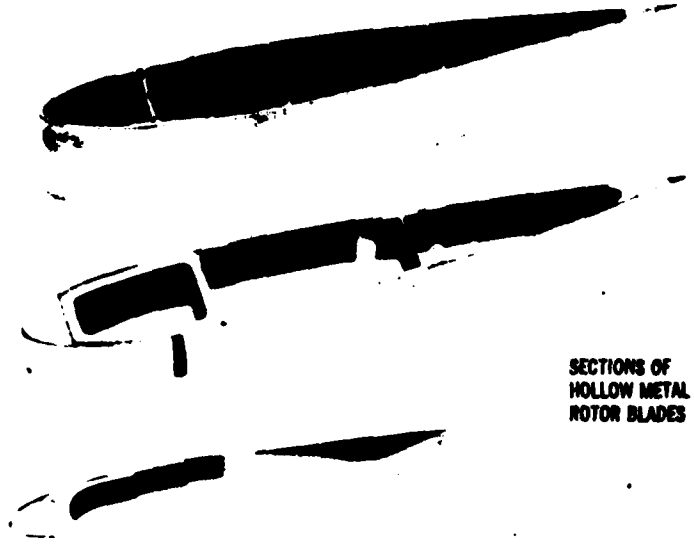

SECTIONS OF
HOLLOW METAL
ROTOR BLADES

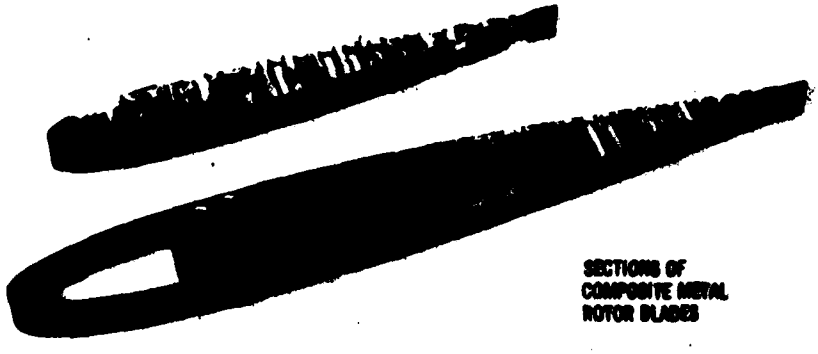

SECTIONS OF
COMPOSITE METAL
ROTOR BLADES

VI. MAIN ROTOR POWER CORRECTIONS

The power required analyses presented in the previous sections have made many simplifying assumptions, some of which severly affect the accuracy of the results. Although more rigorous techniques may not be warranted for qualitative results, some consideration must be given to the more significant restrictions of the simplified approach as they pertain to particular flight regimes. In particular, more analysis is warranted of the induced power in hover and in forward flight and the profile power is forward flight.

A. INDUCED POWER REQUIRED

Induced Power in Hover

The simple momentum theory used to predict induced effects assumes the velocity of the flow induced through the rotor disc to be constant across the entire disc. This implies elliptical span loading and results in minimum induced drag. This ideal situation is not at all typical of an actual rotor, in light of the fact that the element dynamic pressure changes with radial position (see Figure 1), the most significant differences being non-uniform downwash and ineffective lifting area near hub and tips.

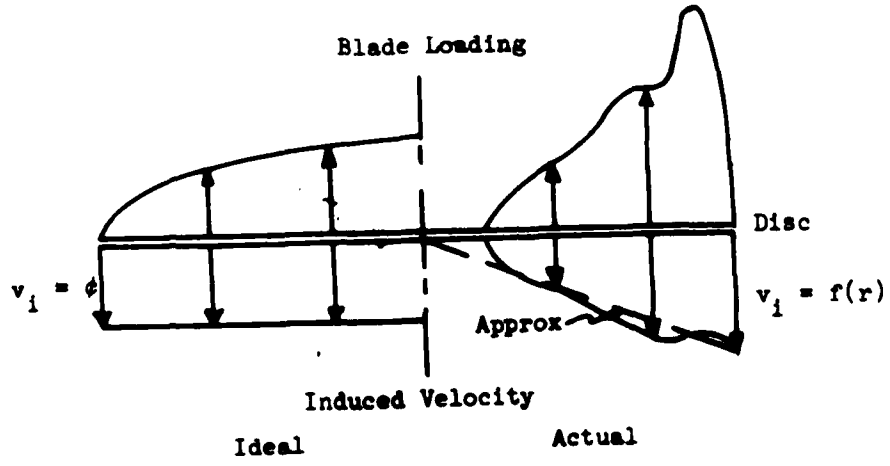

Figure 1
Induced Velocity in Hover

The actual induced velocity is a function of radial position:

$$v_i = f(r)$$

and thus the differential thrust force produced on each annular element of the rotor disc (dA_D in Figure 2) will vary. Integration can be used to determine the total thrust produced by the disc as:

$$T = \int_0^R dT = \int_0^R (\rho dA_D v_i) 2v_i$$

where $v_i = f(r)$ and $dA_D = 2\pi r dr$.

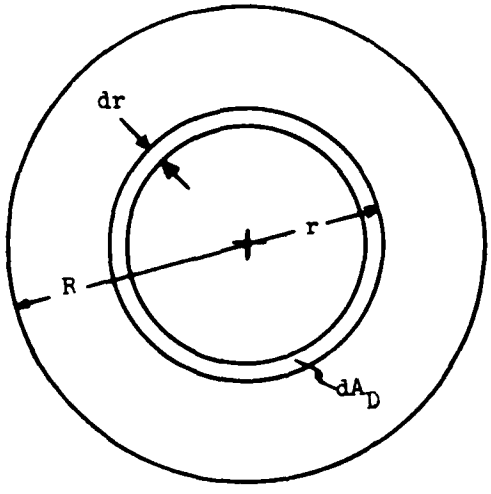

Figure 2
Annular Element of Rotor Disc

To solve the integral, the induced velocity must be expressed explicitly as a function of radius. A linear variation affords a simple solution and is quite close to the actual variation. For this case,

$$v_i = (\text{const})r = \frac{r}{R} v_{i_{tip}}$$

and the integral produces:

$$T = \rho A_D v_{i_{tip}}^2 \qquad \text{where } (v_i')^2 \equiv \frac{W}{2\rho A_D}$$

Recalling the solution obtained by simple momentum theory (constant induced velocity):

$$T = 2\rho A_D (v_i')^2$$

where the prime denotes ideal induced effects. Comparison of the two results shows that for the same thrust:

$$v_{i_{tip}} = \sqrt{2}\ v_i'$$

or, assuming the induced velocity increase linearly with radius, the induced velocity at the tip of the rotor is about 40% greater than that predicted by simple momentum theory (see Figure 3).

The effect on induced power can be determined by integration:

$$P = \int_0^R dT(v_i) = \int_0^R \rho dA_D 2 v_i^3$$

Substituting as before:

$$P = \frac{4}{5}\rho A_D v_{i_{tip}}^3$$

or, in terms of the ideal power required (P_i'):

$$P_i = \frac{4}{5}\sqrt{2}\ P_i' = 1.13\ P_i' \qquad \text{where } P_i' \equiv \sqrt{\frac{W^3}{2\rho A_D}}$$

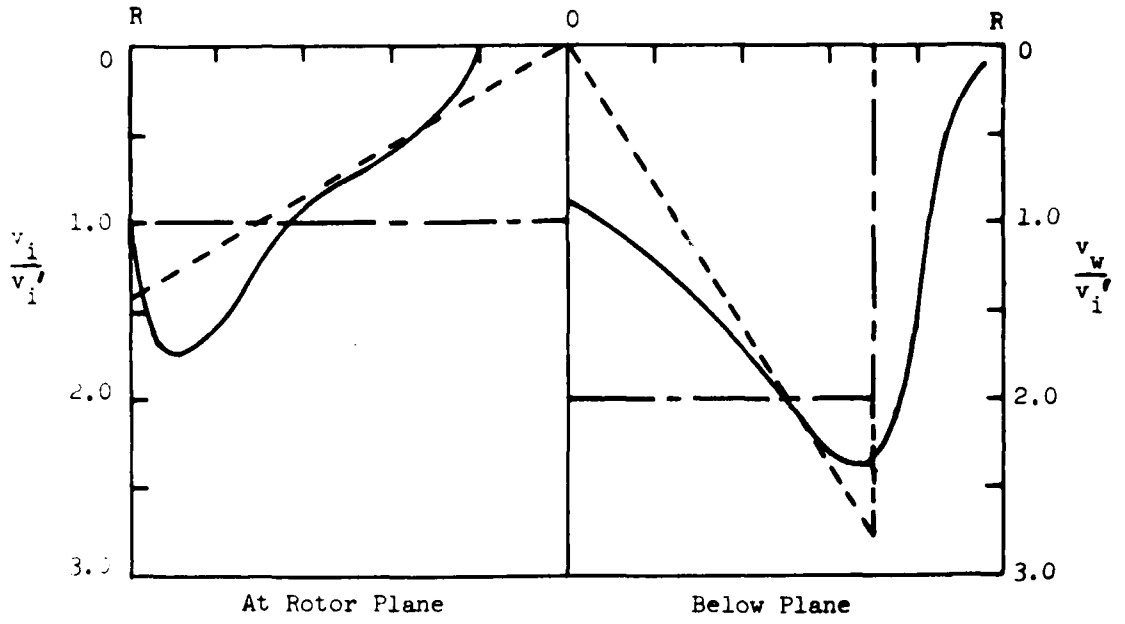

Figure 3
Comparison of Downwash Velocities

Variations of induced velocity with radius other than the simple linear case shown here could be utilized for closer fitting to the actual variation, but the simple case is sufficient to show the increase of induced power and the approximate magnitude.

In the case of a lifting rotor, because of the pressure difference above and below the blade, flow occurs around the blade tip which tends to destroy that pressure difference. The result of this phenomenon, which generates the tip vortex, is a loss of lift near the blade tip (see Figure 4) with essentially no change in profile drag. The change in

induced effects can be analyzed by considering that the tip flow reduces the area of the blade which is effective in producing lift. An approximate correction for the tip loss can be included in the calculations by considering the effective rotor radius to be less than the geometric radius:

$$R_{eff} = BR$$

where B is the tip loss correction factor, a number less than unity. This reduction in effective disc area imposes an increase in induced power:

$$P_i = \frac{w^{3/2}}{\sqrt{2\rho\pi(BR)^2}} = \frac{1}{B} P_i'$$

where P_i' represents the estimate of induced power not considering tip effects.

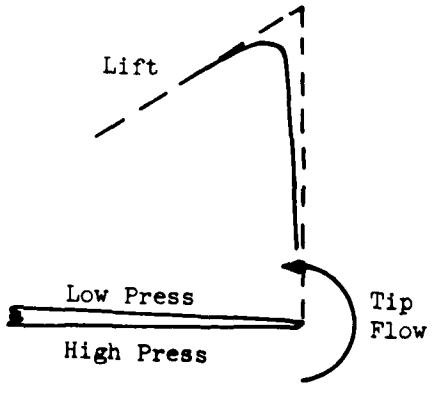

Figure 4
Rotor Blade Tip Effect

Several emperical relationships have been developed for B, one of wnich is shown in Figure 5.

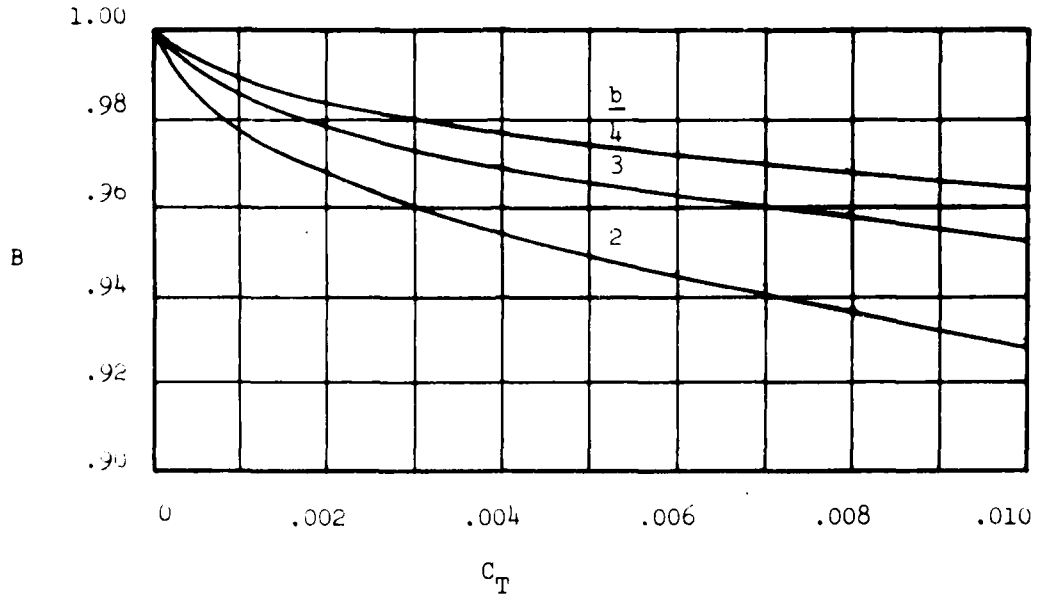

Empirical relationship:

$$B = 1 - \frac{\sqrt{2C_T}}{b}$$

Effective radius = BR

B = Correction Factor

C_T = Thrust Coefficient

b = Number of blades

R = Rotor Radius

Figure 5
Rotor Blade Tip Correction Factor

The significance of the tip loss is the effective increase in disc loading for a given thrust and thus an increase in induced velocity and induced power required. This correction would be cummulative with that for non-uniform downwash.

Fuselage Vertical Drag

The assumption that the vertical force required of the rotor for level flight is equal to the gross weight is reasonably accurate for most conventional helicopters, but is an approximation neglecting the vertical drag produced as a result of the rotor downwash on the fuselage. The most pertinent situation would be in hover where downwash velocities are the largest and power requirements are critical.

Defining f_v as the equivalent flat plate area of the fuselage based on tests with flow from above, the vertical drag (D_v) can be approximated as $f_v q_s$. The equivalent flat plate area is larger for bluff, poorly faired fuselages and the consequences of fitting fixed wings in the rotor wake is obvious. The dynamic pressure, q_s, is that of the slipstream and if the wake is assumed to be fully developed by the time it strikes the fuselage:

$$q_s = \frac{1}{2}\rho(2v_i)^2 = T/A_D$$

The thrust, T, can then be expressed:

$$T = W + D_v = W + T\frac{f_v}{A_D}$$

or the thrust-to-weight ratio required to hover becomes:

$$\frac{T}{W} = \frac{1}{1 - f_v/A_D}$$

This is a number very close to unity for most helicopters but decreases with increasing f_v (winged helicopters, etc.) and with decreasing A_D (increasing q_s).

Induced Power in Forward Flight

In the analysis of forward flight climbs and descents the non-dimensional induced velocity was shown to be

$$\frac{v_i}{v_{i_v}} = \sqrt{\left(\frac{V_f}{v_i}\right)^2 + \left(\frac{V_v}{v_i} + \frac{v_{i_v}}{v_i}\right)^2}$$

This is shown graphically for conditions outside the vortex ring state in Figure 6.

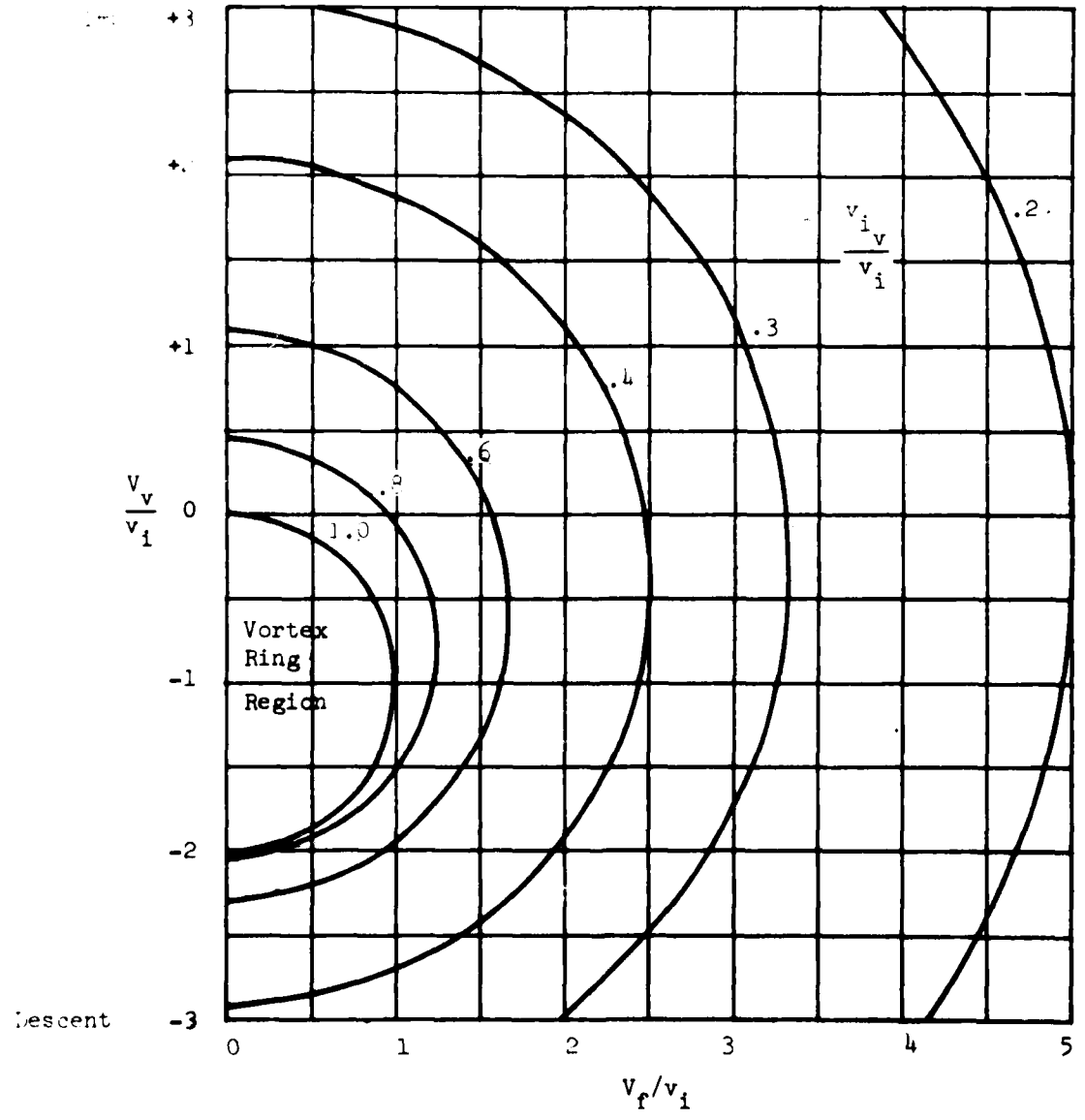

Figure 6
Theoretical Non-Dimensional Induced Velocity

In practice the actual induced velocity in hover is about 1.15 times that indicated by simple momentum analysis. This ratio varies, tending to 1.05 to 1.10 in forward flight and 1.0 for axial flight at high rates. Figure 7, taken from Payne, shows the idealized circles of the above equation distorted to agree with experimental evidence and includes the vortex ring region.

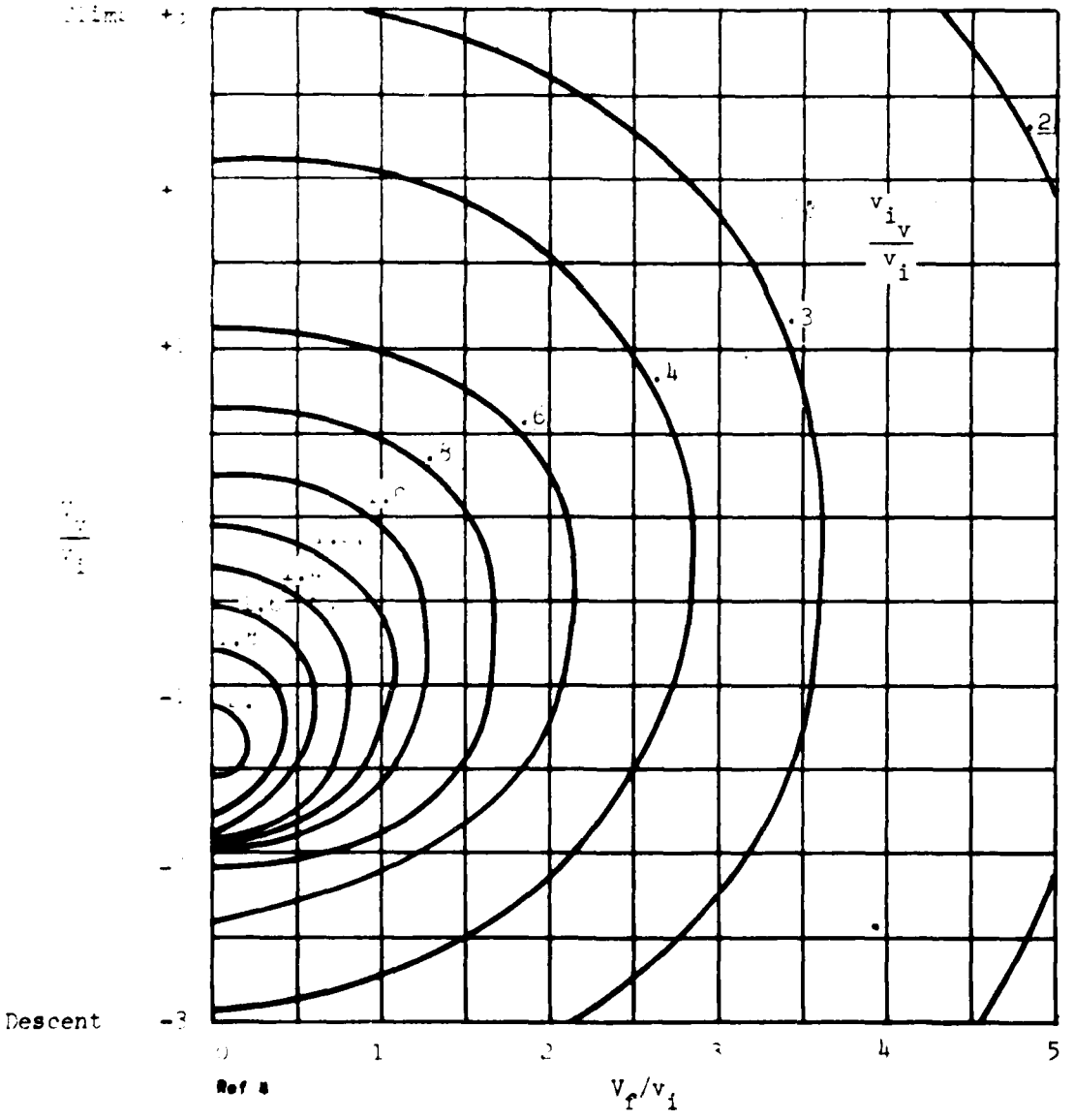

Figure 7
Emperical Variation Of Induced Velocity With Flight Conditions

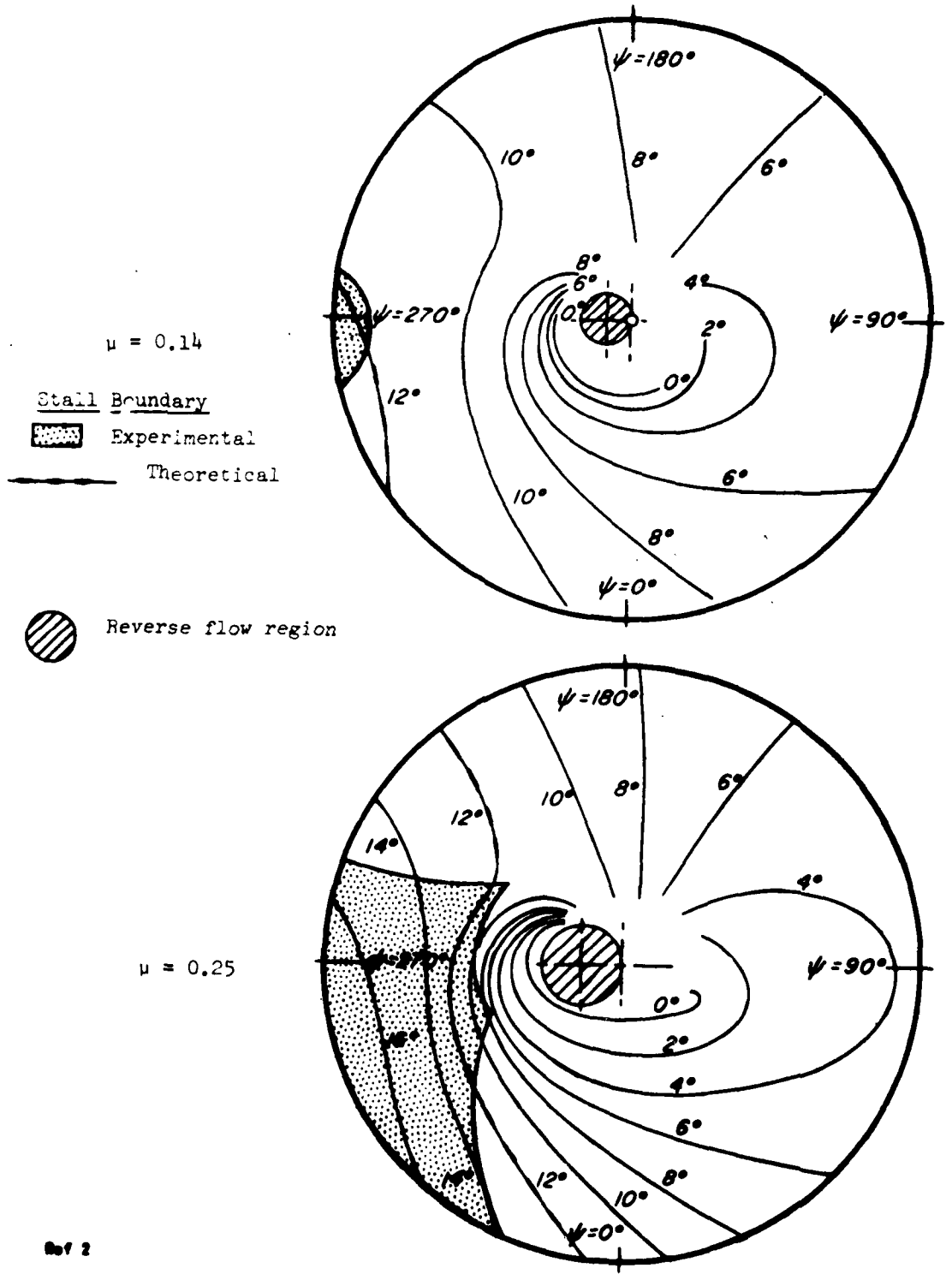

Ref 2

Figure 8
Growth of Blade Stall in Forward Flight

B. PROFILE POWER REQUIRED IN FORWARD FLIGHT

The profile power required in forward flight, developed in Section IV , was based on the assumption that the section profile drag coefficient was constant, independent of r or ψ. The rotor blade in forward flight experiences a cyclic variation of local dynamic pressure producing blade motion normal to the plane of rotation (flapping) thus preventing the dissymmetry of lift that would otherwise occur. The addition of flapping motion results in relatively low angles of attack on the advancing blade, where the local velocities are high, and relatively high angles of attack on the retreating blade, where the local velocities are low. Figure 8 depicts a cyclic variation of section angle of attack, typical of rotors in powered forward flight.

Retreating Blade

The blade flapping produced by forward flight causes the retreating blade to operate at high angles of attack. Prediction of the local angle of attack values should consider blade twist, induced velocity distribution and the component of freestream velocity normal to the disc. Blade twist is commonly a linear washout in an attempt to reduce the variation of induced velocity across the rotor. The freestream normal component acts to reduce the blade angle of attack for the helicopter in forward flight with the rotor tilted to provide forward thrust. The magnitude of the effect depends on the amount of forward thrust the rotor must supply (amount of tilt) and is most pronounced on the disc where the rotor rotational velocity component is small, thus causing higher angles of attack to occur near the blade tip.

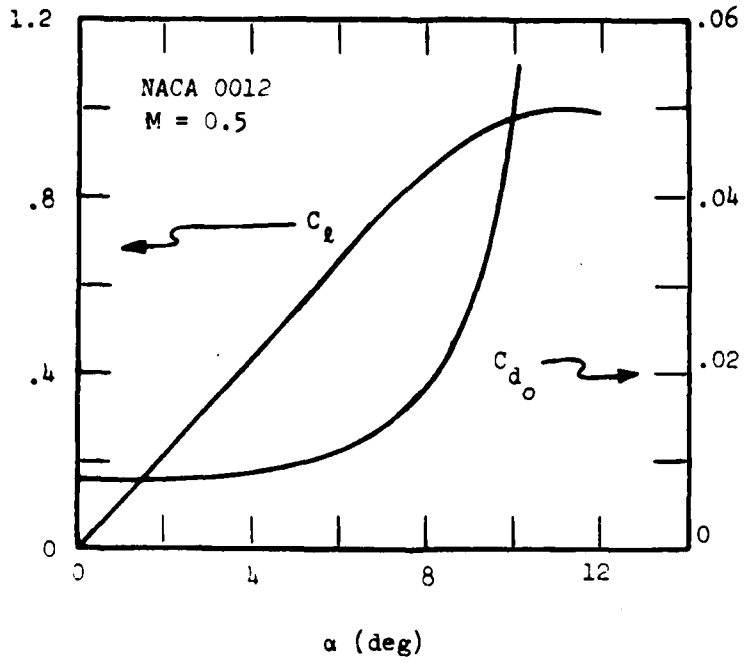

Figure 9
Section Data - Angle of Attack Variation

The consequence of operation at high angles of attack is an increase in profile drag coefficient and possible blade stall (see Figure 9) associated with airflow separation. Correlation of predicted and actual stall is, of course, not exact because of the complexity of predicting local angles of attack and stalling angles for a flexible blade in three-dimensional, transient flow conditions.

Advancing Blade

The addition of the freestream velocity and that due to rotation produces high local Mach numbers on the advancing blade tip. The effect of Mach number on section force coefficients for a constant angle of attack is shown in Figure 10.

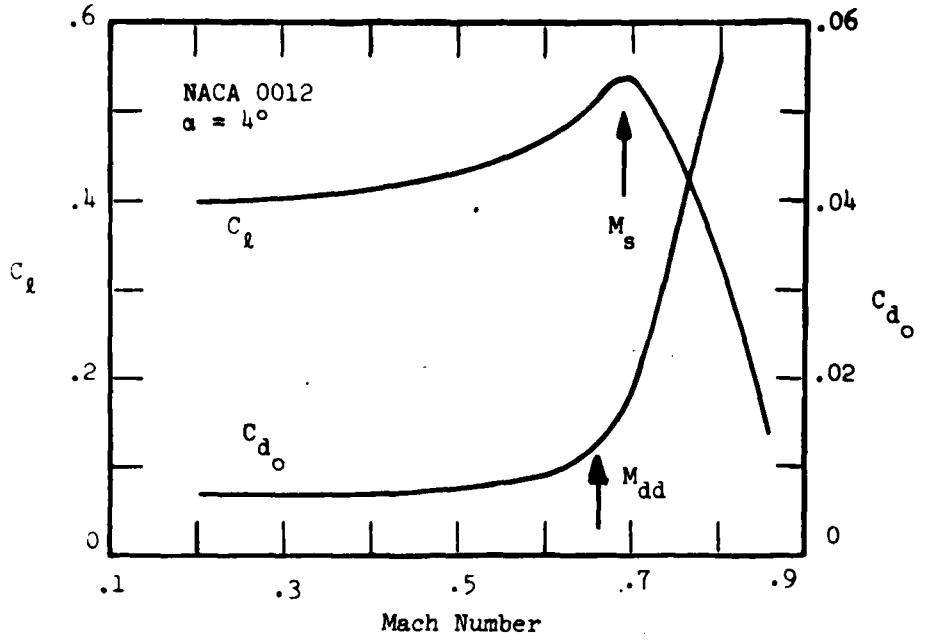

Figure 10
Section Data - Mach Number Variation

Thus, operation at high Mach numbers also results in an increase in profile drag coefficient (C_{d_o}) and a decrease in lift coefficient (C_ℓ). These phenomena are the result of supersonic airflow on the blade, which will occur when the blade is still subsonic because of the acceleration of the air as it passes over the blade. The Mach at which an airfoil section must be moving relative to the air to first produce sonic velocity somewhere on the section is defined as the critical Mach number (M_{cr}). Exceeding this Mach number produces a shock wave on the airfoil causing a rather abrupt increase in C_{d_o}. The freestream Mach number at which $\Delta C_{d_o}/\Delta M = 0.1$ is commonly defined as the drag divergence Mach number (M_{dd}). In general, M_{dd} exceeds M_{cr} by 10 to 15 percent. A further

increase in speed increases the shock intensity which induces separation and causes an abrupt decrease in C_ℓ. The freestream Mach number at which this loss of lift occurs is defined as the shock-stall Mach number (M_s). The change in velocity experienced by the air as it passes over the airfoil depends on the angle of attack of a given section, so that M_{cr}, M_{dd} and M_s are functions of angle of attack. This variation is shown for M_{dd} in Figure11 which represents the section Mach number at which abrupt increases in profile drag coefficient will occur. Airfoil sections thickness and thickness distribution will greatly influence drag divergence characteristics.

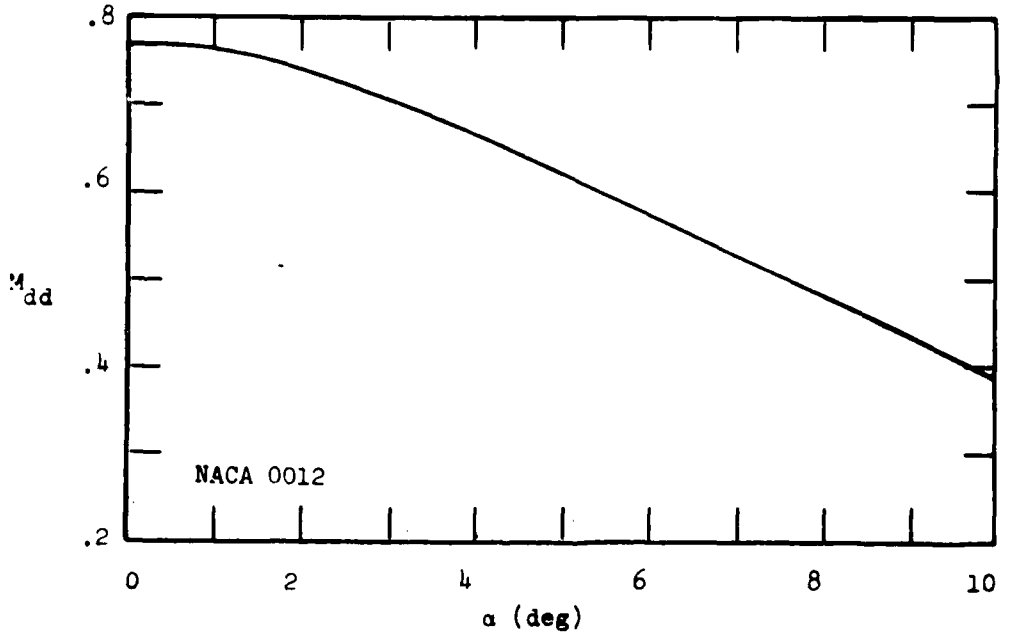

Figure 11
Effect of Angle-of-Attack on Drag Divergence

The advancing blade tip Mach number (M_{adv}) increases directly with rotor RPM (Ω) and forward flight velocity (V_f), and inversely with ambient temperature (T_a), or acoustic speed (V_a):

$$M_{adv} = \frac{V_{adv}}{V_a} = \frac{\Omega R + V_f}{\sqrt{\gamma g R}\sqrt{T_a}}$$

Whether or not a particular M_{adv} is greater than M_{dd} for the blade section depends on the advancing blade tip angle of attack. For a given RPM, the forward velocity at which advancing blade drag divergence occurs will be lower on colder days and under conditions of high C_T. Increasing rotor RPM will aggravate the situation.

Power Required

The effect of increasing forward flight speed, or μ for a fixed RPM, is summarized in Figure 12 by showing the local lift coefficient of

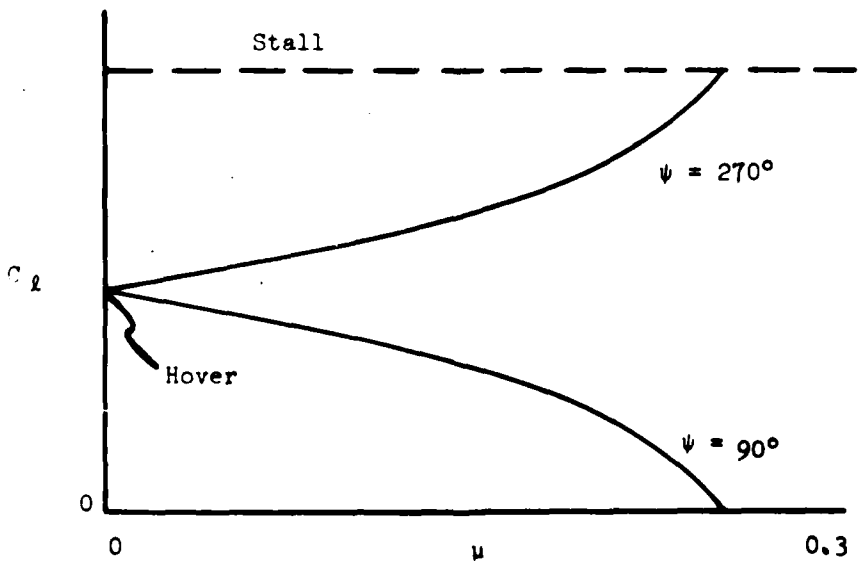

Figure 12
Local C_L in Forward Flight

a section near the blade tip at two azimuth locations. It is seen that the advancing blade is experiencing low angles of attack but high local velocities, while the retreating blade is experiencing high angles of attack. Both of these situations will eventually lead to increases in local drag and thus increase the main rotor power required. Recalling that the forward flight power required analysis presented in Section IV assumed the section profile drag coefficient to be constant, it is apparent that drag rise associated with high angle of attack or high Mach number would necessitate corrections to the section drag coefficient for accuracy in predicting power required at high forward flight speeds.

VII. TAIL ROTOR POWER REQUIRED

For performance analysis of stabilized flight, it is sufficient to consider that the purpose of the tail rotor is to provide a force which balances the torque reaction to the rotation of the main rotor. Thus, the tail rotor thrust, T_{TR}, required for equilibrium is dictated by the main rotor torque, Q_{MR}:

$$T_{TR}\ \ell_{TR} = Q_{MR} = \left(\frac{P}{\Omega}\right)_{MR}$$

or

$$T_{TR} = \frac{(P/\Omega)_{MR}}{\ell_{TR}}$$

where ℓ_{TR} is the distance from the helicopter center of gravity to the tail rotor thrust line, measured normal to the main rotor shaft (see Figure 1). With the relatively limited CG movement allowable in a single rotor helicopter and the fairly constant main rotor RPM, the tail rotor thrust becomes essentially a constant times the main rotor power required.

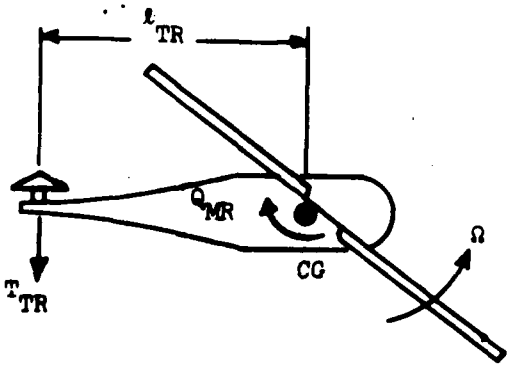

Figure 1
Torque Balance

The power required to drive the tail rotor is composed of induced power and profile power, both of which can be analyzed in the same manner as was the main rotor.

A. HOVER POWER

The momentum theory visualizes the tail rotor thrust as a reaction to the acceleration of the air mass through the tail rotor where the required amount of thrust is dependent upon main rotor torque. If the induced velocity is assumed constant across the disc, the tail rotor induced velocity in hover, $v_{i_{TR}}$, is

$$v_{i_{TR}} = \sqrt{\frac{T_{TR}}{2\rho A_{D_{TR}}}}$$

In terms of main rotor power,

$$v_{i_{TR}} = \sqrt{\frac{(P/\Omega)_{MR}}{2\rho A_{D_{TR}} \ell_{TR}}}$$

or, in non-dimensional form,

$$\frac{v_{i_{TR}}}{(\Omega R)_{MR}} = \frac{1}{\sqrt{2}} C_{P_{MR}}^{1/2} \sqrt{\frac{A_{D_{MR}}}{A_{D_{TR}}}} \sqrt{\frac{R_{MR}}{\ell_{TR}}}$$

Induced Power

The induced power can be evaluated as

$$P_{i_{TR}} = T_{TR} v_{i_{TR}}$$

Defining the non-dimensional tail rotor power coefficient and thrust coefficient as

$$C_{P_{TR}} \equiv \frac{P_{TR}}{\rho A_{D_{MR}} (\Omega R)^3_{MR}} \qquad C_{T_{TR}} = \frac{T_{TR}}{\rho A_{D_{MR}} (\Omega R)^2_{MR}}$$

the induced power can be expressed in coefficient form as:

$$C_{P_i}\Big|_{TR} = \frac{T_{TR}}{\rho A_{D_{MR}} (\Omega R)^2_{MR}} \frac{v_{i_{TR}}}{(\Omega R)_{MR}}$$

Relating T_{TR} to $(P/\Omega)_{MR}$ and using the equation for $v_{i_{TR}}$:

$$C_{P_i}\Big|_{TR} = \frac{1}{\sqrt{2}} C_{P_{MR}}^{3/2} \sqrt{\frac{A_{D_{MR}}}{A_{D_{TR}}}} \left(\frac{R_{MR}}{\ell_{TR}}\right)^{3/2}$$

Recalling from the analysis of the main rotor:

$$C_{P_{MR}} = \frac{1}{\sqrt{2}} C_{T_{MR}}^{3/2} + \frac{1}{8} \left[\sigma_R \bar{C}_{d_o}\right]_{MR}$$

then

$$C_{P_i}\Big|_{TR} = \frac{1}{\sqrt{2}} \left[\frac{1}{\sqrt{2}} C_{T_{MR}}^{3/2} + K_1\right]^{3/2} K_2$$

where

$$K_1 \equiv \left[\frac{1}{8} \sigma_R \bar{C}_{d_o}\right]_{MR} \qquad K_2 \equiv \sqrt{\frac{A_{D_{MR}}}{A_{D_{TR}}}} \left(\frac{R_{MR}}{\ell_{TR}}\right)^{3/2}$$

Profile Power

Blade element analysis of the tail rotor produces the following profile power required:

$$P_{o_{TR}} = \left[\frac{1}{8}\sigma_R \bar{C}_{d_o} \rho A_D (\Omega R)^3\right]_{TR}$$

where each symbol in the equation refers to the value associated with the tail rotor. In coefficient form:

$$C_{P_o}\Big|_{TR} = \frac{1}{8}\left[\sigma_R \bar{C}_{d_o}\right]_{TR} \frac{A_{D_{TR}}}{A_{D_{MR}}} \frac{(\Omega R)^3_{TR}}{(\Omega R)^3_{MR}} \equiv K_3$$

Total Power

The total tail rotor power required for hover, in coefficient form, is

$$C_{P_{TR}} = C_{P_i}\Big|_{TR} + C_{P_o}\Big|_{TR}$$

$$= \frac{1}{\sqrt{2}}\left[\frac{1}{\sqrt{2}} C_{T_{MR}}^{3/2} + K_1\right]^{3/2} K_2 + K_3$$

Thus, if K_1, K_2 and K_3 are constant, the tail rotor power required in hover will generalize as:

$$C_{P_{TR}} = f\left(C_{T_{MR}}\right)$$

A lack of generalization would result from variations in profile drag coefficients or center of gravity location, but $C_{P_{TR}}$ is small compared to

$C_{P_{MR}}$ and these effects would generally be negligible.

B. FORWARD FLIGHT POWER

Induced Power

The variation of the tail rotor induced power required in forward flight can be analyzed using simple momentum analysis to predict the variation in tail rotor induced velocity in forward flight. As a consequence of forward flight the induced velocity required to produce a certain tail rotor thrust decrease due to the increase mass flow rate through the tail rotor. Furthermore, the tail rotor thrust required for equilibrium depends on the main rotor torque, which varies with forward flight speed. Considering the tail rotor plane of rotation to be parallel to the flight path, the variation of induced velocity in forward flight is:

$$v_{i_f}{}_{TR} = \left[-\frac{V_f^2}{2} + \sqrt{\left(\frac{V_f^2}{2}\right)^2 + \left(\frac{P_f}{P}\right)^2_{MR} v_{i_{TR}}^4} \right]^{1/2}$$

or, in non-dimensional form,

$$\frac{v_{i_f}{}_{TR}}{(\Omega R)_{MR}} = \left[-\frac{\mu^2}{2} + \sqrt{\left(\frac{\mu^2}{2}\right)^2 + \left(\frac{C_{P_f}}{C_P}\right)^2_{MR} \left[\frac{v_{i_{TR}}}{(\Omega R)_{MR}}\right]^4} \right]^{1/2}$$

where the subscript "f" implies a parameter evaluate with a forward flight velocity of V_f. Using the expression determined for $v_{i_{TR}}$ (in hover):

$$\frac{\left(v_{i_f}\right)_{TR}}{(\Omega R)_{MR}} = \left[-\frac{\mu^2}{2} + \sqrt{\left(\frac{\mu^2}{2}\right)^2 + \left(\frac{C_{P_f}\Big|_{MR}}{2} \frac{A_{D_{TR}}}{A_{D_{MR}}} \frac{R_{MR}}{\ell_{TR}}\right)^2} \right]^{1/2}$$

The induced power of the tail rotor in forward flight can be expressed as

$$P_{i_f}\Big|_{TR} = T_{f_{TR}} \left(v_{i_f}\right)_{TR}$$

r, in coefficient form as

$$C_{P_{i_f}}\Big|_{TR} = \frac{P_{i_f}\Big|_{TR}}{\rho A_{D_{MR}} (\Omega R)^3_{MR}} = \frac{T_{f_{TR}}}{\rho A_{D_{MR}} (\Omega R)^2_{MR}} \frac{\left(v_{i_f}\right)_{TR}}{(\Omega R)_{MR}}$$

where

$$C_{T_{TR}} \equiv \frac{T_{f_{TR}}}{\rho A_{D_{MR}} (\Omega R)^2_{MR}}$$

The variation of tail rotor thrust coefficient with forward flight speed is:

$$C_{T_f}\Big|_{TR} = \frac{(P_f/\Omega)_{MR}}{\ell_{TR} \rho A_{D_{MR}} (\Omega R)^2_{MR}} = C_{P_f}\Big|_{MR} \left(\frac{R_{MR}}{\ell_{TR}}\right)$$

Using this expression and the induced velocity in forward flight:

$$C_{P_{i_f}}\Big|_{TR} = C_{P_f}\Big|_{MR} \left(\frac{R_{MR}}{\ell_{TR}}\right) \left[-\frac{\mu^2}{2} + \sqrt{\left(\frac{\mu^2}{2}\right)^2 + \left(\frac{C_{P_f}\Big|_{MR}}{2} \frac{A_{D_{TR}}}{A_{D_{MR}}} \frac{R_{MR}}{\ell_{TR}}\right)^2} \right]^{1/2}$$

or, in functional form:

$$C_{P_{i_f}}\Big|_{TR} = f\left[\left(C_{P_f}\right)_{MR}, \mu\right]$$

Profile Power

The profile power of the tail rotor in forward flight can be predicted by blade element analysis, the results of which are the same as for the main rotor if the tail rotor H-forces are considered as contributing to the tail rotor power required. In that case

$$P_{o_f}\Big|_{TR} = \left[\frac{1}{8}\sigma_R \bar{C}_{d_o} \rho A_D (\Omega R)^3 (1 + 4.65\mu^2)\right]_{TR}$$

where

$$\mu_{TR} \equiv \frac{V_f}{(\Omega R)_{TR}}$$

and all other symbols refer to values associated with the tail rotor. This equation can be written as

$$P_{o_f}\Big|_{TR} = P_{o_{TR}}\left[1 + 4.65\mu^2 \frac{(\Omega R)^2_{MR}}{(\Omega R)^2_{TR}}\right]$$

where

$$\mu \equiv \frac{V_f}{(\Omega R)_{MR}}$$

In coefficient form, then

$$C_{P_{o_f}}\Big|_{TR} = \frac{P_{o_f}\Big|_{TR}}{\rho A_{D_{MR}} (\Omega R)^3_{MR}}$$

$$= \frac{1}{8}\left(\sigma_R \bar{C}_{d_o}\right)_{TR} \frac{A_{D_{TR}}}{A_{D_{MR}}} \frac{(\Omega R)^3_{TR}}{(\Omega R)^3_{MR}} \left[1 + 4.65\mu^2 \frac{(\Omega R)^2_{MR}}{(\Omega R)^2_{TR}}\right]$$

For a fixed main rotor/tail rotor tip speed ratio and a particular tail rotor profile drag coefficient:

$$C_{P_{o_f}}\Big|_{TR} = f(\mu)$$

Total Power

The total tail rotor power required in forward flight is

$$P_{f_{TR}} = P_{i_f}\Big|_{TR} + P_{o_f}\Big|_{TR}$$

or

$$C_{P_f}\Big|_{TR} = C_{P_{i_f}}\Big|_{TR} + C_{P_{o_f}}\Big|_{TR}$$

Although the terms of these equations have been explicitly defined above, the influence of the tail rotor power on the generalization of power required can most simply be shown by the functional relationships:

$$C_{P_f}\Big|_{TR} = f_1\left[\left(C_{P_f}\right)_{MR}, \mu\right] + f_2[\mu]$$

$$= f_3\left[\left(C_{P_f}\right)_{MR}, \mu\right]$$

For a given helicopter, the generalization depends on a constant ℓ_{TR} and tail rotor C_{d_o}.

In the forward flight analysis of the main rotor, it was concluded that

$$C_{P_f}\Big|_{MR} = f_4\left(C_{T_{MR}}, \mu\right)$$

if the main rotor C_{d_o} and the fuselage C_{D_p} remain fairly constant. Similarly it has been demonstrated that

$$C_{P_f}\Big|_{TR} = f_5\left(C_{T_{MR}}, \mu\right)$$

and thus the tail rotor power required should generalize in the same manner as the main rotor power required:

$$C_{P_f}\Big|_{MR} + C_{P_f}\Big|_{TR} = f\left(C_{T_{MR}}, \mu\right)$$

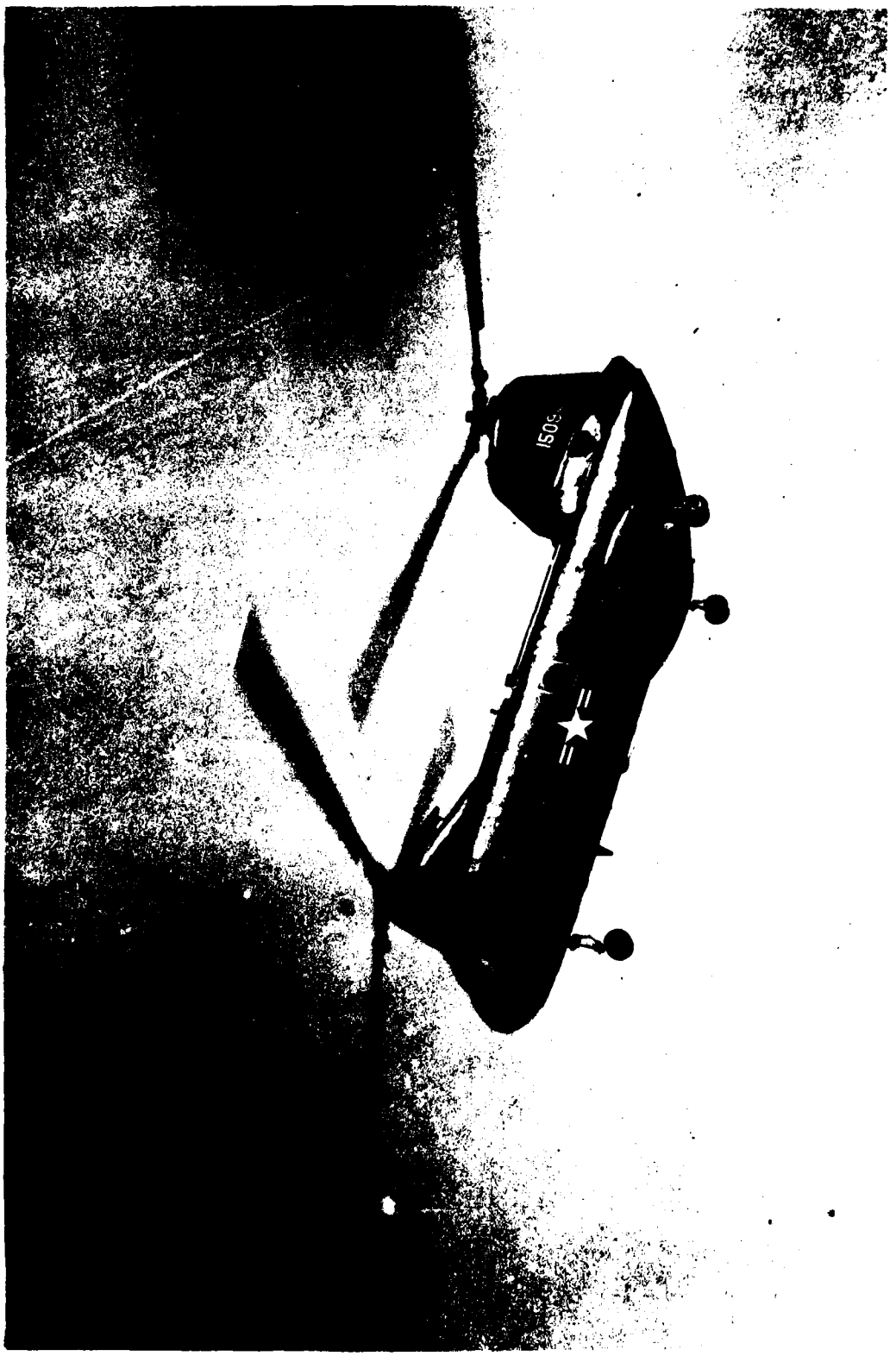

NOTATION

SYMBOLS

A	Area
A_D	Rotor disc area : $A_D \equiv \pi R^2$
B	Rotor tip loss correction factor (p VI - 6)
b	Number of blades per rotor
b	Wing span
c	Chord of rotor section
C_{d_c}	Section drag coefficient
$\bar{C}_{d_o}$	Average C_{d_o} across blade
C_D	Drag coefficient; $C_D \equiv D/qS$
C_ℓ	Section lift coefficient
$\bar{C}_\ell$	Average C_ℓ cross blade
C_L	Lift coefficient; $C_L \equiv L/qS$
C_P	Rotor power coefficient; $C_P \equiv \frac{P}{\rho A_D (\Omega R)^3}$
C_T	Rotor thrust coefficient; $C_T \equiv \frac{T}{\rho A_D (\Omega R)^2}$
D	Drag
D	Diameter
F	Force
f	Equivalent flat plate area (p IV - 16)
H	Rotor hub shear force (p IV - 12)
h	Height

NOTATION

SYMBOLS (continued)

h_p	Pressure altitude
I_R	Rotor moment of inertia
L	Lift
ℓ_t	Length from CG to tail rotor (p VII - 1)
M	Mach number; $M \equiv V/V_a$
M_{cr}	Critical M
M_{dd}	Drag divergence M
M_s	Shock stall M
M'	Figure of merit (p II - 22)
$\dot{m}$	Mass flow rate
P	Power
P	Pressure
Q	Torque
q	Dynamic pressure; $q \equiv 1/2\ \rho V^2$
R	Resultant
R	Rotor radius
r	Radius to blade element
S	Wing area
T	Thrust
t	Time
V	Velocity

NOTATION

SYMBOLS (continued)

V_a	Acoustic velocity
V_e	Blade element velocity
V_f	Forward flight velocity
V_r	Resultant velocity through rotor disc
V_v	Vertical velocity
V'	Uncorrected vertical velocity (p III - 2)
v_i	Induced velocity at rotor
v_{i_f}	Resultant induced velocity in forward flight
v_{i_h}	Horizontal component of v_i
v_{i_v}	Vertical component of v_i
v_w	Wake induced velocity

GREEK SYMBOLS

α	Angle of attack
η_m	Mechanical Efficiency; $\eta_m \equiv \frac{RSHP}{ESHP}$
θ	Blade pitch angle
μ	Tip speed ratio, $\mu \equiv \frac{V_f}{\Omega R}$
ρ	Density
σ	Density ratio, $\sigma \equiv \rho/\rho_{SL}$
σ_R	Rotor solidity, $\sigma_R \equiv bc/\pi R$

NOTATION

GREEK SYMBOLS (continued)

ϕ	Inflow angle (p V - 6)
ϕ'	Arctan drag - lift ratio (p V - 6)
ψ	Blade azimuth angle (p IV - 9)
Ω	Angular rotation rate

SUBSCRIPTS

a	Ambient
E	Engine
e	Rotor blade element
f	Freestream
f	Forward flight
h	Hover
i	Induced
IGE	In ground effect
MR	Main rotor
o	Profile
o	Two-dimensional
o	Zero velocity
OGE	Out of ground effect
p	Parasite
R	Resultant

NOTATION

SUBSCRIPTS (continued)

TR	Tail rotor
v	Vertical or vertical component
w	Wing
ΔPE	Change potential energy

ABBREVIATIONS

AR	Aspect ratio
ESHP	Engine shaft horsepower
IGE	In ground effect
OGE	Out of ground effect
R/C	Rate of climb
RSHP	Rotor shaft horsepower

REFERENCES

1. Lodge, D.: "Introduction to the Helicopter", Hiller Aircraft Corporation, 1962

2. Gessow, A. and Meyers, G. C.: "Aerodynamics of the Helicopter", The MacMillan Company, New York, 1952

3. Shapiro, J.: "Principles of Helicopter Engineering", McGraw-Hill, New York, 1956

4. Payne, P. R.: "Helicopter Dynamics and Aerodynamics", The MacMillan Company, New York, 1959

VIII. TWIN-ROTOR INTERFERENCE

Aerodynamic interference between rotors of a multirotor helicopter are not well defined but the consequences may be significant and the analysis of performance would not be complete without some discussion. Under certain conditions of flight, interference may exist between main rotor and tail rotor of a single main-rotor helicopter but the discussion here is directed toward interference between the main rotors of a counter-rotating dual main rotor machine which needs no tail rotor.

The problem to be considered is that of a comparison between the induced power required to support a given weight in hover with a two rotor system which has the same total disc area, solidity and tip speed as the single rotor. It is assumed that profile power is not affected by interference.

Momentum analysis shows that for the same total disc area and thrust (same T/A_D) the induced loses are the same regardless of the number of discs, if there is no interference. In the actual case there is a significant amount of interference which must be considered.

The aerodynamic consequence of operating two rotors in close proximity to one another are, primarily: (1) each rotor is operating in a flow field which may be influenced by the induced velocity of the other rotor and (2) the two rotors in combination may influence a larger air mass than if they were far apart. These effects predominate to different degrees depending on geometric parameters such

as comparative size and relative location of the rotors (overlap and vertical displacement) and on the aerodynamic situation such as flight velocity, attitude, rotor thrust, etc. Presented here is only an extension of simple momentum theory to show the major consequence of interference on power required. The case considered is that of two rotors of the same size and thrust with varying degrees of overlap but where the vertical displacement is small. The degree of overlap is expressed as ℓ/D (where ℓ is the distance between main rotor centers and D is the rotor diameter) and is considered here to vary from a number near unity (tandem) to zero (co-axial).

A. HOVER

Considering first the co-axial situation with small vertical displacement, simple moment analysis can produce an approximate solution to the interference problem by considering each rotor to be operating in a moving air mass induced by the other rotor. The problem can then be analyzed by vertical climb analysis.

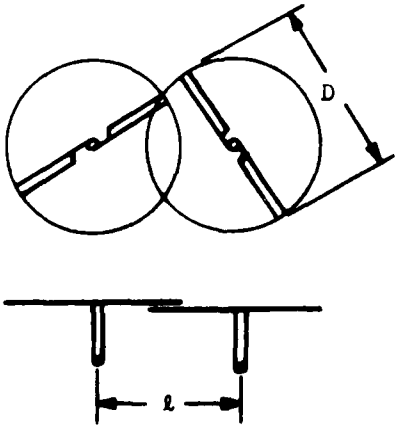

Figure 1
Twin-Rotor Configuration

When a rotor is operating in a stabilized climb with respect to the air mass, the induced velocity (v_{i_v}) in the presence of a vertical velocity (V_v), assuming parasite drag to be zero, is (see page III - 3):

$$v_{i_v} = \sqrt{(V_v/2)^2 + v_i^2} - V_v/2$$

where v_i is the induced velocity required for the same thrust with no climb rate:

$$v_i = \sqrt{\frac{T}{2\rho A_D}}$$

For the case presented here, $V_v = v_{i_v}$ and

$$v_{i_v} = v_i \sqrt{2}$$

The resultant flow through each rotor disc (V_r) is then the sum of the self-induced velocity plus that induced by the other rotor, or,

$$V_r = 2 \frac{v_i}{\sqrt{2}} = \sqrt{2}\ v_i$$

and the induced power for each rotor with this mutual interference is:

$$P_i = T\ V_r = \sqrt{2}\ T\ v_i$$

Thus, for a given thrust, the induced power is seen to increase on each rotor of a co-axial system by 41% of that if the rotors were far apart.

Assuming that the interence has no effect on profile power, the total power of the two rotors (P_{2MR}) is:

$$P_{2MR} = 2\,(Po + Pi)$$
$$= 2\left\{\frac{1}{8}\,\sigma_R\,\bar{C}_{do}\rho A_D\,(\Omega R)^3 + \sqrt{2}\,T\sqrt{\frac{T}{2\rho A_D}}\right\}$$

where A_D is the disc area of each rotor.

In order to compare the coefficient form to that for two rotors operating without interference, the total area must be taken as the sum of the individual disc areas so that, with interference:

$$C_p \equiv \frac{P}{\rho 2A_D\,(\Omega R)^3}$$
$$= \frac{1}{8}\,\sigma_R\,\bar{C}_{do} + \sqrt{2}\sqrt{\frac{C_T^3}{2}}$$

where

$$C_T \equiv \frac{T}{\rho A_D\,(\Omega R)^3}$$

or, if each rotor has $T = W/2$ (this may not be the case),

$$C_T = \frac{W}{\rho 2A_D\,(\Omega R)^3}$$

It is interesting to note that the same conclusion can be obtained by simply considering that the total system is producing thrust equal to weight with a total disc area of $2\,A_D$ for the separated rotors, whereas the co-axial system is producing thrust equal to weight with an effective disc area of A_D. Thus the co-axial has effectively twice the disc loading of the single rotors which would directly explain the increase of induced effects by $\sqrt{2}$. This approach is more easily applied to the case of varying degrees of overlap than is the downwash analysis and will be used subsequently.

In terms of effective rotor system area (A_e):

$$P_i = \sqrt{\frac{W^3}{2\rho A_e}}$$

For two separated rotors, $A_e = 2A_D$ and

$$P_{i_{sep}} = \sqrt{\frac{W^3}{2\rho\ 2A_D}}$$

whereas if the two rotors are co-axial

$$P_{i_{coax}} = \sqrt{\frac{W^3}{2\rho A_D}} = \sqrt{2}\ P_{i_{sep}}$$

This "effective disc area" analysis can be readily extended to include various degrees of overlap. However, it has been observed exterimentally that the stream tube influenced by two rotors in tandem ($\ell/D \simeq 1.0$) is larger than the sum of the individual rotor disc areas and the induced power is less than that for the two rotors if placed far apart. This is analogous to the lift produced by the nonexistent center section of a fixed wing aircraft. Thus it is indicated that the effective disc area is actually larger than the area swept by the rotors and the <u>effective area</u> chosen here, which correlates well with the limited experimental results available, is defined as (see Figure 2):

$$A_e \equiv A_D + \ell\ D = A_D\ (1 + \frac{4}{\pi}\ \frac{\ell}{D})$$

where $A_D \equiv \pi D^2/4$ and ℓ/D is limited to a maximum value of about unity.

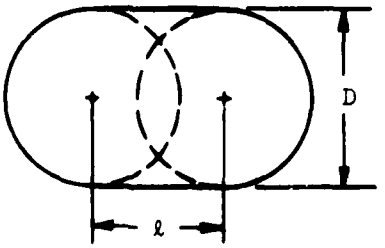

Figure 2

Effective Area For Overlapping Rotors

The induced power required by both rotors can be expressed for any degree of overlap as:

$$P_i = \sqrt{\frac{W^3}{2\rho A_e}} \qquad \ell/D \lesssim 1.0$$

whereas for separate rotors:

$$P_i = \sqrt{\frac{W^3}{2\rho\ 2A_D}} \qquad \ell/D >> 1.0$$

The induced power ratio, $P_{i_{ratio}}$, is defined as the total induced power with overlap to that of two separate rotors and is:

$$P_{i_{ratio}} = \frac{\sqrt{W^3/2\rho A_e}}{\sqrt{W^3/2\rho 2A_D}} = \sqrt{\frac{2A_D}{A_e}}$$

$$= \sqrt{\frac{2}{1 + \frac{4}{\pi}\frac{\ell}{D}}}$$

Figure 3

Induced Power Ratio For Overlapping Rotors

Simple Momentum Analysis

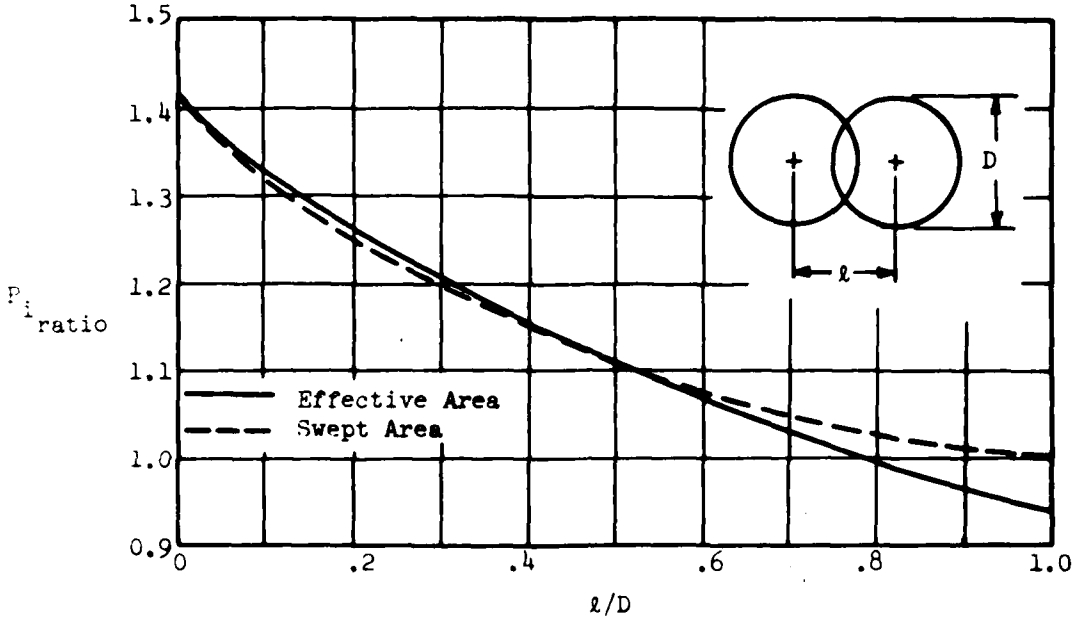

The induced power ratio variation is shown graphically in Figure 3.

The large air mass influenced by the twin rotor system indicates that the diameter of a single rotor should not be used in assessing the effective value of h/D in the determination of ground effect. Possibly the diameter to use should be an effective diameter (D_e) such as:

$$D_e = \sqrt{\frac{4}{\pi} A_e}$$

$$= D \sqrt{1 + \frac{4}{\pi} \frac{\ell}{D}}$$

for $\ell/D \lesssim 1.0$

The conclusions of the main rotor power required analysis must be tempered by other considerations. For example, although the tandem configuration ($\ell/D \approx 1.0$) has no tail rotor power required and has favorable main rotor interference, the

configuration usually results in more fuselage area subjected to rotor downwash which may well negate the favorable aspects. Other design criteria must also be considered such as the system size, weight and complexity, the influence of the rotor configuration on handling qualities and on high forward-flight speed operating problems.

B. FORWARD FLIGHT

Once the tandem rotor ($\ell/D \approx 1.0$) proceeds into forward flight, the front rotor wake trails back over the rear rotor creating a significant change in the interference effects. The characteristics exhibited depend on the geometric relationship between the two rotors or, more specifically, on the rotor's respective pylon heights and the attitude of the machine with respect to the freestream. Generally, the front-rotor downwash on the rear rotor causes an interference effect which increases the rear rotor power required. This can be visualized as an effective increase in overlap. As a consequence, the rear rotor power required increase at low forward flight speeds, exceeding that required by the front rotor and the favorable interference effect realized in hover is rapidly lost.

The co-axial system experiences little change in the interference effects because the rotors are close together and the unfavorable interference prevails in forward flight as well as in hover.

In forward flight, the twin-rotor configurations generally exhibits unfavorable interference effects to a degree which more than compensates for the power saved by having no tail rotor.